YscP, a key player in the Type Three Secretion System of *Yersinia enterocolitica*

Inauguraldissertation

zur

Erlangung der Würde eines Doktors der Philosophie

vorgelegt der

Philosophisch-Naturwissenschaftlichen Fakultät

der Universität Basel

von

Céline AGRAIN

aus Strasbourg, France

2005

Genehmigt von der Philosophisch-Naturwissenschaftlichen Fakultät

auf Antrag von

- Prof. Dr. Guy Cornelis
- Prof. Dr. Urs Jenal

Basel, den 25/10/2005

Prof. Dr. Hans-Jakob Wirz

ACKNOWLEDGEMENTS

First, I would really like to thank Prof. Dr. Guy Cornelis for all the support throughout my PhD. He always had an opened door and showed strong interest in my topic of research, pushing me always further. I also specially enjoyed his trust and advices.

J'aimerais remercier le Dr. Jean-Marie Meyer pour m'avoir donné goût à la recherche scientifique, m'avoir fait partager sa passion pour les pyoverdines et les petites "bestioles" et sans qui je ne me serai pas lancée dans l'aventure du doctorat. De meme, je tiens à remercier le Dr. Valérie Geoffroy et Christelle Gruffaz pour m'avoir montré les bases du travail en laboratoire.

Dann würde ich gern ganz herzlich Frau Dr. Isabel Sorg danken für Ihren Einsatz und die erfolgreiche Mitarbeit am YscP Projekt. Sie war eine Spitzenhilfe und besonders wichtig waren unsere konstruktiven Diskussionen. Trotz all der Mühe und des enormen Zeitaufwands am EM, hatten wir viele lustige Momente in der Dunkelheit. Ich hoffe, dass unsere Freundschaft, die im Anatomie Institut entstand, noch weiter gehen wird.

Besonders möchte ich auch Catherine Müller danken für die Einführung in das "Schwiezerdütsche Leben" besonders der "Ruebli Torte" und der Fastnacht. Ich hatte ganz viel Spass an unseren Mittwoch Abenden (nicht nur am Tanzen, sondern auch am gemeinsamen Essen und Plaudern).

I also would like to acknowledge Dr. Luis Jaime Mota for all the inputs and advices he gave me. He was an amazing source of knowledge.

J'aimerais également remercier le Dr. Laure Journet pour son accueil au sein du labo et sur le projet YscP. Elle m'a non seulement initiée aux différentes techniques utilisées (notamment la microscopie électronique) mais elle a aussi été une amie avec laquelle nous avons partagé de très bons moment en dehors du labo.

Ich möchte auch Marina Kuhn danken für Ihre stete Hilfsbereitschaft sowie dafür, dass sie immer ein offenes Ohr hatte für die kleinen und grossen Probleme des Labor- und des Büroalltags.

Egalement un grand merci à "Dorie" Cécile Paroz pour sa bonne humeur, son dynamisme et la motivation dont elle a fait preuve durant les quelques mois ou elle m'a donné un "coup de main" pour les constructions. Je n'oublie pas non plus les centaines de séquençage des mutants qu'elle a réalisé...avec le sourire.

I would also like to thank Dr. Hwain Shin for her availabity and her help, not only each time I needed to write in correct english but also concerning the purification of YscP.

Ein spezieller Dank gilt Nadine Shracke, "die strahlende", die mich dazu brachte Milchschnitten und Latte Macchiato zu probieren. Obwohl wir nur eine kurze Zeit miteinander in Basel hatten , werde ich ihren Sinn für Humor, ihre Witze und ihre Lebensfreude vermissen.

Many thanks to the different people who were interested and contributed to the project, namely Dr. Caroline Peneff (Biozentrum), Dr. Isabelle Callebaut (Paris) and Prof. Kelly Hughes (Salt Lake City).

I would also like to thank all the past and present members of the lab that I did not mentionned previously for a really nice atmosphere, great moments of fun and all the help they provided me : Petr Broz, Michel Letzelter, Manuella Mally, Steffi Wagner, Dr. Mario Feldman, Dr. Gottfried Eisner, Paul Troisfontaines, Tamara Codilupi, and the students : Yvonne Lussi, Kerstin Maylandt, Emilie Clément, Viola Huschauer, Jacqueline Stalder, Silke Lützelschwab, Franziska Fischer.

Enfin, un très grand merci à mes parents pour leur soutien inconditionnel durant toutes mes études, leurs encouragements et leurs conseils. Et également à Jean-Marc pour sa presence à mes côtés.

TABLE OF CONTENTS

1- INTRODUCTION

Length control in microorganisms

1. Length control in micro-organisms

Size and shape determination of multi-component structures are critical for their proper assembly and function. To ensure length control of structures, organisms have evolved a certain number of mechanisms. The presence of such a mechanism governing the size of a given structure is inferred whenever this structure adopts a narrow distribution of sizes. The study of these length-controlling mechanisms in biology is complicated by the 3-dimensional structure of organelles, which makes their size difficult to measure or even to define. Therefore most of the studies performed so far are considering linear structures. Two major ways of size determination have been highlighted:

- either the size of the overall structure is determined in comparison with the size of an individual molecule, a so-called “molecular ruler”
- or length control is involving a steady-state balance of assembly and disassembly, in which one or the other rate is inherently length dependent.

1.1. Bacteriophage tail length determination

One of the main features of bacteriophages is to remain attached to the bacteria outer cell surface during infection. A vast majority of phages have evolved to use a tubular structure called a tail for host recognition, attachment and genome delivery into the cell. This tail connects the capsid (head), containing the phage genome, to an adsorption organelle called the baseplate, which consists of a basal structure and fibers. Bacteriophages self assemble into these remarkably complex structures whose size is highly reproducible.

As for the head, the size is commonly fixed by the geometrical relations between the interacting subunits. On the contrary, the tails, which are simple polymers could, in principle, grow to any size. Nevertheless their observed length distribution is very narrow, far narrower than expected for a simple polymerization process at equilibrium. The way this tail length determination is achieved has been one of the pioneer work in understanding how organisms regulate their protein assembly systems.

1.1.1. Bacteriophage lambda

a. Structure of the tail complex (for review, [1-3])

The first organism extensively studied was the bacteriophage λ. Its tail is a thin flexible tube (135nm long), ending in a small conical part (15nm long, often with side fibers) with a single tail fiber (23nm). The tubular part consists of 32 disks each of which seems to be a

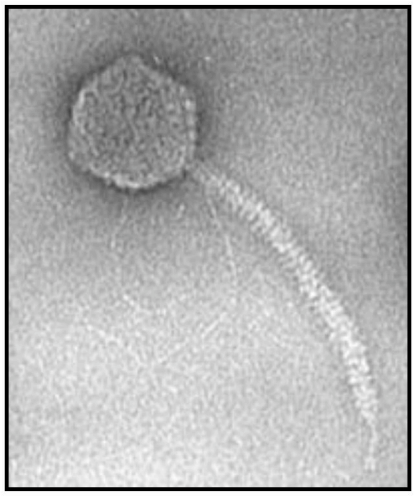

Fig. 1: The bacteriophage λ virion. Electron micrograph of λ negatively stained with uranyl acetate. The length of the tail, excluding fibers, is around 150 nm. (www.steve.gb.com/science/model_organisms.html)

	Lambda Tail	**T4 tube**
Structure		
Length (nm) (nb of disks)	135 32	100 24
Outer diameter (nm)	17	9
Central channel (nm)	3-3.5	3.2-3.8
Major protein	gpV	gp18
Tape-measuring molecule or ruler		
Protein	gpH	gp29
Length (aa)	853aa	591aa
Molecular Weight	93KDa → 79KDa (cleaved)	64KDa
Number of protein/particle	6	4-7
Length of the tube/residue (Å)	1.6	1.7
Growth-terminating protein		
	gpU	gp3

Table 1: Major characteristics of the λ tail and the T4 tube

ring-like hexamer of the major tail protein gpV. Eleven genes Z, U, V (major tail protein), G, T, H, M, L,K , I and J (tail fiber) have been shown to be necessary for assembly of the tails.

b. Proposed length determination models

Early in the study process, three theories had been proposed for the length determination of the phage tails (reviewed by [1-3]) :

- **Cumulative model**
  The subunits polymerizing at the growing end of the tail become increasingly deformed as the tube elongates, thereby blocking the addition of further subunits. In this model, the length would be somehow specified by the intrinsic properties of the subunits.
- **Vernier model**
  An internal component of the tube elongates alongside the tube subunits to co-measure length. The elongation stops when the ends of the two proteins structures come into register like the marks of a mechanical Vernier and create a binding site for a terminator molecule.
- **Ruler model**
  Tail length is controlled by a ruler or tape measure protein, around which the tail tube monomers polymerize; the length of this ruler protein would determine the length of the tail.

The two first theories proved to be wrong. Indeed, the cumulative model would imply that a change in gpV (deletion, amino acid substitution) would affect tail length. However, none of the gpV mutant lead to longer or shorter tails. As for the Vernier model, it would require another protein, besides gpV, present in a large number. The only two proteins fitting this requirement are gpG and gpU. The latter can be excluded as it has been shown not to be necessary for the pause of the assembly of gpV. The function of gpG is unknown but it is suggested that it could be involved in the initiator assembly.

c. gpH, a molecular ruler

Besides the investigation on the Cumulative and on the Vernier model, the search for a potential ruler protein was initiated. The most probable candidate was gpH, that had also been shown to be contained in the baseplate or initiator. Indeed it had been calculated that in order to measure a tail tube of 135 nm with all or part of the length of a protein, this protein would need to contain at least 400 amino acids. This left gpH as the only possible candidate.

Furthermore it had been shown that in a λ-related phage φ80, both the tail and the protein homologous to gpH are longer than in λ (19% and 22% higher as for the tail and the molecular weight, respectively)[3].

Experimental evidences have demonstrated that gpH controls the length of the tail. Indeed, deletion mutants in gpH produce phage tails abnormally short while engineered duplications within gpH produce correspondingly longer tails [4]. The length of mutated gpH is proportional to the length of the tails produced by these mutants [5], except for the C-term part of the protein which is needed for initiator assembly [3]. This means that nearly the whole protein serves as a ruler. In fact, the middle part of gpH has a relatively uniform structure with respect to length per residue (about 1,6Å/residue) and no or only weak, non-specific interactions with other proteins. Secondary structures prediction on the whole protein shows that gpH consist mainly in α-helices, which comprise about 60% of the residues, connected by random structures, β-turns and β-structures. Although gpH must be extended when it measures the tail length, the coefficient of friction of the initiator suggests that gpH exists in a relatively compact form in the initiator. This initiator is thought to contain, among others, 6 molecules of the ruler proteins gpH [6], attached via their C-term and folded into a somewhat compacted form. This explains the phenotype observed in mutants with deletions in the C-term of gpH, which are blocked in the initiator assembly. In addition of having a different function, the C-term part has also a different pattern than the rest of the protein; it is more glycine-rich and predicted to be less α-helical. The fact that a deletion in the N-term part of the protein still enables a correct assembly and a sharp distribution of the tail lengths disfavours the idea of a ruler protein analogous to a thread with two sticky ends. It rather leads to envision a model in which the N-term end does not adhere to the top of the tail tube (Fig. 4).

d. gpU, the terminator protein

To describe the full tail length determination process it is important to mention another important actor, gpU. Indeed, the only mutants displaying polytails or polytubes structures, meaning structures whose polymerization never ended, are mutants in the gene U. Therefore, a function of terminator was assigned to gpU. Although in these mutants the distribution is broad and a lot of tails are extra-longs, still some have a WT size, indicating that the mutation in gpU is not affecting the pause in the polymerization which occurs once the proper length has been attained [3].

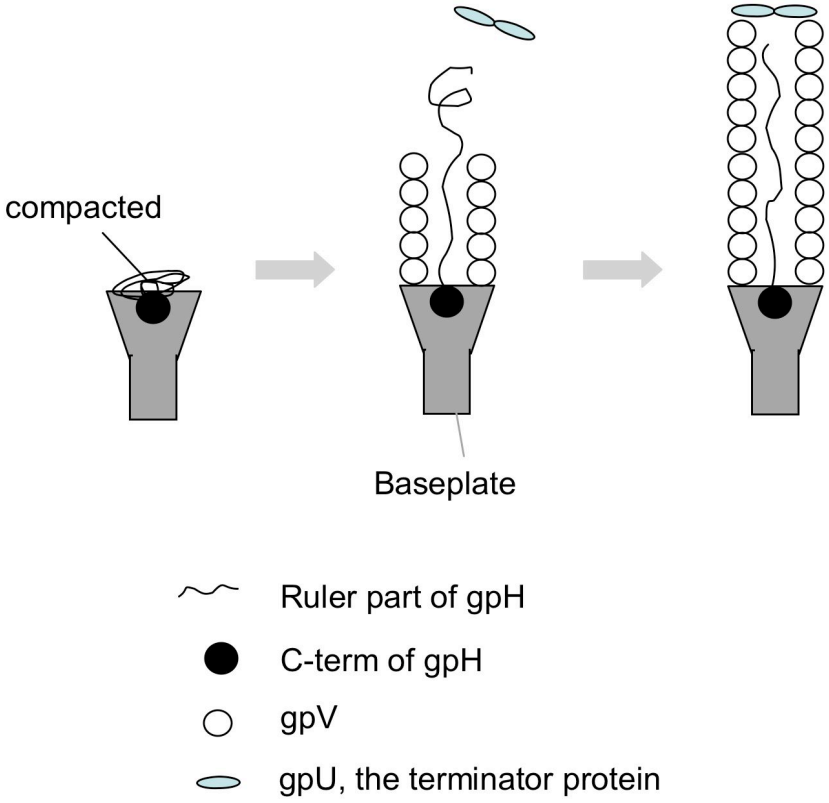

Fig. 2 : Proposed model for tail length determination by gpH and gpU. Modified from [3].

e. gpH and gpU co-acting to determine tail length during its assembly

The proposed tail assembly pathway can be summarized as follows (Fig.2):

1) The major tail protein gpV polymerizes on the baseplate, which requires 8 gene products for its formation, among which 6 molecules of gpH, which are compacted and attached via their C-terms.
2) Although there is no direct evidence, the ruler proteins seem then to unfold into a fibrous, length-measuring form as tails elongate by polymerization of gpV. They are considered to be located inside the tail tube except for a small part at one end, which protects the tail from the growth-termination factor gpU.
3) Once the correct length is reached and the tail becomes longer than gpH stretched, further growth carries the end of the tail past the end of gpH, which can no longer protect the tail from the inhibitory action of gpU.
4) The terminator gpU joins to the top of the tails, which terminates assembly of gpV, triggers cleavage of gpH into gpH*.

Thus, the tail length is regulated by a 2-steps process. First, there is a molecular ruler setting the standard length. Then, there is a growth-terminating molecule that binds to the tail end during the pause and locks in the correct length.

1.1.2. Bacteriophage T4

a. Structure of the tail complex (Fig.3, Table 1)(For review, [7])

The main organization is similar to that of λ, even though the degree of complexity is a little higher. The baseplate is composed of 150 subunits including at least 16 different gene products, many of which are oligomeric. It is assembled from six identical wedges that surround a central hub. Six copies of gp29 initiate the assembly of the central hub of the baseplate. One central hub complex (gp5, gp27 and gp29) then combines with six wedges (gp25, gp53, gp6, gp7, gp8, gp10 and gp11) to produce the hexagonal baseplate. Assembly of the baseplate is completed by attaching gp9 and gp12 forming the short tail fibers; and also gp48 and gp54 that are required to initiate polymerization of the tail tube, that is constructed of 138 copies of gp19. The tail tube serves then as a template for the assembly of 138 copies of gp18 that form the contractile sheath. In the absence of tail tube, gp18 assembles into long polysheaths. When the baseplate attaches the phage to the cell surface, it undergoes a conformational change. This initiates the contraction of the sheath, which drives the tail tube trough the cell envelope. Subsequently, the phage genome passes through the tail tube into the cytoplasm.

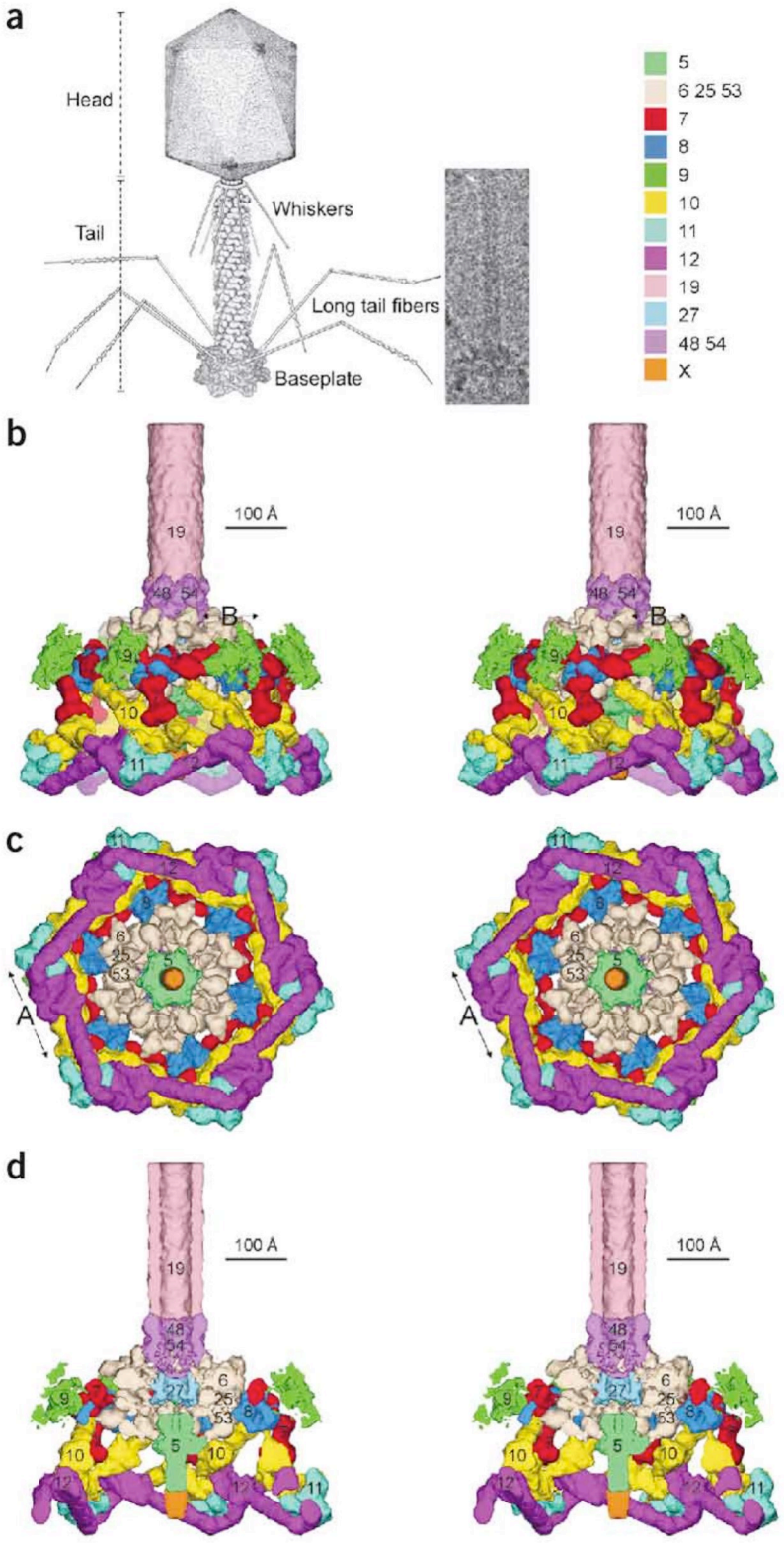

Fig. 3: Structure of the baseplate-tail tube complex. (a) Model of the T4 virus and cryoEM image of the baseplate-tail tube complex. (b-d) The baseplate and the proximal part of the tail tube are shown. Colors identify proteins labeled with their respective gene numbers, as shown on the right hand side. gp5, spring green; gp6+gp25+gp53, beige; putative gp7, red; gp8, dark blue; gp9, green; putative gp10, yellow; gp11, cyan; gp12, magenta; gp19, salmon; gp27, sky blue; putative gp48 or gp54, pink; unidentified protein X at the tip of gp5, orange. (b) Side view. (c) End-on view. Published in [77].

b. gp29 is acting as ruler

In comparison to the λ phage and as mentioned before, the T4 phage has an outer contractile sheath. But as its absence does not affect correct tube length, it cannot be considered as participating in the determination of the tail length. Therefore the tail length determinant is the tube length.

Structural studies have shown that the tail tube contains an internal component in the center of the tube. It was then suggested that this protein could be responsible for controlling tail length. This internal component could have been one of the 3 baseplate proteins (29, 48 or 54) that were shown to remain firmly bound to the purified structures. However, attempts to elongate gp48 have not shown any increase in tail length. On the contrary, mutations in some regions of gp29 that increase or decrease its length, produce corresponding changes in the length of the tail. Furthermore, sequence and structure analysis predicted that Gp29 could be long enough to extend over the length of the tube [8] as it is the largest of the hub proteins with 64 KDa molecular weight. Taking all these evidences into account, it seems that gp29 could be the counterpart of gpH in the T4 tail length determination system.

Deletions in the N-term or in the central part of the gp29 protein affect baseplate and thus tail assembly demonstrating that these regions are essential for phage particles assembly. Deletions in the C-term produce phage particle that are shorter than WT, suggesting that the C-term can be altered as a length regulator without affecting its ability to initiate a hub structure [9]. What is worth mentioning here is that the short tails observed do not have long tail fibers. The few particles that have tail fibers display an abnormally contracted sheath. In fact, the deleted portions at the C-term end of gp29 could result in a defective sheath-baseplate connection, suggesting that the C-term affect sheath-baseplate anchoring, or that the baseplate is assembled in a sensitive form that switches and loses its connection to the sheath upon tail fiber attachment [9].

c. gp3 as a terminator

Similarly to gpU, a gp3 mutant has abnormally long tails but a peak at WT length. Therefore it is likely that gp3 is acting as a growth-terminator protein once the tail tube has attained its correct length [10]. Consistent with this idea, gp3 has been shown to form an hexameric ring terminating the tube once it has attained its proper length [11] .

d. assembly pathway

- gp29 initially assembles in a compact form and provides binding sites for other proteins in the central hub around which the baseplate forms
- then, several molecules of the ruler protein must be reorganized into an extended fiber that is forced out of the baseplate as the tail tube grows in length.
- the addition of tail tube subunits to the growing structure stops when the ruler is fully extended, and the tube-fiber terminus creates a new binding site for gp3.

Gp29 is thought to remain attached by one end to the baseplate and at the other to the growing end of the tail tube, where it blocks the growth-terminator protein gp3 from binding and arresting polymerization.

1.1.3. Other ruler examples

Recent studies on two others λ-related phages HK97 and HK022, and the morphologically similar T5 are extending the list of ruler examples. Indeed, these phages, which have gpH homologs that are longer or shorter produce correspondent tail lengths that are respectively 17% longer, 11% shorter and 27% longer than lambda.

Tape-measure proteins (TMP) or rulers are found not only in T and lambdoid coliphages but in all phages with flexible non-contractile tails. A close correspondence between TMP gene length of 13 mycobacteriophages and phage tail length was recently observed [12]. The relationship is consistent with length determination by an extended alpha-helical protein, although for some of the phages, the TMP is somewhat longer than needed to span the tail as an α helix, suggesting that these proteins may have segments that do not participate in the length determination [12].

In bacteriophage TP901-1 that infects *Lactococcus*, deletions and duplications within a gene located at the same locus as gpH produce corresponding changes in tail length. This tends to suggest that the gene product also behaves as a molecular ruler.

1.1.4. Similarities and differences

Obviously the general mechanism of tail length regulation, as well as its main determinants, is well conserved among bacteriophages.

Both ruler proteins, gp29 and gpH, share a certain number of features. First, they are multi-functional proteins. Indeed, they are not only necessary for baseplate assembly but they also regulate tail length. Recently it has also been speculated that they could be playing a role in infection. Further functions in the initiation of infection and DNA injection are presently investigated. The so-called “pull-chain” model predicts that a tail protein transduces

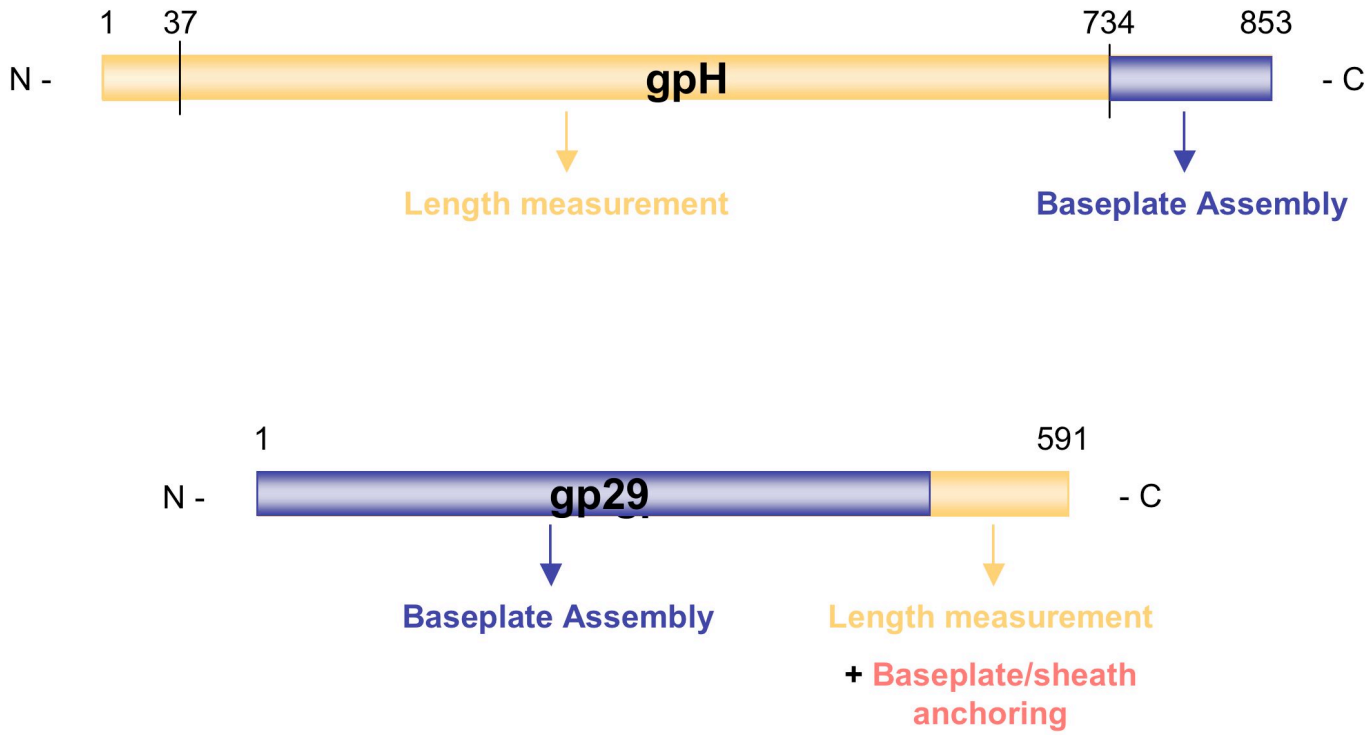

Fig. 4: Structure-function analysis of two phage tail rulers, gpH (λ phage) and gp29 (T4 phage).

a signal from the baseplate to the head to initiate DNA injection. And since rulers are located inside the tail, they could very well be the signalling molecules, especially as they are elongated during assembly. Their stretching could provide the connection between the baseplate and the head [13].

Although ruler proteins seem to perform the same function they are very diverse in their sequence. Their gene can usually be identified due to their location immediately downstream from a pair of genes expressed via a translational frameshift and their large size (>2000 bp). The size criteria is however not so accurate since size can vary according to the species. The biochemical properties of the ruler proteins are also different. Indeed, gpH is cleaved during assembly while gp29 is not and gp29 is reported to have an enzymatic function as folyl glutamate synthetase [14] which has never been shown for gpH.

Not only the sequence is diverse but also the domain distribution (Fig.4). Whereas in gpH both the N-term and the central part are dispensable for particles assembly, in gp29, they are essential in forming baseplates and thereby, crucial for assembly. In gpH, only the C-term is essential for assembly and likely to be the end attached to the baseplate. As for the ruler function, it seems that it is assigned to the N-term and central parts of gpH but to the C-term of gp29. The latter also appears to play a structural role in anchoring the sheath to the baseplate. Considering the regions devoted to each function in both proteins, gp29 probably contains more assembly information and has more complex protein-protein interactions than gpH.

Another major difference worthwhile to be highlighted is the lack of infectivity of T4 with altered tail lengths, in contrast to λ, in which particles with altered tail lengths remain infective. The absence of long tail fibers in T4 phage particles with altered tail lengths could render them not infective.

1.1.5. Conclusion

Bacteriophage tail length is primarily governed by a tape-measuring protein or ruler but is also assisted by a termination factor that recognizes the naked end. The ruler should have 2 domains; one that binds the site of initiation for assembly of the structure to be regulated and another that tracks the growing end and prevents binding of the growth-terminating protein. When the structure becomes longer than the ruler, the growth-terminating protein can access and bind the tip of the tail thereby arresting further growth.

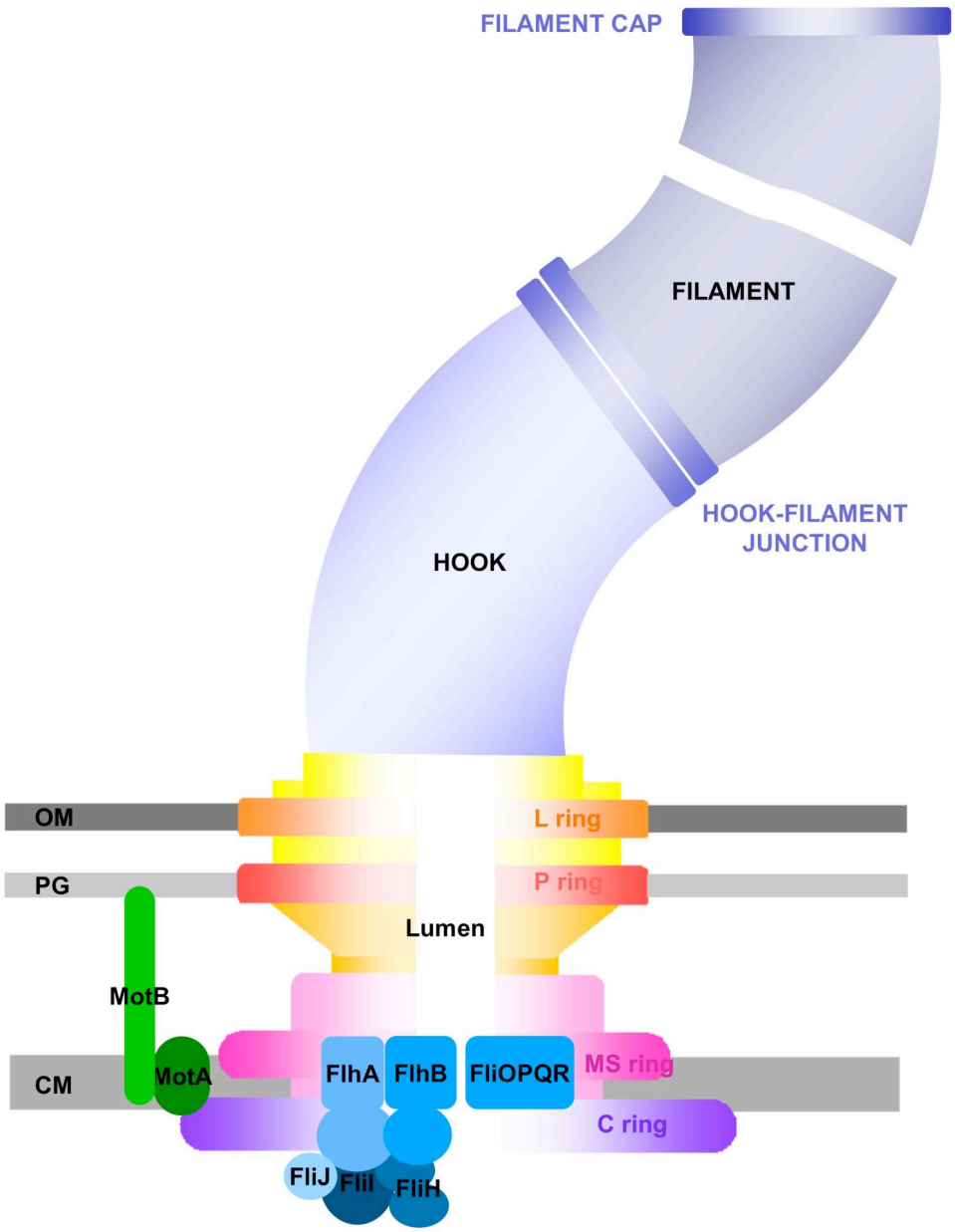

Fig. 5 : Schematic drawing of the flagellum. Components of the TTSS apparatus are in different tinges of turquoise. The colors refer to Table 2. Please note that the drawing is not on scale.

	Protein	Function	Location	Assembly	*Yersinia* inj
Soluble components	**FlhC**	global regulator, class II	C		
	FlhD	global regulator, class II	C		
	FliI	ATPase; drives type III flagellar export	C		YscN
	FliH	Negative regulator of FliI	C		YscL
	FliJ	General chaperone	C		YscO
	FlgN	Specific chaperone of FlgL and FlgK	C		
	FliS	Specific chaperone of FliC	C		LcrH
	FliT	Specific chaperone of FliD	C		YscY ?
Motor/Switch proteins	**FliG**	Rotor/Switch protein, torque generation	Peripheral	SA	
	FliM	C-ring component, rotor/switch protein	Peripheral	SA	YscQ ?
	FliN	C-ring component, rotor/switch protein	Peripheral	SA	
	MotA	Stator protein	CM	Sec	
	MotB	Stator protein	CM	Sec	
MS ring	**FliF**	MS-ring protein	CM	Sec	
Export apparatus	**FlhA**	Export component	CM, center of MS ring	Sec?	YscV
	FlhB	Export component, **Substrate-specificity switch**	CM, center of MS ring	Sec?	YscU
	FliO	Export component	CM, center of MS ring	Sec?	
	FliP	Export component	CM, center of MS ring	Sec?	YscR
	FliQ	Export component	CM, center of MS ring	Sec?	YscS
	FliR	Export component	CM, center of MS ring	Sec?	YscT
P-ring	**FlgI**	P-ring protein	PS	Sec	YscC
	FlgA	Specific chaperone of FlgI	PS	Sec	
L ring	**FlgH**	L-ring protein	OM	Sec	YscW
MS ring/ rod junction	**FliE**	MS ring/ rod junction protein	PS	TT	
Rod	**FlgB**	Proximal rod component	PS	TT	
	FlgC	Proximal rod component	PS	TT	
	FlgF	Proximal rod component	PS	TT	
	FlgG	Distal rod	PS	TT	
Rod cap	**FlgJ**	Rod capping protein	PS	TT	
Hook	**FlgE**	Hook component	E	TT	YscF
Hook cap	**FlgD**	Hook capping protein	E	TT	YscI
Hook/Filament junction	**FlgK**	HAP1, 1st hook/filament junction protein	E	TT	YopB
	FlgL	HAP3, 2nd hook/filament junction protein	E	TT	YopD ?
Filament	**FliC**	Filament component, flagellin	E	TT	LcrV ?
Filament cap	**FliD**	HAP2, filament capping protein	E	TT	YscX ?
	FliK	**Hook-length control protein**	Secreted	TT	YscP
	FlgM	Anti sigma factor	Secreted	TT	

Table 2 : Proteins of the flagellum and its export apparatus, arranged by cellular location. For each protein the function, the location, the mode of export/assembly and the counterpart in the *Yersinia* injectisome is given. C, cytoplasm; CM, cytoplasmic membrane; PS, periplasmic space; E, cell exterior; SA, self-assembly; TT, Type III export. Colors refer to the sub structures (Fig. 5) in which the proteins can be found.

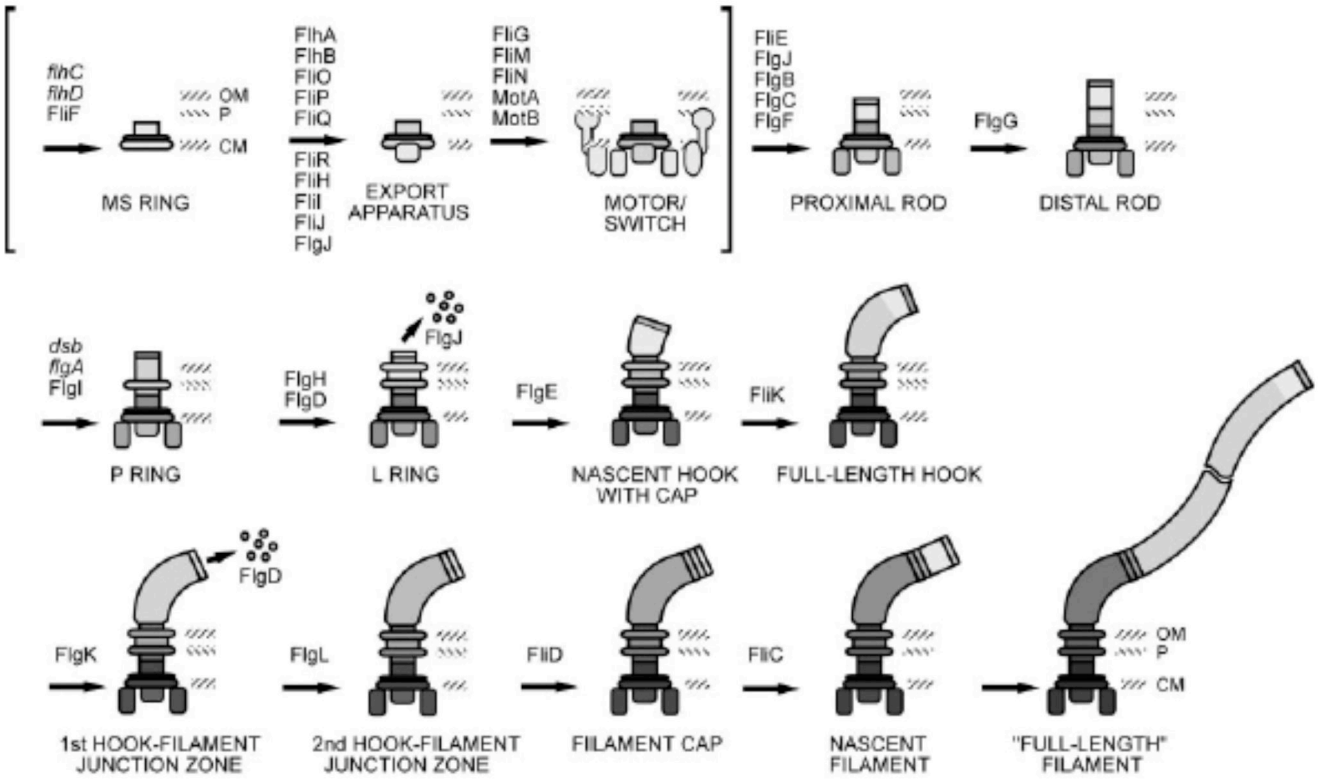

Fig. 6: Morphogenetic pathway for the flagellum of *Salmonella*. The brackets indicate substructures that are assembled prior to the utilization of the type III export pathway. The Mot proteins constitute the stator element of the motor and are integral membrane proteins surrounding the MS ring, while FliG and the C ring (FliM and FliN) constitute the rotor/switch element of the motor and are peripheral membrane proteins mounted on the MS ring. Genes (italics) or proteins necessary at each stage are indicated. Published in [15].

1.2. Flagellum hook length determination (State of the art in 2002)

1.2.1. The Flagellar structure and its assembly

The flagellum is a remarkably complex nanomachine whose organization is extremely optimized and efficient. It is composed mainly of 3 substructures: the basal body, the hook and the flagellum itself (for review, [15]).

a. The basal body [16]

The basal body consists of an integral membrane ring called the MS ring, a rod that spans the periplasmic space, a periplasmic P ring, and an outer membrane L ring. At least 8 different proteins composed the basal body; 4 of them in the rod (FlgB, FlgC, FlgF and FlgG) [17], FlgH forms the L ring, FlgI the P ring and FliF the MS ring, and FliE [18,19].

Around the basal body, there are several copies of an integral membrane structure made from two proteins, MotA and MotB. This assemblage sets up the stator part of the flagellar motor. The stator is attached noncovalently to the peptidoglycan layer and therefore is stationary in the frame of reference of the cell. The rotor/switch part of the motor, which is responsible for the reversal of the direction of rotation of the motor between counterclockwise and clockwise, is quite a large structure [20,21]. This structure consists of numerous subunits of three proteins: 26 subunits of FliG [22], 37 of FliM and 110 of FliN [23,24]. Morphologically, the latter proteins, FliM [25,26] and FliN, form a cytoplasmic cup- or ring-like structure called the C ring [20,21].

In the first stage of the basal body assembly, integral membrane proteins, including FliF, the Mot proteins and six components of the export apparatus (FlhA, FlhB, FliO, FliP, FliQ and FliR), which will be described, in the next section are inserted into the membrane using the Sec-pathway. Also assembled at this stage is the C ring which assembles onto the MS ring complex [27]. It is believed that the soluble components of the export apparatus, which are presumably in dynamic association with the membrane components [28], also can be included in this stage.

In the second stage the rod is assembled from proteins that have been exported by the export apparatus.

In the third stage the proteins of the periplasmic P ring and the outer membrane L ring are exported by the Sec pathway with signal peptide cleavage, and assemble as rings around the rod. They may be exported before stage two is complete, but probably can only assemble when the rod is in place and can act as a nucleation center.

b. The hook

The hook is a sharp bend outside the membrane, in the continuity with the basal body. It functions as a universal joint, connecting the hollow core of the basal body and the flagellum. The hook has a well-defined length of 55 nm ± 6 [29] and consists of about 130 subunits of FlgE. Once FlgD joins the rod tip, the hook starts to elongate by polymerizing these FlgE subunits at the distal end of the growing structure. FlgD, also called the hook cap is acting as a scaffolding protein. Its displacement by FlgK (also called Hook-Associated Protein 1: HAP1) terminates the hook assembly [30].

c. The filament

The filament is a long, thin cylindrical structure that is helical in shape. It represents by far the major component in terms of mass. It is of variable length (typically 5 to 10 μm) but has a constant diameter of about 20 nm throughout its length. An indefinite assembly of around 20,000 subunits of a single protein, flagellin (FliC) builds up the filament. The assembly starts after the distal addition of two others hook-associated proteins, FlgL and FliD (HAP3 and HAP2, respectively) [31] to FlgK [32,33]. FliD is forming the cap that enables flagellin subunits to polymerize at the distal end of the nascent filament. In contrast to the hook cap, the filament cap is retained indefinitely.

1.2.2. The TTSS of the flagellum

a. The export apparatus

Six proteins (FlhA, FlhB, FliO, FliP, FliQ and FliR)[34-37] are central to the flagellar export apparatus, in the sense that they participate in the export of all known substrates. They are integral membrane proteins and are believed to be located in a patch of specialized membranes within a central pore in the basal-body MS ring (Suzuki et al., 1998; [28,34,38]. They range in size from 10 kDa (FliQ) to 75 kDa (FlhA), and vary in the predicted number of membrane spans from one (FliO) to eight (FlhA). Two of them (FlhA and FlhB) have large C-terminal cytosolic domains that interface with the soluble components. The evidences for an association with the MS ring are still weak. FliP and FliR have been found in the basal body but attempts to detect the others have been unsuccessful so far. But, given the physical pathway by which exported subunits reach their destination, the core of the MS ring seems the only logical location for the export apparatus. For FliO, FliP, FliQ, and FliR, all what can be said is that they are essential for flagellar protein export. As for FlhA, it appears to be important for association of the export complex with the MS ring. Indeed, a genetic evidence (extragenic suppression) suggests an interaction between FlhA and FliF, the MS ring protein.

Besides FliF, FlhA seems also interact with the ATPase FliI [38-40] and its partner, FlhB. FlhB plays a central role in the type three secretion systems by being the gatekeeper, determining the export substrate specificity of the machinery [29,41-43].

b. The soluble components

Three proteins, FliH, FliI and FliJ, are thought to interact with the export apparatus. FliH is the regulator of the FliI ATPase [44,45]. FliJ is a general chaperone [46] whereas FlgN, FliT [47,48] and FliS [44] are three specific cytoplasmic chaperones, which associate with the hook filament junction proteins, flagellin, and the filament capping protein, respectively. Whether or not they play a direct role in presenting their substrates to the export apparatus is not clear, but they do prevent substrate degradation. There is also a specific periplasmic chaperone, FlgA [49], for the P-ring protein.

Finally, there are other proteins secreted via the export apparatus, involved in various aspects of the assembly process, such as the muramidase/rodcapping protein FlgJ [50], the hook-capping protein FlgD, the filament-capping protein FliD, and FliK whose role will be discussed below. With the exception of FliD, these proteins are not present in the final flagellar structure.

1.2.3. Hook-length control in the flagellum

In contrast with the filament, which can adopt any sizes, the length of the wild-type hook shows a narrow distribution with a peak at 55.0 +/- 5.9 nm (+/- standard deviation). This deviation of 10% of the mean is larger than the one found for tobacco mosaic virus (2%) or the bacteriophage λ tail (5%). Hook length control implies a proper functioning of the substrate-specificity switch of the export apparatus from the rod/hook-type to the filament type substrates. Indeed the substrate switch terminates the secretion of FlgE and thereby the assembly of the hook. Thus, to study the hook length control mechanism it is necessary to include also the proteins involved in the specificity switch.

a. FliK, a major actor

Contrary to WT, a *fliK* mutant shows a broad distribution of hook lengths ranging from 40 to 900 nm, with a failure to assemble filament (polyhooks phenotype). The phenotype of this *flik* mutant suggest that FliK is involved in hook length control but also in the substrate-specificity switch from rod/hook-type to filament-type substrates [29]. The double failure i.e. the inability to terminate the hook at its proper length and the inability to initiate filament assembly suggest that FliK is a bi-functional protein.

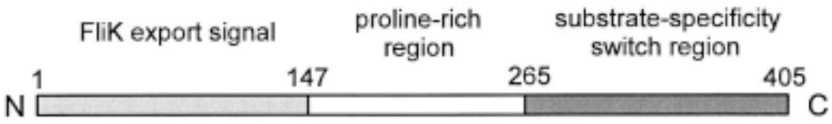

Fig. 7: The primary structure of the hook-length control protein FliK. Its 405 amino acid sequence can be roughly divided into three regions. The C-terminal region is known to be essential for switching the substrate specificity of the export apparatus from hook-type proteins to filament-type proteins. The central region is proline rich, and may perform a hinge-like function between the N and C-terminal domains. The function of the N-terminal region contains the information necessary for FliK export by the type III flagellum-specific apparatus [51].

Among pseudorevertants isolated from such polyhook mutants, *fliK* intragenic suppressors restore filament assembly, but the cells remain defective in hook-length control (polyhook-filament phenotype). These intragenic suppressors mutations are found to restore the C-term of FliK which could thus be playing a role in the substrate-specificity switch [29,41]. In fact, linker insertion mutagenesis of the conserved C-terminal region completely abolished motility (meaning filament assembly), whereas disruption of the less conserved N-terminal and central regions had little or no effect. Therefore it is likely that the C-term region constitute a domain, distinct from the rest of the protein. When comparing FliK from S. *typhimurium* and *E. Coli*, it appears that the C-terminal sequence, rich in glutamine residues is the most conserved part (71% identity in the last 154 amino acids). Conversely, the N-term and the central region, which is proline rich, have low identity especially for homologous flagellar proteins.

While examining the location of FliK during flagellar morphogenesis, it was found that FliK is most efficiently exported prior to the completion of hook assembly [51]. Furthermore, its export is impaired by deletions within the N-term, but not by C-term truncations. Altogether these results indicate that FliK can be roughly divided into 3 regions (Fig. 7) [51]:

- the C-term which is known to be essential for switching the substrate-specificity of the export apparatus,
- the central region which is proline rich and may perform a hinge-like function between the N-term and the C-term domains. It is poorly conserved and of substantially different sizes which seems to argue agains any highly specific function.
- The N-term contains the information necessary for FliK export by the type III flagellum-specific apparatus.

The question of how FliK is measuring the length is still not addressed. The idea that it could function as a ruler has been put aside. The groups of Aizawa and Macnab bring up several arguments against FliK functioning as a ruler. The main argument is that its amino acid sequence makes it unlikely to function as an α-helical molecular ruler. Predictions of secondary structure show no pronounced tendency towards an α-helix, and the central region, with its high proline content, is almost certainly not α-helical. Furthermore, the highly asymmetric composition of the molecule is not a characteristic that one would expect to be associated with a molecular ruler. Two other reasons to doubt that FliK functions as a ruler were mentioned. First, it appears to be needed for terminating elongation rather than enabling it, since its absence results in abnormally long hooks rather than zero-length hooks. Then, deletions in FliK lead to polyhook structures and not shorter hooks as it would be expected for shortened rulers.

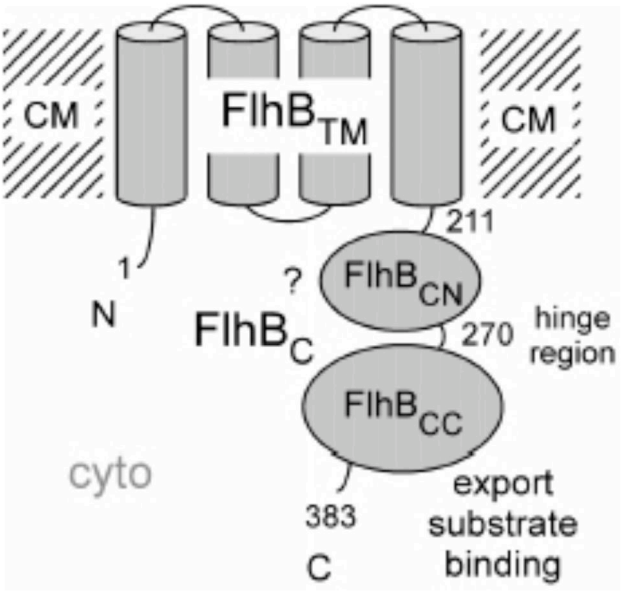

Fig. 8: Cartoon of the FlhB structure, consisting of an N-terminal transmembrane domain, $FlhB_{TM}$, and a C-terminal cytoplasmic domain, $FlhB_C$. The boundary between $FlhB_{TM}$ and the cloned $FlhB_C$ protein is at Phe-211. $FlhB_C$ consists of two subdomains, $FlhB_{CN}$ and $FlhB_{CC}$, linked by a proteolytically sensitive hinge centered at Pro-270. $FlhB_{CC}$ appears to be directly involved in binding export substrates. The role of $FlhB_{CN}$ is less clear (as indicated by the question mark), but since the two subdomains physically interact, its role may be to control the binding specificity state of $FlhB_{CC}$ [43].

Rather than a ruler, it has been hypothesized that FliK could function as a regulatory protein. Indeed, FliK is present in the cell at a low level. Furthermore, variations in the expression of FliK results in modulation of hook lengths [52]. So, underexpression of the wild-type *fliK* gene decreased both the number of flagella and the ability to swarm, but did not abolished either flagellation or motility. At levels of FliK lower than WT, most flagella had polyhooks. With increasing amounts, the morphology progressively changed to polyhook-filament, and eventually to wild-type hook-filaments. When FliK was overproduced, the hook length was slightly shorter (46+/-7 nm) than when FliK was produced at WT level (55+/-9 nm) [52].

Another feature that favors the idea of FliK being a regulatory protein is its glutamine-rich C-term, with one stretch of about 100 residues having a glutamine content of over 20%. Indeed, this unusual high glutamine content is typical from activation domains that exist in a number of eukaryotic transcription factors.

The basic idea behind the regulatory model is that FliK, in some way (wether directly or indirectly), could receive the information indicating that the hook has reached its mature length. At that point it would interact (directly or indirectly) with the export apparatus, in such a fashion that the specificity for the exported substrate is changed. The signal captured by FliK has been proposed be the shift in the kinetics of the hook elongation process [53].

b. FlhB

Not only intragenic suppressors of the polyhook phenotype are observed but also intergenic ones. All these suppressive mutations map to *flhB* and also give rise to polyhook-filaments [29,41]. Thus, FlhB seems to be a partner of FliK in the substrate-specificity switching process. However, genetic analysis of the suppressive mutations has revealed no allele specificity suggesting that there may not be direct interaction between FliK and FlhB at the molecular level.

Introduction of the intergenic suppressor *flhB* mutations into an otherwise wild-type genetic background display an average hook length similar to wt but with more examples of longer hooks (as long as 100nm) [41]. This suggests that FlhB is also somehow involved in hook length control. What is worth mentioning is that FlhB N-term is essential for basal body assembly and therefore, all the mutants considered here have mutations only affecting the C-term cytoplasmic portion of the protein. Another argument in favour of FlhB participating in hook length control is the obtention of long polyhooks in *flhB flgK* double mutants [41]. This is reinforcing the idea that there is also a FliK-independant way of regulating hook length, that was already suspected while observing the peak at WT hook length in *fliK* null mutant.

Full-length wild-type FlhB is subjected to cleavage within its cytoplasmic region. The coproduction of the cleavage products, $FlhB_{\Delta CC}$ and $FlhB_{CC}$ (C-term of the cytoplasmic region

of FlhB), resulted in restoration of both motility and flagellar protein export to an *flhB* mutant host, indicating that the two polypeptides are capable of productive association. The cleavage products of wild-type $FlhB_C$, existing as a $FlhB_{CN}$-$FlhB_{CC}$ complex binds the rod- and hook-type substrates more strongly than the filament-type substrates. Therefore it is proposed that $FlhB_C$ has two substrate specificity states and that a conformational change, mediated by the interaction between $FlhB_{CN}$ and $FlhB_{CC}$, is responsible for the specificity switching process [43]. FliK itself is an export substrate and thus, its binding properties for $FlhB_C$ resemble those of an early substrate (FlgD, for example) and do not provide any evidence for a physical interaction beyond that of the export process [43].

c. FlgE

As the major hook component, FlgE could very well be a hook length determinant. Therefore its role was investigated. When FlgE was overproduced in a wild-type strain, a *fliC* (flagellin) mutant, or a *fliD* (filament capping protein) mutant, the hooks remained at the wild-type length. However in a *fliK* mutant, which produces long hooks (polyhooks), here the overproduction of FlgE resulted in extraordinarily long hooks (superpolyhooks). In a flgK (HAP1, first hook-filament junction protein) mutant or a flgL (HAP3, second hook-filament junction protein) mutant, the overproduction of FlgE also resulted in longer than normal hooks [54]. Thus, at elevated hook protein levels not only FliK but also FlgK and FlgL are necessary for the proper termination of hook elongation. When FlgE was severely underproduced, basal bodies without hooks were often observed . However, those hooks that were seen were of wild-type length, demonstrating that FlgE underproduction decreases the probability of the initiation of hook assembly but not the extent of hook elongation [54].

d. FliG, FliM and FliN

So far only mutants producing elongated hooks have been mentioned. Nevertheless to study a length control mechanism it is important to focus on all the cases in which the length is aberrant; either longer or shorter.

The only strains displaying hooks shorter than wt have a mutation in the *fliG*, *fliM* and *fliN* genes, the switch genes involved in the formation of the C ring. All these mutants have hooks shorter than wt that fall into 2 groups : 25 nm and 45 nm hooks, comprising 99 subunits and 55 of FlgE, respectively. The lengths of these short hooks are discontinuous. Assuming that the subunits accumulate in the C ring with binding sites in the inner wall, one could envision that the C ring would hold the 120 subunits of FlgE that are necessary to a WT hook. If there are initially 4 binding sites and if the number of binding sites decreases to 3 and 2, the total number of hook subunits would be 90 or 60, respectively, which is what is observed. These findings lead to the proposal that the physical capacity of the C ring may determine the

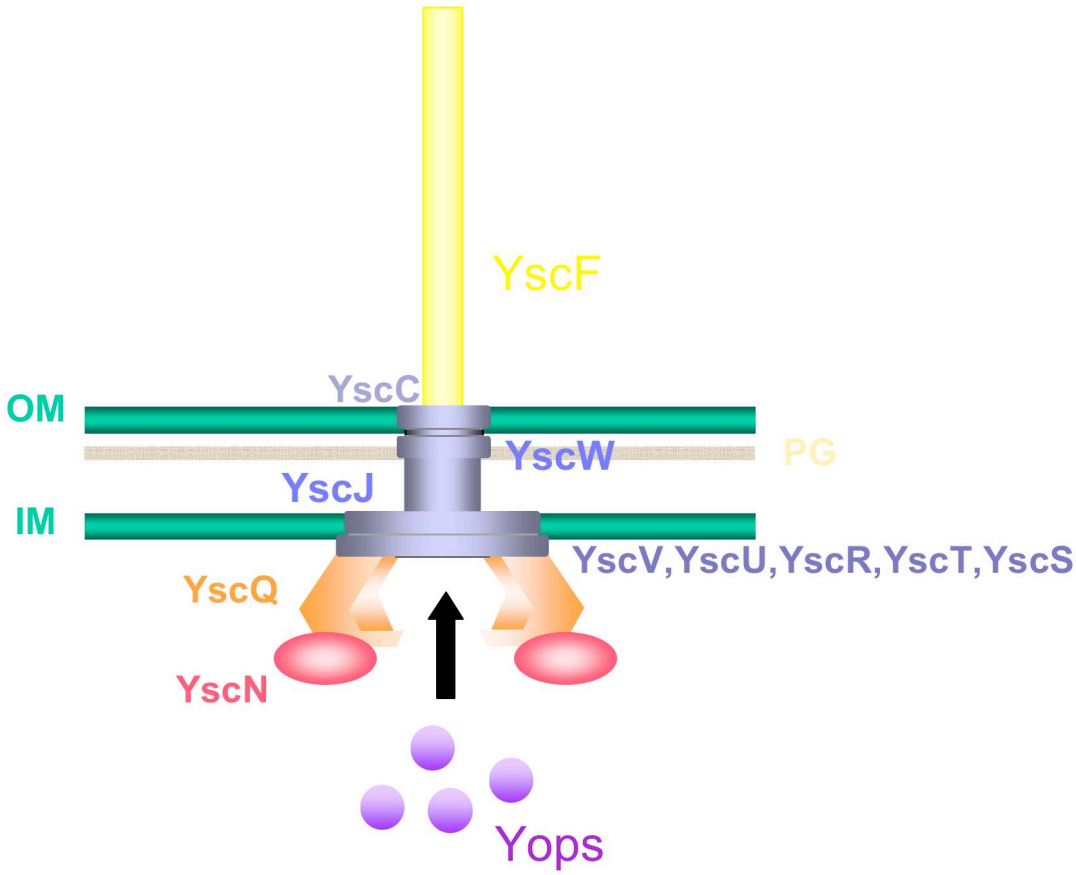

Fig. 9: Hypothetical model of *Yersinia* injectisome

hook length and that it could act as a quantized measuring cup [55]. In this model, FliK is likely to be required in the termination of the hook length by changing the mode of secretion.

e. Conclusion

Several proteins have revealed to be somehow involved in hook length control. Some producing only elongated hooks of any size (polyhooks) and some other only shorter ones of definite size. The understanding of the length control mechanism has improved by identifying the different possible actors and by studying their functioning as single protein. However the course of the hook length control process is still vague and the link between the different actors, among others FliK and the C ring component, still undefined.

Although the cup model is an elegant model, taking some of the observed phenotypes into account, direct proofs that could validate it are missing. Furthermore, this model cannot explain some observations, like for instance, the effect of overproduction of FliK on hook length. It is also important to mention that no adequate experiments have been performed to invalidate the ruler hypothesis. Indeed, a systematic deletion/insertion mutagenesis of FliK has not been done.

1.3. Needle length determination in injectisome (State of the art in 2002)

Although exerting a completely different function, the flagellum share similarities with the injectisome, a machine found in certain classes of pathogenic bacteria. Indeed, although the flagellum and the injectisome are different machines, they have a similar structure and exploit a common secretion pathway: the Type Three Secretion (TTS) pathway. Thus, the TTSS fall in two groups:

- the virulence associated TTSS found in animal (*Shigella*, *Salmonella*, *Yersinia*) or plant (*Erwinia*, Pseudomonas *syringae*...) pathogens
- the flagellar related TTSS

The TTSS can be defined by the features common to the two different groups, which can be summarized as follows:

- the proteins to be exported do not have the Sec-dependent signal sequences. They do not undergo any cleavage while secreted. Furthermore, the regions involved in targeting do not show any primary sequence conservation.
- The export apparatus, consisting of many protein components, spans both the inner and outer membranes. Therefore, there is no periplasmic secretion intermediate.

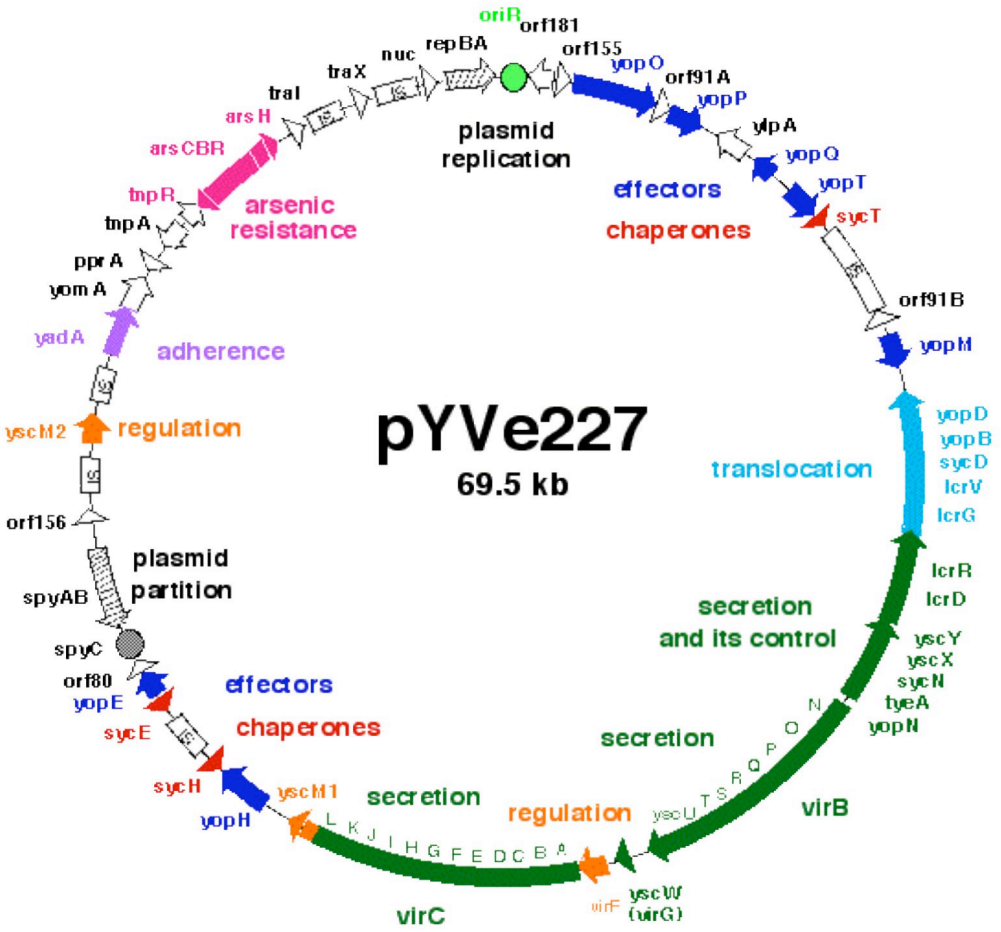

Fig. 10 : Genetic organization of the pYV plasmid of *Y. enterocolitica*

- Energy is required for protein secretion.
- Dedicated chaperones are present for some secreted proteins

Besides these common features, both systems share morphological similarities, especially considering their core structure, and have sequence homologues (Table 2 and Fig. 10)[56]. About half of the virulence-associated TTSS proteins are similar in sequence or membrane topology to cytoplasmic or inner membrane proteins of the flagellar basal body. Some others have no significant sequence homology but they show “functional conservation”. Indeed, when they are knocked out, they lead to similar phenotypes. Both injectisome and flagellum assembly pathways also share organizing principles.

It is the obvious difference in the function (motility vs host cell infection) that is responsible for the main differences between the two systems, that is to say the host contact-mediated TTSS induction and the ability to translocate proteins into eukaryotic cells.

1.3.1. Structure of the injectisomes (Fig. 9)

The injectisomes consist of a basal body that spans both the inner and outer membrane and a needle-like structure protruding at the surface of the bacteria (For a review, see [57]). This TTS apparatus enables secreted effector proteins, called Yops in *Yersinia*, to be delivered directly into the eukaryotic cell cytosol where they can exert their function. The delivery of these Yops across the two bacterial membranes requires over 35 genes of the 70 kb pYV plasmid (Fig. 10). These genes encode the Syc cytosolic chaperones [58-60], the 27 Ysc proteins, most of which constitute the machinery, and the translocators proteins [61-64]. The genes encoding the Ysc proteins are clustered in three large neighbouring operons called *virA*, *virB* and *virC*. Among the Ysc proteins, two groups can be distinguished: the Ysc proteins composing the basal body and the ones that are released in the extracellular media.

The former group contain some proteins having highly homologous counterparts in the flagellum basal body, notably YscN, YscR, YscS, YscT, YscU (table 2). Some of the Ysc proteins involved in the machinery have been well characterized. For example, there is the YscC secretin which has been shown to form a ring-shaped structure in the bacterial outer membrane, with an apparent central pore of about 50Å [65]. YscN is the ATPase of the system and energizes the secretion process [66].

The latter group is composed of proteins less understood, many of which have unknown functions. Indeed, apart from the 9 Kda YscF protein, which is the major component of the needle part of the system, the functions of the others, YscP [67,68], YscO [69], YscX [70], YscI remains to be elucidated.

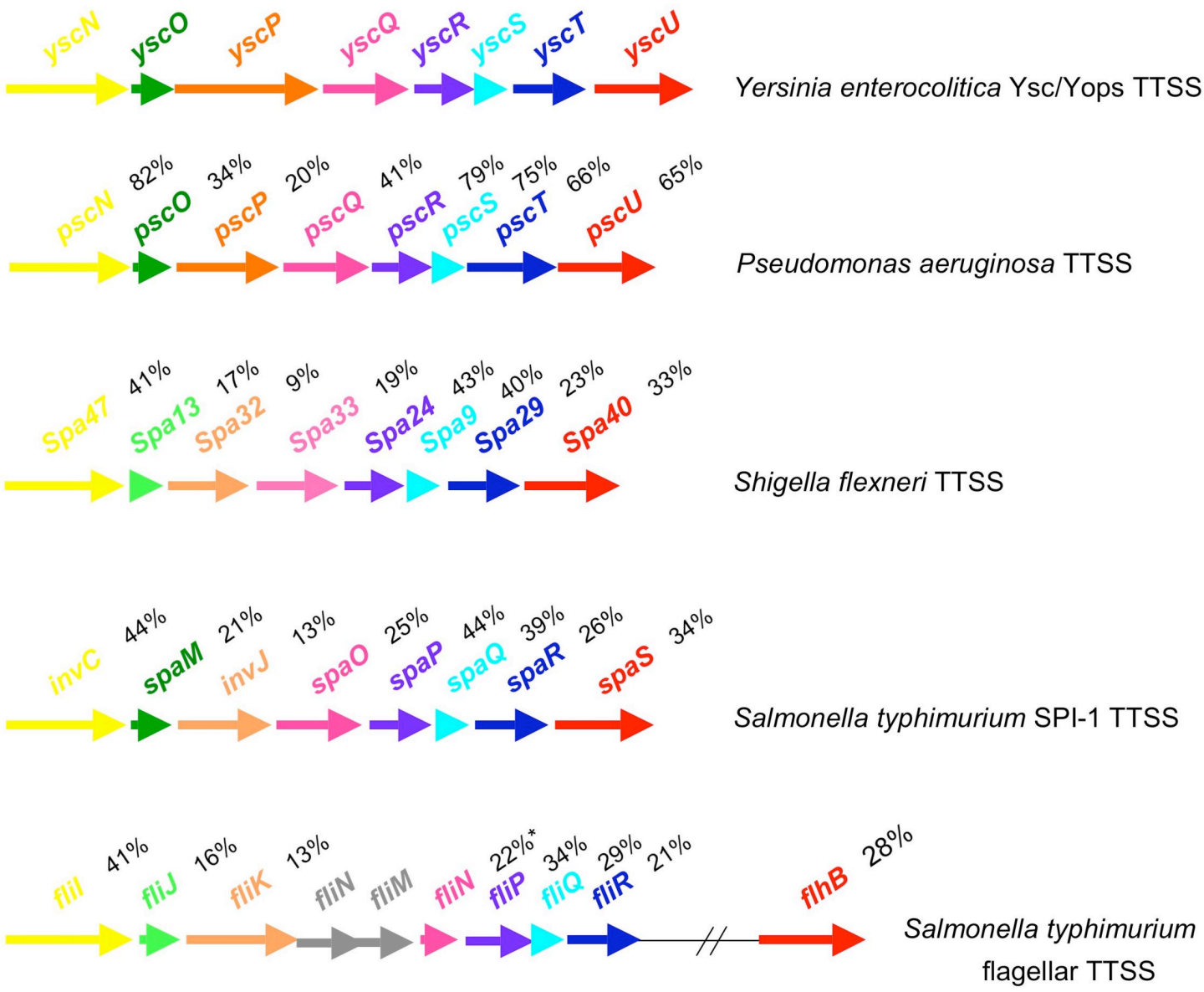

Fig. 11: **The *Yersinia* virB operon and its counterpart in *Pseudomonas*, *Salmonella*, *Shigella* TTSS virulence-associated and in *Salmonella* flagella-related TTSS**.
The genes that are considered similar (either on structural level or functional level) are represented with the same color. Following the gene name, the % of identity of the considered gene product with the equivalent *Yersinia* protein is indicated. The size of the arrow representing the genes reflects the size of the gene. (*) The % of identity given is between FliN and the C-term of YscQ.

Whereas the basal body is well conserved among the virulence-associated TTSS, the needle length is varying according to the species: 45 nm in *Shigella* [71] and 80 nm in *Salmonella* [72,73], for example. In a given bacterium, however, the needle length is well defined and tightly regulated. The understanding of the needle length determination mechanism has improved by following the initial step forward achieved in the study of the hook length control.

1.3.2. Needle length controlling proteins

a. Spa32 and InvJ

Similarly to the polyhooks phenotype observed in *flik* mutants, needles of deregulated length were found in *invJ* and *spa32* mutants in *Shigella* and *Salmonella*, respectively. Although these proteins do not show any significant homology, the phenotype observed suggest that their functioning is similar. Both Spa32 and InvJ could be functional counterparts of FliK in injectisomes and thus, needle length-controlling proteins.

b. YscP, a putative length controlling protein

In *Yersinia*, there is a gene synthenic to *spa32* and *invJ* but its product shows no significant sequence identity with Spa32, InvJ and FliK. This gene is found in the virB *yscN-yscU* operon. Most of the proteins encoded by this operon share sequence homology to their counterparts in *Salmonella typhimurium*, *Shigella flexneri* or in the *S.t.* flagellum (Fig.11), whereas YscP (515aa) and its neighbour YscO have little similarity to their counterparts. However, on the functional level, YscP behaves as FliK or Spa32. Indeed, it is necessary for Yops secretion [68] as Spa32 is necessary for the secretion of the Ipa proteins [74] and FliK for the secretion of the filament-type substrates [75]. YscP is an original protein with a high proline content. Another interesting feature concerning this protein is that large deletions within it do not affect its functions.

1.3.3. YscU and the substrate-specificity switch

Another protein of the same operon that would deserve further investigations is YscU, an inner membrane protein with a large cytoplasmic region [76]. YscU is homologous to FlhB which is involved in the substrate-specificity switch of the flagellar export apparatus and thereby in the termination of the hook assembly at the proper length [29,41,43].

2- AIM OF THE THESIS

2- Aim of the thesis

The aim of my thesis was to characterize the role of the YscP protein in the determination of the needle length as well as in Yops secretion. Indeed, as suggested by the observed phenotype [58], YscP appeared to be a key protein of the TTSS and therefore, its study was not only a regular structure/function analysis but could also turn to provide insights into the assembly and the functioning of the injectisome.

Judging from the complexity of the system it was likely that YscP shared closed connections to other proteins. As studies in the flagellum [28,40,42] had pointed out a partnership between FlhB and FliK that could be at the core of the functioning of the apparatus, it was also decided to start an investigation on YscU (FlhB homologue) in parallel.

3- RESULTS

3.1- The needle length of bacterial injectisomes is determined by a molecular ruler

Journet, L., Agrain, C., Broz, P., and Cornelis, G.R.

Science 302: 1757-60

(2003)

Summary

The *Yersinia* injectisome needle has a remarkably constant length of around 60 nm suggesting that it is genetically controlled. Mutants affected in the *yscP* gene display abnormally long needles, indicating that the needle length is indeed controlled and that YscP is involved in this process, as it is the case for its counterparts in other TTSS.

To determine how YscP is exerting its length control function, we engineered a set of deletions and insertions in the protein. Deletions affecting either the extreme N- or C-term lead to needles of deregulated lengths suggesting that they are required for the control of the length of the needles. In contrast, the central part can be shortened or lengthened without loss of function. Moreover, deletions or insertions in this central part give rise to shorter or longer needles, respectively and a strict linear relationship between the number of residues of YscP and the needle length can be observed. Altogether these results demonstrate that YscP is acting as a molecular ruler to determine needle length.

Statement of my work

I contributed to this paper by constructing the pCA plasmids encoding various deletions in YscP, as well as pCA23, the plasmid in which permissive restriction sites have been engineered in YscP. I also contributed to their analysis.

lines was 1.23 and 1.26 mm, whereas it was 1.23 mm for the $ds2^M$ line (Wilcoxon rank-sum test $P > 0.1$ for all comparisons, sample sizes $N = 18$). If anything, one of the $ds2^Z$ lines shows an effect in the wrong direction.

Lack of sex specificity of the influence of *ds2* on both starvation and cold tolerance suggests that this effect is not due to differences in cuticular hydrocarbons per se. Perhaps it is due to an influence of *ds2* on phospholipid composition, as in many other organisms (*22*). Whatever the exact mechanism of *ds2* action, our results strongly suggest that it is involved in stress resistance. Note, however, that the $ds2^M$ allele appears to be the derived one (*6*). Consequently, we have restored the ancestral state at the *ds2* locus of the Cosmopolitan line, whereas the actual adaptation involved the loss of the $ds2^Z$ allele from the African population.

The possibility that ecologically driven adaptation at the *ds2* locus results in sexual isolation as a pleiotropic by-product is certainly intriguing. The role *ds2* may play in Z-M sexual isolation is being debated. The genetic basis of Z behavior is complex (*12*, *39*). Thus, *ds2* cannot be the only gene involved and, because the Caribbean flies carry the African $ds2^Z$ allele but exhibit M-type behavior, the locus has initially been excluded as a candidate sexual isolation gene (*4*). However, this lack of association across genetic backgrounds is inconclusive. A comparison within populations, in which the genetic background is randomized, is more informative. Indeed, when three African populations polymorphic for both Z behavior and *ds2* were tested, a positive correlation between the presence of $ds2^Z$ and the strength of female Z behavior was found in all of them (*11*). Thus, loss of $ds2^Z$ from the average African background may reduce Z-M sexual isolation.

Although the role of *ds2* in premating isolation remains to be firmly established, we have identified a potential ecological basis for the maintenance of pheromone polymorphism as a result of strong geographical differentiation at the *ds2* locus. Our ability to detect the role of *ds2* in differential adaptation depended crucially on manipulating the gene at its locus while leaving the rest of the genome intact. The phenotypic differences associated with *ds2* allele replacement are small enough to be drowned out by the noise introduced by the genetic background in conventional genetic analyses. Precise allele substitution thus promises to lead to insights into the molecular and evolutionary mechanism of adaptation and speciation.

References and Notes

1. D. Schluter, *The Ecology of Adaptive Radiation* (Oxford Univ. Press, 2000).
2. C.-I Wu, *J. Evol. Biol.* **14**, 851 (2001).
3. D. Presgraves, L. Balagopalan, S. Abmayr, H. Orr, *Nature* **423**, 715 (2003).
4. J. A. Coyne, C. Wicker-Thomas, J. M. Jallon, *Genet. Res.* **73**, 189 (1999).
5. R. Dallerac *et al.*, *Proc. Natl. Acad. Sci. U.S.A.* **97**, 9449 (2000).
6. A. Takahashi, S. C. Tsaur, J. A. Coyne, C.-I Wu, *Proc. Natl. Acad. Sci. U.S.A.* **98**, 3920 (2001).
7. J. M. Jallon, *Behav. Genet.* **14**, 441 (1984).
8. J. Tillman, S. Seybold, R. Jurenka, G. Blomquist, *Insect Biochem. Mol. Biol.* **29**, 481 (1999).
9. J. A. Coyne, A. P. Crittenden, K. Mah, *Science* **265**, 1461 (1994).
10. J. Coyne, *Genetics* **143**, 353 (1996).
11. S. Fang, A. Takahashi, C.-I Wu, *Genetics* **162**, 781 (2002).
12. H. Hollocher, C. T. Ting, M. L. Wu, C.-I Wu, *Genetics* **147**, 1191 (1997).
13. H. Hollocher, C. T. Ting, F. Pollack, C.-I Wu, *Evolution* **51**, 1175 (1997).
14. C.-I Wu *et al.*, *Proc. Natl. Acad. Sci. U.S.A.* **92**, 2519 (1995).
15. C. C. Laurie-Ahlberg, L. F. Stam, *Genetics* **115**, 129 (1987).
16. D. J. Hawthorne, S. Via, *Nature* **412**, 904 (2001).
17. M. Doi, M. Matsuda, M. Tomaru, H. Matsubayashi, Y. Oguma, *Proc. Natl. Acad. Sci. U.S.A.* **98**, 6714 (2001).
18. Y. S. Rong, K. G. Golic, *Genetics* **157**, 1307 (2001).
19. Y. Rong *et al.*, *Genes Dev.* **16**, 1568 (2002).
20. A detailed description of allele substitution line construction can be found in the "Gene Targeting" section of Materials and Methods on *Science* Online.
21. J. Hazel, E. Williams, *Prog. Lipid. Res.* **29**, 167 (1990).
22. A. R. Cossins, Ed., *Temperature Adaptation of Biological Membranes* (Portland Press, London, 1994).
23. T. Ohtsu, M. Kimura, C. Katagiri, *Eur. J. Biochem.* **252**, 608 (1998).
24. P. Tiku, A. Gracey, A. Macartney, R. Beynon, A. Cossins, *Science* **271**, 815 (1996).
25. M. T. Kimura, *Evolution* **42**, 1288 (1988).
26. P. Gibert, B. Moreteau, G. Petavy, D. Karan, J. David, *Evolution* **55**, 1063 (2001).
27. P. Gibert, R. Huey, *Physiol. Biochem. Zool.* **74**, 429 (2001).
28. A. A. Hoffmann, A. Anderson, R. Hallas, *Ecol. Lett.* **5**, 614 (2002).
29. A. A. Hoffmann, J. G. Sørensen, V. Loeschcke, *J. Therm. Biol.* **28**, 175 (2003).
30. D. Knipple, C. Rosenfield, R. Nielsen, K. You, S. Jeong, *Genetics* **162**, 1737 (2002).
31. J. David, P. Capy, *Trends Genet.* **4**, 106 (1988).
32. A detailed description of fly rearing and stress tolerance experimental conditions can be found in the "Fly Rearing and Stress Tolerance Assays" section of Materials and Methods on *Science* Online.
33. D. Karan, J. David, *J. Therm. Biol.* **25**, 345 (2000).
34. R. Parkash, A. K. Munjal, *Evol. Ecol. Res.* **2**, 685 (2000).
35. A. A. Hoffmann, R. Hallas, C. Sinclair, P. Mitrovski, *Evolution* **55**, 1621 (2001).
36. K. Lockey, *Comp. Biochem. Physiol. B-Biochem. Mol. Biol.* **89**, 595 (1988).
37. L. Partridge, B. Barrie, K. Fowler, V. French, *Evolution* **48**, 1269 (1994).
38. J. Coyne, *Evolution* **37**, 1101 (1983).
39. C. T. Ting, A. Takahashi, C.-I. Wu, *Proc. Natl. Acad. Sci. U.S.A.* **98**, 6709 (2001).
40. Statistical tests were performed with the R package, version 1.6.1. To assess significance levels, survival curves were treated as cumulative distributions and compared with the two-sample Kolmogorov-Smirnov test.

41. Funding for this work was provided by NIH grants for C.-IW. and J.A.C. and an NIH Ruth L. Kirschstein National Research Service Award fellowship to A.J.G. We thank K. Golic and Y. Rong for advice and materials, S. Fang and A. Takahashi for information on *desaturase2* sequence and primers, J. Huie and J. Fay for comments on the manuscript, J. Shapiro for help with the production and injection of some of the constructs, and M.-L. Wu, V. I, and E. Chang for help with fly work.

Supporting Online Material

www.sciencemag.org/cgi/content/full/302/5651/1754/DC1

Materials and Methods

14 August 2003; accepted 16 October 2003

The Needle Length of Bacterial Injectisomes Is Determined by a Molecular Ruler

Laure Journet, Céline Agrain, Petr Broz, Guy R. Cornelis*

Size determination represents a fundamental requirement for multicomponent biological structures. Some pathogenic bacteria possess a weapon derived from the flagellum. Like the flagellum, this type-III secretion apparatus, called the injectisome, has a transmembrane basal body, but the external component is a needle-like structure instead of a hook and a filament. Here, we provide evidence that the length of this needle is determined by the size of a protein, YscP, acting as a molecular ruler.

Yersinia pestis and *Y. enterocolitica*, the infectious agents of bubonic plague and gastroenteritis, respectively, share a common plasmid-encoded type-III secretion system consisting of the Ysc (Yop secretion) injectisome and the Yops (*Yersinia* outer proteins) that are secreted by this apparatus (*1*). The injectisome, made of 27 Ysc proteins, is thought to resemble those of *Salmonella enterica* and *Shigella flexneri*. These injectisomes, or "needle complexes," appear as two pairs of rings that are anchored to the inner and outer membranes of the bacterial envelope, joined by a central rod and supporting a hollow needle about 10 nm thick and 60 nm long (*2–4*). It is thought that the injectisome serves as a hollow conduit through which the secreted proteins travel across the two bacterial membranes and the peptidoglycan in one step.

Several Ysc proteins that are anchored in the inner membrane and form the core of the secretion apparatus are similar to proteins from the basal body of the flagellum, suggesting a common evolutionary origin (*5*). Not surprisingly, the *Salmonella* and *Shigella* injectisomes resemble the flagellar basal body (*6*) except that they are topped by a

Biozentrum, Universität Basel, 4056 Basel, Switzerland.

*To whom correspondence should be addressed: E-mail: guy.cornelis@unibas.ch

needle instead of a hook and a flexible filament. The length of the flagellar hook (55 nm) is genetically controlled. Mutations in the gene *fliK* give rise to hooks of indefinite length (*7*), but it is unclear how FliK exerts its control. The fact that all truncated FliK proteins engineered so far lead to longer hooks rather than shorter hooks is presented as an argument that FliK cannot act as a simple molecular ruler (*8*). In addition, certain mutations in genes that encode the cytoplasmic ring lead to shorter hooks (*8*), supporting an elegant model in which this structure controls the hook length by acting as "a quantized measuring cup," storing the subunits before their export (*8*). In this model, the role of FliK would be to terminate hook elongation by changing the secretion mode from hook-monomer to flagellin-monomer secretion (*8*). As for the injectisome of *Salmonella* and *Shigella*, mutants affected in a gene called *invJ* or *spa32*, respectively, display needles of various lengths, ranging from normal (60 nm) to as long as 1 μm (*2*, *9*, *10*). Thus, InvJ and Spa32 behave as FliK homologs, although they do not share any substantial sequence homology with FliK.

Here, we address the question of what controls the injectisome needle length in *Yersinia*. We first examined by electron microscopy *Y. enterocolitica* E40 bacteria incubated under conditions that artificially induce secretion of the Yops (*11*). We observed many needle-like structures that were about 6 to 7 nm thick and 60 nm long (*12*). Many of these needles were detached from the bacterial body (Fig. 1). We purified these detached needles and confirmed that they were made of the 6-kD YscF protein (*12*). Because it is difficult to define the exact insertion point of needles on bacteria, we measured only the detached needles. The length was distributed with an average of 58 ± 10 nm (Fig. 1), suggesting that the needles either detached or broke at a precise point close to the bacterial surface. Next, we examined *Y. enterocolitica* with a large deletion (codons 97 to 465 out of 515) in *yscP* ($yscP_{\Delta 97-465}$) (*13*). This gene is synthenic to *spa32* and *invJ*, but its product has no substantial sequence identity with Spa32, InvJ, or FliK. The $yscP_{\Delta 97-465}$ mutant bacteria produced needle-like structures with an indefinite length ranging from 45 nm up to 1570 nm (Fig. 1). When the $yscP_{\Delta 97-465}$ mutation was complemented with the $yscP^{+}$ allele, control of the length was restored (55 ± 8 nm), indicating that YscP played an essential role in length control.

YscP from *Y. enterocolitica* E40 ($YscP_{entero}$) carries a duplication of 60 central residues (*13*) (Fig. 2). YscP from *Y. pestis* KIM5 ($YscP_{pestisKIM5}$) is 90% identical in sequence to $YscP_{entero}$, but it is shorter (455 residues) because of the lack of such repetition (*14*). To explore whether the two proteins lead to needles of the same length, we complemented the *Y. enterocolitica* $yscP_{\Delta 97-465}$ mutation with the $yscP_{pestisKIM5}{}^{+}$ gene (*15*). The shorter *Y. pestis* gene restored length control but programmed shorter needles (41 ± 8 nm) (Fig. 2).

To investigate whether the needle length reduction was a result of the shortening of YscP and not subtle residue changes, we complemented the $yscP_{\Delta 97-465}$ mutation with

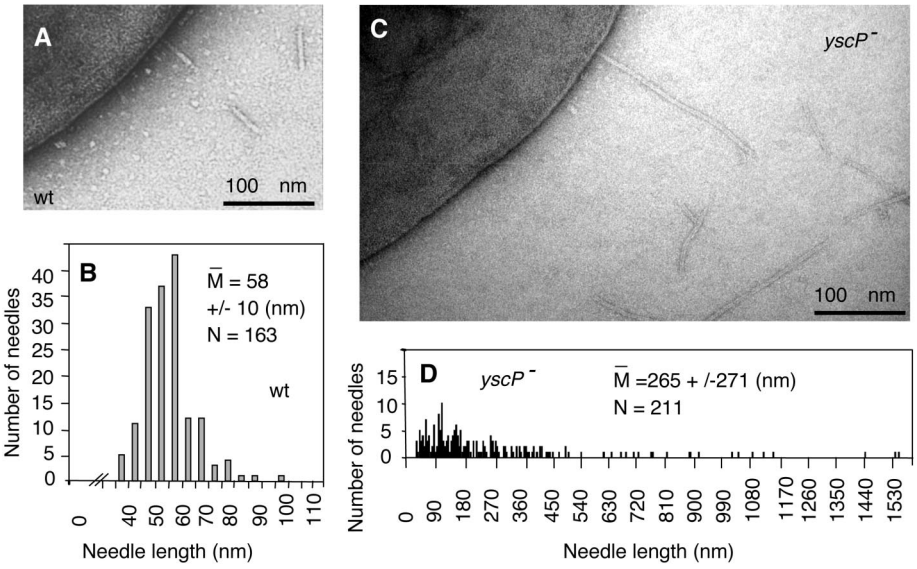

Fig. 1. YscP is required for needle-length control. Electron micrographs of *Y. enterocolitica* wild type (wt) (**A**) and $yscP_{\Delta 97-465}$ mutant (**C**) showing the needles of the injectisomes. Detached needles were measured at the vicinity of at least 10 to 15 different bacteria. Histograms of lengths are given in (**B**) (for wild type) and (**D**) (for $yscP_{\Delta 97-465}$ mutant). Note the altered distribution of lengths in the mutant. $\overline{M}$, mean of the lengths; *N*, number of needles measured.

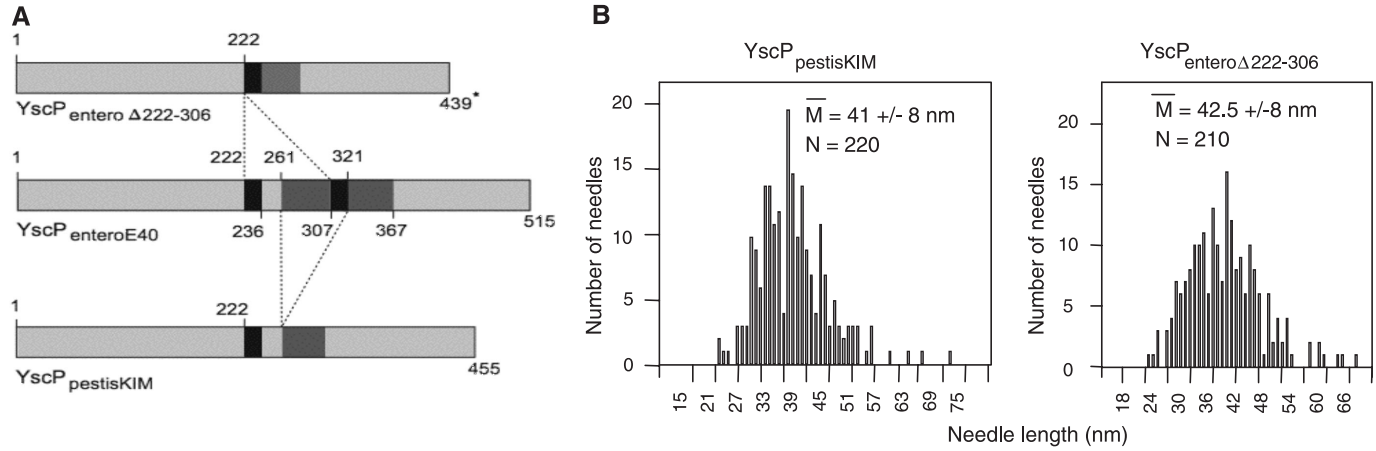

Fig. 2. YscP is shorter in *Y. pestis* than in *Y. enterocolitica* and determines shorter needles. (**A**) Residues 222 to 236 and 261 to 306 from YscP are duplicated in *Y. enterocolitica* E40 and W22703 but not in *Y. pestis* KIM. The *yscP* gene from *Y. pestis* KIM and the *yscP* gene from *Y. enterocolitica* deprived of these repeats were cloned downstream from an arabinose-inducible promoter and expressed in the *Y. enterocolitica* $yscP_{\Delta 97-465}$ mutant. The figure marked with an asterisk includes a few amino acids inserted to generate the deletion. (**B**) Histograms of the needle lengths from recombinant *Y. enterocolitica* bacteria.

A

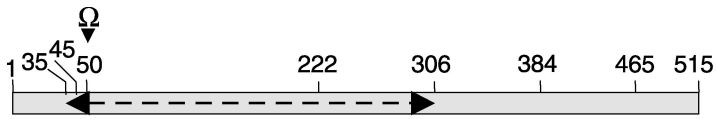

B

Construct	N.aa*	Control	Needle length (nm)	Nr of particles measured	Lane
YscP $_{46\text{-}96+\ 222\text{-}306}$	388	+	30 +/- 7	168	1
YscP $_{222\text{-}306}$	439	+	43 +/- 8	210	2
YscP $_{46\text{-}96}$	464	+	45 +/- 7	205	3
YscP $_{36\text{-}45}$	505	+	53 +/- 8	216	4
YscP $_{wt}$	515	+	55 +/- 7	198	5
YscP $_{\Omega\ YscP307\text{-}381}$	595	+	72 +/- 10	212	6
YscP $_{\Omega\ FliK147\text{-}266}$	640	+	75 +/- 14	223	7
YscP $_{\Omega\ YscP222\text{-}381}$	680	+	88 +/- 12	209	8
YscP $_{16\text{-}25}$	505	-	108 +/- 93	205	9
YscP $_{26\text{-}35}$	505	-	158 +/- 119	203	10
YscP $_{385\text{-}424}$	475	-	343 +/- 278	209	11
YscP $_{467\text{-}515}$	479	-	544 +/- 361	203	12

* including the aa inserted to create the Ω restriction site and some deletions

C

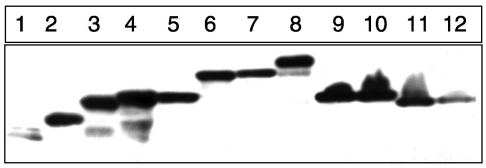

D

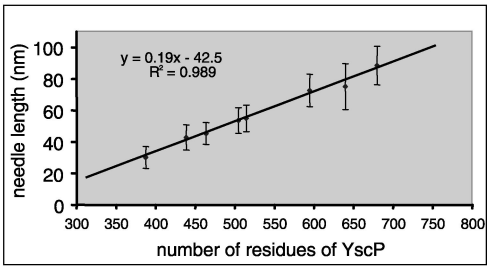

Fig. 3. The needle length is proportional to the number of residues in YscP. (**A**) Various deletions and insertions were introduced in *yscP*$_{enteroE40}$, cloned downstream from the arabinose promoter. Insertions occurred in a restriction site inserted after residue 49 (Ω). The dotted arrow spans the region where deletions and insertions modify the needle length. (**B**) Needle length measurements. N. aa, number of amino acids; Nr, number. (**C**) Expression of the various constructs in *Y. enterocolitica yscP*$_{\Delta 97-465}$, monitored by Western blotting. (**D**) Plot of the lengths versus the number of residues in YscP.

the allele *yscP*$_{entero\Delta 222-306}$$^{+}$ encoding YscP$_{entero}$ without its repeat. The truncated YscP$_{entero\Delta 222-306}$ programmed short needles (42.5 ± 8 nm) (Fig. 2), suggesting that the needle length indeed correlated with the size of YscP. To further investigate this hypothesis, we engineered a set of deletions within the cloned *yscP*$_{entero}$ gene and used them to complement the *yscP*$_{\Delta 97-465}$ mutation (Fig. 3). Proteins truncated within the first 35 or the last 130 residues were unable to control the length, even though their expression levels were comparable to that of the wild type (Fig. 3). In contrast, YscP with deletions up to 126 amino acids between residues 36 and 306 retained length control but programmed shorter needles. Moreover, the length of the needles was proportional to the size of the YscP protein (Fig. 3). We then inserted a second copy of residues 307 to 381 or 222 to 381 after residue 49, thus generating YscP proteins containing the same 60-residue sequence three or four times (Fig. 3). These mutants programmed longer needles with lengths of 72 ± 10 nm and 88 ± 12 nm, respectively. Insertion of residues 147 to 265 from FliK at the same position also resulted in a functional protein but longer needles (75 ± 14.5 nm). Thus, a strict linear relationship existed between needle length and the number of amino acids in YscP, with 1.9 Å per YscP residue (Fig. 3). To rule out bias as a result of an inadequate gene dosage or gene expression of the complementation plasmids, we replaced the wild-type *yscP* allele on the virulence plasmid by two truncated alleles (*yscP*$_{\Delta 46-96}$ and *yscP*$_{\Delta 222-306}$). In this native genetic environment, the two alleles again programmed shorter needles than those of the wild type (47.5 ± 10 nm and 44 ± 8.5 nm, respectively). Thus, YscP appeared to serve as a ruler determining the length of the needle. This is unprecedented in bacteria but it evokes the molecular rulers controlling the length of bacteriophage tails (*16*–*18*), which are structures resembling the needle in morphology, size, and even function. A difference between the two systems is that tails do not assemble in the absence of the ruler whereas needles are of undetermined length in the absence of YscP. The length per residue is also slightly different for tail rulers (1.5 Å per ruler residue).

If YscP acts as a ruler measuring the growing needle, one might expect it to be associated

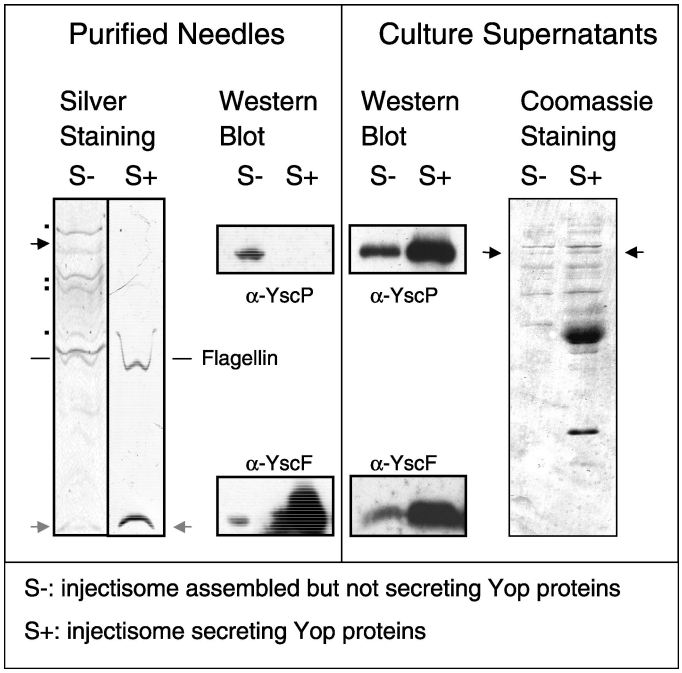

Fig. 4. Association of YscP with the needles. *Y. enterocolitica* E40 deprived of the effectors (ΔHOPEMT) was grown in conditions that are (S+) or are not (S–) permissive for Yop secretion (*11*). Detached needles purified from 2 × 10^{9} (S+) or 10^{10} (S–) bacteria were analyzed by silver stained SDS–polyacrylamide gel electrophoresis (SDS-PAGE) and Western blotting (WB) (**left**). Needle samples prepared from S+ bacteria contain YscF (bottom arrows) and flagellin (middle) as a contaminant but no YscP (top). In contrast, needle samples prepared from S– bacteria contain YscF, YscP (top arrow), flagellin, and unidentified contaminants (dots). Proteins from the supernatant from 10^{8} bacteria from the same cultures were analyzed by Coomassie-stained SDS-PAGE and WB (**right**). YscP is visible as a faint band in both the S+ and the S– supernatants (arrows). The darkest band stained in the S+ supernatant is YopB+D. YscF is not visible by Coomassie staining. The prominent bands in the supernatant of S– are cellular contaminants.

with the needle, at least during the needle elongation stage. To test this, we purified needles from *Y. enterocolitica* incubated in conditions that are either nonpermissive or permissive for secretion (*11*). Under nonpermissive conditions, some YscP was found in the needle fraction as well as in the culture supernatant, whereas under secretion-permissive conditions YscP was found only in the culture supernatant and not in the needle fraction any more (Fig. 4). These data, fitting with previous reports on the localization of YscP (*13*, *14*), show that YscP is associated with newly synthesized needles that are not secreting Yops but not with needles that are secreting Yops.

We propose that YscP controls the length of the needle by acting as a molecular ruler during the stepwise assembly of the injectisome. Because deletions affecting both N- and C-termini of YscP lead to a loss of length control, we hypothesize that the two ends of YscP act as anchors. One end would be attached to the basal body, whereas the other would be connected to the growing tip of the needle. Whatever the anchor mechanism may be, when the needle reaches its mature length, YscP would be fully stretched and signal, via its internal anchor, to the secretion apparatus, which would stop exporting YscF and switch to other substrates. This model (fig. S1) does not contradict the switch function of YscP (*8*, *19*, *20*) but rather includes it in a more complex dual function, which may also exist in some phage tail rulers (*21*). Taking into account the length of 1.9 Å per residue, the ruler domain of YscP would consist of about 300 to 350 residues, leaving more than 150 residues for anchoring and signaling. The fact that YscP is secreted also fits the model, because an internal ruler would be expected to obstruct the 2- to 3-nm-wide secretion channel (*22*). This evokes again the phage tail rulers, which are thought to exit the tail before the tail exerts its function (*21*, *23*). Given the similarity between all the type-III secretion systems (*5*) and the fact that Spa32 (*9*, *10*) InvJ (*24*), and FliK (*25*) are also secreted proteins, it is likely that the mechanism demonstrated here for YscP may apply to the control of the needle length in the other bacteria as well as the length of the flagellar hook. The proposed organization of FliK in three regions—export, hinge$_{(147–265)}$, and switch (*25*)—is also compatible with this view. Finally, the fact that YscP, InvJ, Spa32, and FliK diverged more during evolution than other proteins from type-III secretion suggests that rulers are subjected to fewer constraints. They nevertheless have to share intrinsic properties still to be discovered.

References and Notes

1. G. R. Cornelis, *Nature Rev. Mol. Cell Biol.* **3**, 742 (2002).
2. T. Kubori, A. Sukhan, S. I. Aizawa, J. E. Galan, *Proc. Natl. Acad. Sci. U.S.A.* **97**, 10225 (2000).
3. T. G. Kimbrough, S. I. Miller, *Proc. Natl. Acad. Sci. U.S.A.* **97**, 11008 (2000).
4. A. Blocker *et al.*, *Mol. Microbiol.* **39**, 652 (2001).
5. S. I. Aizawa, *FEMS Microbiol. Lett.* **202**, 157 (2001).
6. R. M. Macnab, *Annu. Rev. Microbiol.* **57**, 77 (2003).
7. T. Hirano, S. Yamaguchi, K. Oosawa, S. Aizawa, *J. Bacteriol.* **176**, 5439 (1994).
8. S. Makishima, K. Komoriya, S. Yamaguchi, S. I. Aizawa, *Science* **291**, 2411 (2001).
9. K. Tamano, E. Katayama, T. Toyotome, C. Sasakawa, *J. Bacteriol.* **184**, 1244 (2002).
10. J. Magdalena *et al.*, *J. Bacteriol.* **184**, 3433 (2002).
11. *Yersinia* builds injectisomes when temperature reaches 37°C, the host temperature. However, Yop secretion is only triggered upon contact with a target cell or artificially by chelating Ca^{2+} ions. The usual procedure consists of growing bacteria at 28°C in oxalated rich medium and then switching the culture to 37°C. In these secretion-permissive conditions, the production of injectisomes is also stimulated. When bacteria are grown at 37°C in the presence of 5 mM Ca^{2+}, they make injectisomes but they do not secrete Yops (nonpermissive conditions). Materials and methods are available as supporting material on *Science* Online.
12. E. Hoiczyk, G. Blobel, *Proc. Natl. Acad. Sci. U.S.A.* **98**, 4669 (2001).
13. I. Stainier *et al.*, *Mol. Microbiol.* **37**, 1005 (2000).
14. P. L. Payne, S. C. Straley, *J. Bacteriol.* **181**, 2852 (1999).
15. For complementation, *yscP* DNA was amplified by polymerase chain reaction and cloned in the pBAD expression vector. Expression was induced with arabinose.
16. I. Katsura, *Nature* **327**, 73 (1987).
17. I. Katsura, R. W. Hendrix, *Cell* **39**, 691 (1984).
18. N. K. Abuladze, M. Gingery, J. Tsai, F. A. Eiserling, *Virology* **199**, 301 (1994).
19. T. Minamino, R. M. Macnab, *J. Bacteriol.* **182**, 4906 (2000).
20. P. J. Edqvist *et al.*, *J. Bacteriol.* **185**, 2259 (2003).
21. M. L. Pedulla *et al.*, *Cell* **113**, 171 (2003).
22. F. S. Cordes *et al.*, *J. Biol. Chem.* **278**, 17103 (2003).
23. R. L. Duda, M. Gingery, F. A. Eiserling, *Virology* **151**, 296 (1986).
24. C. M. Collazo, M. K. Zierler, J. E. Galan, *Mol. Microbiol.* **15**, 25 (1995).
25. T. Minamino, B. Gonzalez-Pedrajo, K. Yamaguchi, S. I. Aizawa, R. M. Macnab, *Mol. Microbiol.* **34**, 295 (1999).

26. We thank M. Duerrenberger for the electron microscopy facility; V. Huschauer for contributing to the needle purification protocol; S. I. Aizawa for advice; M. Kuhn for technical assistance; S. Straley and K. Hughes for supplying *yscP$_{pestisKIM}$* and *Salmonella* LT2; and C. Thompson, U. Jenal, H. Shin, and J. Mota for suggestions. This work was supported by the Swiss National Science Foundation (grant 32-65393.01) and the Swiss Office Fédéral de l'Education et de la Science (European Union Human Potential–Research Training Network CT-2000-00075).

Supporting Online Material

www.sciencemag.org/cgi/content/full/302/5651/1757/DC1
Materials and Methods
Fig. S1
References

11 September 2003; accepted 16 October 2003

Inflammatory Blockade Restores Adult Hippocampal Neurogenesis

Michelle L. Monje, Hiroki Toda, Theo D. Palmer*

Cranial radiation therapy causes a progressive decline in cognitive function that is linked to impaired neurogenesis. Chronic inflammation accompanies radiation injury, suggesting that inflammatory processes may contribute to neural stem cell dysfunction. Here, we show that neuroinflammation alone inhibits neurogenesis and that inflammatory blockade with indomethacin, a common nonsteroidal anti-inflammatory drug, restores neurogenesis after endotoxin-induced inflammation and augments neurogenesis after cranial irradiation.

The birth of new neurons within the hippocampal region of the central nervous system continues throughout life, and the amount of neurogenesis correlates closely with the hippocampal functions of learning and memory (*1*, *2*). The generation of new neurons within the hippocampus is mediated by proliferating neural stem or progenitor cells (NPC) (*3–5*) that are widespread within the adult brain but instructed by local signaling to produce neurons only in discrete areas (*6*, *7*). Alterations in the microenvironment of the stem cell may allow ectopic neurogenesis to occur (*8*, *9*) or even block essential neurogenesis, leading to deficits in learning and memory (*10–12*) such as that observed in patients who receive therapeutic cranial radiation therapy (*13*). In animal models, cranial irradiation ablates hippocampal neurogenesis, in part by damaging the neurogenic microenvironment, leading to a blockade of endogenous neurogenesis (*12*, *13*). Injury induces pro-inflammatory cytokine expression both peripherally and within the central nervous system and induces stress hormones, such as glucocorticoids, that inhibit hippocampal neurogenesis (*10*). The extensive microglial inflammation and release of pro-inflammatory cytokines that accompanies this irradiation-induced failure suggests that inflammatory processes may influence neural progenitor cell activity (*12*, *14*, *15*).

To determine the effects of inflammation on adult hippocampal neurogenesis, we injected bacterial lipopolysaccharide (LPS) into adult female rats to induce systemic inflammation (*16–19*). The intraperitoneal (i.p.) administration of LPS causes a peripheral in-

Stanford University, Department of Neurosurgery, MSLS P309, Mail Code 5487, 1201 Welch Road, Stanford, CA 94305–5487, USA.

*To whom correspondence should be addressed. E-mail: tpalmer@stanford.edu

Supporting Online Material

Materials and Methods

Yersinia enterocolitica MRS40(pYV40) (*S1*), an ampicillin-sensitive derivative of E40(pYV40)(S*2*) was used for genetics and electron microscopy. An effector multimutant, called ΔHOPEMT, MRS40(pIML421)(*S3*) was used to prepare needles. The various pYV plasmid mutants and the expression plasmids are listed in Table S1. The oligonucleotides used for genetic constructions are given in table S2.

Bacteria were routinely grown on Luria-Bertani agar plates and in liquid Luria-Bertani medium. For the induction of the *yop* regulon, *Y. enterocolitica* bacteria were inoculated to an OD_{600} of 0.1 and cultivated in brain-heart infusion (BHI; Remel) supplemented with 4 mg/ml glycerol, 20 mM $MgCl_2$ and 20 mM sodium oxalate (BHI-Ox) for 2 h at 28 °C, then shifted to 37 °C and incubated for 4 h(*S4*). Expression of the different *yscP* genes cloned downstream from the pBAD promoter was induced by adding 0.2 % arabinose to the culture just before the shift at 37 °C, and again two hours later. Ampicillin was used at a concentration of 200 µg/ml to select for the expression plasmids.

Alleles to be inserted in the pYV plasmids were subcloned into the pKNG101 suicide vector and the allelic exchange was selected by plating diploid bacteria on sucrose(*S5*).

Proteins from the supernatant were precipitated overnight at 4°C with trichloroacetic acid 10% (w/v) final. Electrophoresis was carried out in 12 % or 15 %(w/v) polyacrylamide gels in the presence of SDS (SDS-PAGE). Proteins secreted by $3x10^8$ bacteria were loaded by lane. For the total bacterial cells, the proteins from 10^7 bacteria were loaded by lane. After electrophoresis, proteins were stained with Coomassie brilliant blue (Pierce) or transferred by electroblotting to a nitrocellulose

membrane. Immunoblotting was carried out using rabbit polyclonal antibodies (anti-YscP(*S6*)), polyclonal anti-YscF antibodies raised against the synthetic YscF peptide (NFSGFTKGNDIADLDAVAQTLK) (Centre d'Economie Rurale, Marloie, Belgium). Detection of immunoblots was performed with secondary antibodies conjugated to horse-radish peroxidase (1:2000; Dako) before development with supersignal chemiluminescent substrate (Pierce).

Visualization of the needle-like structures at the cell surface of the bacteria was done by electron microscopy as described by Hoiczyk and Blobel(*S7*). After 4 hours of induction at 37 °C, bacteria were harvested at 2,000 *x g* and resuspended gently in Tris-HCl, pH 7.5. Droplets were applied for 1 min to freshly glow-discharged, formvar-carbon coated grids, and negatively stained with 1% (wt/vol) uranylacetate. Bacteria were visualized in a Philips Morgagni 268D electron microscope at a nominal magnification of *x* 44,000 and an acceleration voltage of 80 kV. Sizes were measured with the "Soft Imaging System" software (Hamburg, Germany). The corresponding cells were analysed in parallel for the presence of YscF by immunoblot.

In order to purify needles, bacteria were cultivated for 2h at 28 °C in BHI-Ox or BHI-Ca^{2+}, then shifted to 37 °C and incubated for 4h(*S4*). Bacteria were harvested by centrifugation (10 min at 5'700 *x* g) and washed once in 1/30 of the culture volume with 20 mM TrisHCl (pH 7.5). The washing supernatant was passed through a 0.45 µm mesh filter and centrifugated for 30 min at 17'500 *x* g. The pellet was resuspended in 1/60 of the initial culture volume of TrisHCl 20 mM (pH 7.5), CHAPS 0.1% (w/v) and centrifuged again for 30 min at 17'500 *x* g. The supernatant was collected and the needles were precipitated for one hour one ice with polyethylene glycol 6000 (10% w/v) and NaCl (100 mM). The needles were then collected by 30-

min centrifugation at 17'500 *x* g and resuspended in 1/300 of initial culture volume of 20 mM TrisHCl (pH 7.5).

Figure S1

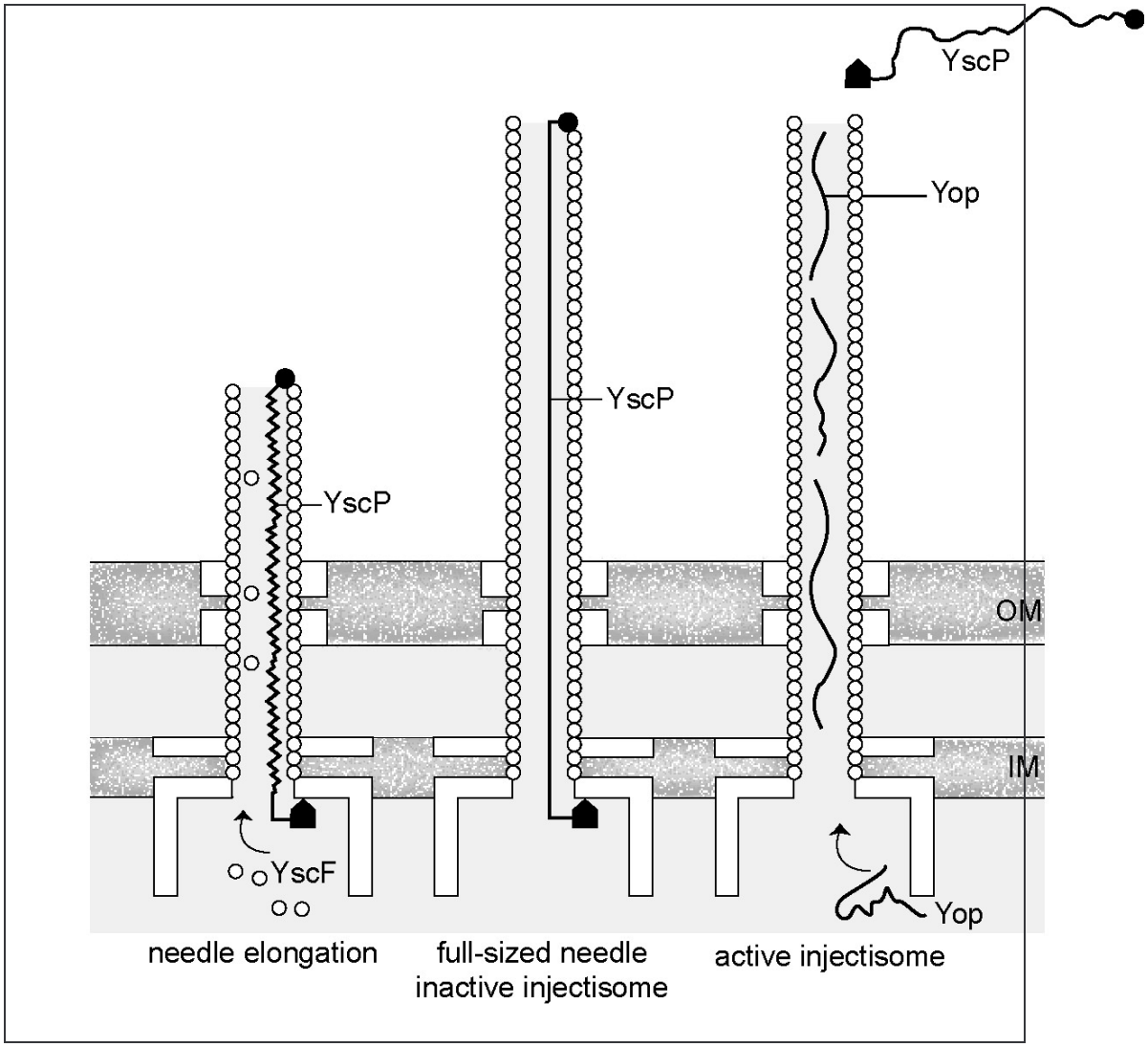

Legend to fig S1

Proposed model for the control of the YscF-needle length by the YscP ruler.

Table S1: Genetic constructs used in this study

Expression Vectors			**refs**
pBAD/*Myc*-HisA			Invitrogen
pEF6/*Myc*-His*lacZ*			Invitrogen
Suicide Plasmids			**refs**
pKNG101			(*S5*)
Mutator plasmids	**Construction**	**Encoded protein**	**refs**
pLJ16	*Sal*I/*Bam*HI fragment of pCA9 cloned in corresponding sites of pKNG101	$YscP_{æ46-96}$	This work
pLJ17	*Sal*I/*Bam*HI fragment of pLJ11 cloned in corresponding sites of pKNG101	$YscP_{æ222-306}$	This work
pYV plasmids	**Construction**	**Encoded protein**	**refs**
pLJC4016	pYV40 $yscP_{\Delta 46-96}$	$YscP_{æ46-96}$	This work
pLJC4017	pYV40 $yscP_{\Delta 222-306}$	$YscP_{æ222-306}$	This work
pSIL4009	pYV40 $yscP_{\Delta 97-465}$	$YscP_{æ97-465}$	(*S6*)
pYV40	Wild-type virulence plasmid of *Y. enterocolitica* E40	$YscP_{entero\ wt}$	(*S2*)

Expression plasmids	**Construction**	**Encoded protein**	**refs**
pCA3	Amplification of *yscP*$_{pestis}$ allele of pYscP.2 using primers 3072 and 3073. Cloning of the resulting fragment in pBAD/*Myc*HisA digested by *Nco*I and *Eco*RI.	YscP$_{pestis}$	This work
pCA5	Deletion of codons 16 to 25 of *yscP*$_{entero}$ from pLJ6 by inverse PCR using phosphorylated oligonucleotides 3066 and 3067, followed by a ligation.	YscP$_{æ16\text{-}25}$	This work
pCA6	Deletion of codons 26 to 35 of *yscP*$_{entero}$ from pLJ6 by inverse PCR using phosphorylated oligonucleotides 3068 and 3069, followed by a ligation.	YscP$_{æ26\text{-}35}$	This work
pCA7	Deletion of codons 36 to 45 of *yscP*$_{entero}$ from pLJ6 by inverse PCR using phosphorylated oligonucleotides 3070 and 3071, followed by a ligation.	YscP$_{æ36\text{-}45}$	This work
pCA9	Deletion of codons 46 to 96 of *yscP*$_{entero}$ from pLJ6 by inverse PCR using phosphorylated oligonucleotides 3124 and 3126, followed by a ligation.	YscP$_{æ46\text{-}96}$	This work

pCA18	Deletion of codons 385 to 424 of *yscP*$_{entero}$ from pLJ6 by inverse PCR using phosphorylated oligonucleotides 3242 and 3243, followed by a ligation.	YscP$_{æ385-424}$	This work
pCA20	Deletion of codons 46 to 96 and 222 to 306 of *yscP* $_{entero}$ from pLJ11 by inverse PCR using phosphorylated oligonucleotides 3124 and 3126, followed by a ligation.	YscP$_{æ46-96+æ222-306}$	This work
pCA23	Introduction of a *Not*I and a *Xba*I site between codons 49 and 50 of *yscP*$_{entero}$ by inverse PCR on pLJ6 DNA using primers 3187 (introducing both sites) and 3188 (introducing *Not*I site), followed by *Not*I digestion and ligation.	YscP$_{Ý}$	This work
pLJ5	*Hind*III digestion of pLK1 and religation to remove sequence encoding codons 467 to 515 of YscP.	YscP$_{æ467-515}$	This work
pLJ6	pBAD :: *yscP*$^{+}$ $_{entero}$ Cloning of the entire yscP coding sequence amplified with oligos 3072 and 3073 (introducing *Nco*I and *Eco*RI sites, respectively) in pBAD/*Myc*HisA digested by *Nco*I and *Eco*RI.	YscP $_{wt}$	This work
pLJ7	Inverse PCR on pLJ6 with primers 3075 (introducing *Not*I site) and 3076 (introducing *Not*I site) to delete the region encoding the repeats of YscP$_{entero}$ (from codon 222 to 381). *Not*I digestion of the amplified vector and ligation.	YscP$_{æ222-381}$	This work
pLJ11	The DNA encoding the second repeat of YscP (aa307 to aa381) was amplified from pLJ6 with primers 3078 (introducing *Not*I and *Xba*I) and 3079 (introducing *Not*I). This 258-bp amplified fragment was digested by *Not*I and ligated in pLJ7 cleaved with *Not*I.	YscP$_{æ222-306}$	This work
pLJ18	Insertion of aa147 to aa266 from FliK into YscP$_{Ý.}$ Amplification of *fliK*$_{147-265}$ of *Salmonella typhimurium* LT2 using primers 3083 (introducing *Xba*I and *Not*I sites) and 3084 (introducing *Not*I site) as primers. The obtained fragment was cloned in pCA23 digested by	YscP$_{Ý\ FliK147-266}$	This work

	*Xba*I and *Not*I.		
pLJ19	Duplication of aa222 to aa381 from $YscP_{entero}$. Amplification of DNA encoding aa222 to aa381 using oligos 3078 (introducing *Xba*I and *Not*I sites) and 3079 (introducing *Not*I site). The obtained fragment was cloned in pCA23 digested by *Xba*I and *Not*I.	$YscP_{Ý\ YscP222\text{-}381}$	This work
pLJ20	Duplication of aa307 to aa381 from $YscP_{entero}$. Amplification of region encoding aa307 to aa381 of YscP using oligos 3078 (introducing *Xba*I and *Not*I sites) and 3079 (introducing *Not*I site). The obtained fragment was cloned in pCA23 digested by *Xba*I and *Not*I.	$YscP_{Ý\ YscP307\text{-}381}$	This work
pLK1	pBAD :: $yscP^{+}_{entero}$, $yscQ^{+'}_{entero}$ (only 3' end of yscQ)	$YscP_{entero\ wt}$	(*S6*)
pSI63	pBlueScript II KS^{-} :: $yscP_{entero\ æ97\text{-}465}$	$YscP_{æ97\text{-}465}$	(*S6*)
pYscP.2	pBlueScript KS^{+} :: $yscP_{pestis}$ expressed under the control of p_{Lac}	$YscP_{pestis}$	(*S8*)

Table S2: Oligonucleotides used in this study

Oligo code	Oligonucleotide sequence	Underlined
3072	gatcccatggccaataaaatcaccactcgt	*Nco*I
3073	gatcgaattcttattcttcagcctcccactc	*Eco*RI
3066	ttcatactcaggttctaatgg	
3067	gcacgtgccgattttgagcaa	
3068	ttgcaaatcatgatgcagctt	
3069	cataataataagggtaatcgt	
3070	caacagcgcttgctcaaaatc	
3071	gaagagccgcgtagacctgta	
3078	gtcagcggccgcttgtctagacgaagaaccgttacctctt	*Not*I, *Xba*I
3079	gtcagcggccgcatacatctccagcaaggt	*Not*I
3124	tttgggatgacgattacc	
3126	catgatttaaacttatct	
3187	gatcgcggccgcaatctctagacgcggctcttct	*Not*I, *Xba*I
3188	gatcgcggccgctagacctgtacgtccgcatgac	*Not*I
3239	gtcatggcggacgtacaggtc	
3240	gaagaaccgttacctcttca	
3242	agacaaggaatacatctc	
3243	ctgcgcggcggctcatcc	
3244	ttctagttctaccgctag	
3245	gaagctttaagaatttta	
3083	gtcagcggccgcttgtctagagctgcccggacaacctgtc	*Not*I, *Xba*I
3084	gtcagcggccgctaacggcgcgctgagtac	*Not*I

Supplementary references

S1. M. R. Sarker, M. P. Sory, A. P. Boyd, M. Iriarte, G. R. Cornelis, *Infect. Immun.* **66**, 2976 (1998).

S2. M. P. Sory, G. R. Cornelis, *Mol. Microbiol.* **14**, 583 (1994).

S3. M. Iriarte, G. R. Cornelis, *Mol. Microbiol.* **29**, 915 (1998).

S4. G. Cornelis, J. C. Vanootegem, C. Sluiters, *Microb. Pathog.* **2**, 367 (1987).

S5. K. Kaniga, I. Delor, G. R. Cornelis, *Gene* **109**, 137 (1991).

S6. I. Stainier *et al.*, *Mol. Microbiol.* **37**, 1005 (2000).

S7. E. Hoiczyk, G. Blobel, *Proc. Natl. Acad. Sci. U. S. A.* **98**, 4669 (2001).

S8. P. L. Payne, S. C. Straley, *J. Bacteriol.* **181**, 2852 (1999).

3- RESULTS

3.2- Characterization of a Type III secretion substrate specificity switch (T3S4) domain in YscP from Yersinia enterocolitica

Agrain, C., Callebaut, I., Journet, L., Sorg, I., Paroz, C., Mota, L.J., and Cornelis, G.R.

Mol Microbiol 56: 54-67 (2005)

Summary

YscP has also been shown to be required for Yop secretion (Stainier et al., 2000). Analyzing now all the constructed mutants for their capacity to secrete Yops led to the conclusion that the C-term part of YscP was crucial for Yops secretion. As this region was shown previously to be also necessary for needle length control, it is probably involved in the substrate-specificity switch of the machinery, from the needle component YscF to Yops. The study of this region by Hydrophobic Cluster Analysis led to a characterization of a new domain that we called T3S4 (Type 3 Secretion Substrate-Specificity Switch) and which can be found in all counterparts of YscP in other injectisomes but also in the flagellum. The remarkable conservation of the T3S4 structure suggests a similar function for all these proteins. The T3S4 domains found in injectisomes happened to be partially exchangeable. So, what matters seems to be the overall structure of the domain. This is further supported by the fact that single alanine-replacement, of the few conserved amino acids not affecting the structure, did not impact the functions.

The HCA was performed by Dr. Isabelle Callebaut, Département de Biologie Structurale, Laboratoire de Minéralogie-Cristallographie, Paris (CNRS/UMR 7590), Universités Paris 6 and Paris 7, France.
The EM work (measurements and pictures) was done jointly with Dr. Isabel Sorg.

Molecular Microbiology (2005) **56**(1), 54–67 doi:10.1111/j.1365-2958.2005.04534.x

Characterization of a Type III secretion substrate specificity switch (T3S4) domain in YscP from *Yersinia enterocolitica*

Céline Agrain,[1‡] Isabelle Callebaut,[2‡] Laure Journet,[1†] Isabel Sorg,[1] Cécile Paroz,[1] Luís Jaime Mota[1] and Guy R. Cornelis[1]*

[1]*Biozentrum der Universität Basel, Basel, Switzerland.*
[2]*Département de Biologie Structurale, Laboratoire de Minéralogie-Cristallographie Paris (CNRS/UMR 7590) Universités Paris 6 and Paris 7, France.*

Summary

The length of the needle ending the *Yersinia* Ysc injectisome is determined by YscP, a protein acting as a molecular ruler. In addition, YscP is required for Yop secretion. In the present paper, by a systematic deletion analysis, we localized accurately the region required for Yop secretion between residues 405 and 500. As this C-terminal region of YscP has also been shown to control needle length it probably represents the substrate specificity switch of the machinery. By a bioinformatics analysis, we show that this region has a globular structure, an original α/β fold, a P-x-L-G signature and presumably no catalytic activity. In spite of very limited sequence similarities, this structure is conserved among the proteins that are presumed to control the needle length in many different injectisomes and also among members of the FliK family, which control the flagellar hook length. This region thus represents a new protein domain that we called T3S4 for Type III secretion substrate specificity switch. The T3S4 domain of YscP can be replaced by the T3S4 domain of AscP (*Aeromonas salmonicida*) or PscP (*Pseudomonas aeruginosa*) but not by the one from FliK, indicating that in spite of a common global structure, these domains need to fit their partner proteins in the secretion apparatus.

Introduction

Injectisomes are multicomponent nanomachines involved in molecular *trans*-kingdom communication between bacteria and eukaryotic cells. They are encountered in Gram-negative bacteria that are either pathogenic for animals and plants or are symbionts (Viprey *et al*., 1998; Dale *et al*., 2001; Dale *et al*., 2002). They allow extracellular bacteria to inject proteins across the plasma membrane of eukaryotic cells and they enable intracellular bacteria to inject proteins across the host membrane limiting their compartment. For reviews see References (Cornelis and Wolf-Watz, 1997; Anderson and Schneewind, 1999; Galan and Collmer, 1999; Cornelis and Van Gijsegem, 2000; Plano *et al*., 2001; Cornelis, 2002).

Based on a phylogeny analysis made on three highly conserved proteins, the injectisomes can be grouped into five major families (Foultier *et al*., 2002). The injectisomes from animal pathogens cluster in three families. The plasmid encoded Ysc injectisome common to *Yersinia enterocolitica, Yersinia pestis* and *Yersinia pseudotuberculosis* represents an archetype for the largest family, which also includes the injectisomes from *Pseudomonas aeruginosa* (Psc), *Aeromonas salmonicida* (Asc), *Bordetella pertussis*, *parapertussis* and *bronchiseptica* (Bsc), *Photorhabdus luminescens* (Lsc and Sct) and an unnamed injectisome from *Vibrio parahemolyticus* (called here Vsc). A second family includes the *Shigella* spp. Mxi-Spa injectisome, the *Salmonella* spp. Inv injectisome (encoded by SPI-1 in *S. enterica*), the Ysa injectisome from *Y. enterocolitica*, an injectisome from *Burkholderia pseudomallei* and one from *Sodalis glossinidius*. A third family includes the Ssa injectisome from *S. enterica* (encoded by SPI-2), the Esc injectisome from enteropathogenic (EPECs) and enterohaemorrhagic (EHECs) *E. coli* and a chromosome-encoded injectisome from *Y. pestis*. The injectisomes from plant pathogens cluster in two families called Hrp1 (*Erwinia amylovora* and *Pseudomonas syringae*) and Hrp2 (*Xanthomonas campestris*, *Ralstonia solanacearum*).

The amino acid sequence of many injectisome constituents has significant similarity to proteins from the flagellum with whom they share Type III secretion (T3S) (Allaoui *et al*., 1994; Fields *et al*., 1994; Van Gijsegem *et al*., 1995; Aizawa, 2001; Blocker *et al*., 2003). Both structures have a similar basal body consisting of a pair of rings that span the inner and outer bacterial membranes, hold together by a short tube. In most animal pathogens, the injectisome

Accepted 15 December, 2004. *For correspondence. E-mail guy.cornelis@unibas.ch; Tel. (+41) 61 267 2110; Fax (+41) 61 267 2118. †Present address: CNRS, UPR9050; E-mail: Laure.Journet@esbs.u-strasbg.fr ‡These authors contributed equally to this work.

ends up with a needle that protrudes outside the bacterium. Therefore, the injectisome is also called needle-complex (Kubori *et al*., 1998; Blocker *et al*., 1999; Kimbrough and Miller, 2000; Kubori *et al*., 2000; Sukhan *et al*., 2003; Marlovits *et al*., 2004). A long flexible pilus terminates the Hrp and Esc injectisomes (Roine *et al*., 1997; Knutton *et al*., 1998; Van Gijsegem *et al*., 2000). In the flagellum, the filament is connected to the basal body via a hook. The length of this hook is genetically determined and a protein called FliK has been shown to play the key role in this process (Patterson-Delafield *et al*., 1973; Suzuki and Iino, 1981). Mutants deficient in FliK make extra-long hooks (called polyhooks) and no filament. Extragenic suppressive mutations restoring filament assembly on polyhook structures (polyhook-filament phenotype) have been mapped in *flhB*, a gene encoding a major component of the export apparatus (Suzuki and Iino, 1981; Kutsukake *et al*., 1994; Williams *et al*., 1996; Fraser *et al*., 2003a). The study of these *fliK* suppressors mutations led to the proposal that the C-terminal domain of FlhB has two substrate specificity states and that a conformational change, mediated by FliK and accompanied by a proteolytic cleavage of FlhB is responsible for the specificity-switching process allowing secretion of flagellin once assembly of the hook is completed (Minamino and Macnab, 2000; Makishima *et al*., 2001; Fraser *et al*., 2003b). The length of the injectisome-needle is also genetically determined. Mutations in *spa32* from *Shigella*, in *invJ* from *Salmonella* (SPI-1) (Kubori *et al*., 2000; Magdalena *et al*., 2002; Tamano *et al*., 2002) and in *yscP* from *Yersinia* (Journet *et al*., 2003) lead to needles with undefinite length and no substrate secretion. The homologues of FlhB in injectisomes form the well-conserved YscU family (Allaoui *et al*., 1994). Introduction into YscU of the FlhB substitutions that suppress the *fliK* phenotype restores Yop secretion in *yscP* mutants (Edqvist *et al*., 2003). Moreover, like FlhB, YscU undergoes a proteolytic cleavage (Lavander *et al*., 2003). Thus, very much like FliK, YscP is presumably involved in the substrate specificity switch, interacting with the basal-body component YscU to stop secretion of the YscF needle subunits and to start Yop secretion. In addition to this switch function, YscP was recently shown to act as a molecular ruler determining the length of the needle (Journet *et al*., 2003). YscP is thus a protein with a dual function. In the molecular ruler model, the N-terminus and C-terminus of YscP are proposed to act as anchors of the central ruler part, one extremity being attached to the basal body and the other one to the growing tip of the needle (Journet *et al*., 2003). However, no information exists regarding the regions of YscP involved in its switch role.

Here, by systematic deletion mutagenesis of YscP and a bioinformatics analysis, we localized accurately the switch domain in the C-terminal domain of the protein and we show that this switch domain is globular and conserved among the proteins controlling length in injectisomes as well as in the flagellum. In contrast to most of the proteins of the injectisomes and flagella, the relationship between Spa32/InvJ, YscP and FliK had remained to date unrevealed because of the too high divergence in their sequences (in the range of 10% identity).

Results

YscP385–500 is required for Yop secretion

We showed previously that in frame deletions and insertions in the central part of YscP (36–96 and 222–306) defined a ruler region (Journet *et al*., 2003), and that in frame deletions in the N-terminus (16–25 and 26–35) as well as in the C-terminus (385–424 and 467–515) identified regions of the protein that are necessary for YscP to exert its needle length control function (Journet *et al*., 2003). However, the deletion mutants were not analysed for their capacity to secrete Yops. In this work, we generated new deletions in the *yscP* gene that together with the ones generated before (see above) encompass almost the entire gene (Fig. 1A) and we tested the mutants for their capacity to secrete Yops. The ruler region of YscP is characterized by a duplication of 60 central residues (Stainier *et al*., 2000), which hampers the engineering of deletions. For this reason, we could only construct one large deletion between residues 222 and 306 of YscP, and not smaller ones as in the rest of the protein. We cloned the mutated alleles downstream from an arabinose-inducible promoter (pBAD) and the recombinant plasmids were introduced in *Y. enterocolitica* E40 (pLJ4036), a new *yscP* null mutant constructed for this study. In the pLJ4036 pYV plasmid, the *yscP* gene is completely removed, from start to stop, in order to prevent any interference from left-over domains or sites. All the recombinant bacteria, incubated at 37°C in Ca^{2+}-deprived medium containing arabinose, synthesized YscP proteins of the expected size (Fig. 1B). We then analysed the phenotype of all the mutants with regard to Yop secretion. As shown in Fig. 1C, the deletions removing parts of the protein before residue 381 and after residue 500 had no impact on Yop secretion. In contrast, deletions between amino acids 385–500 affected Yop secretion. This indicates that this C-terminal region (385–500) is required for both functions, length control (Journet *et al*., 2003) and Yop secretion, and hence is responsible for the substrate specificity switch function. Interestingly, there was no strict correlation between the phenotype of Yop secretion deficiency and tight length control. Indeed, deletions affecting the N-terminus (YscPΔ16–25 and YscPΔ26–35) (Journet *et al*., 2003) led only to a loss of length control but not to a loss of Yop secretion.

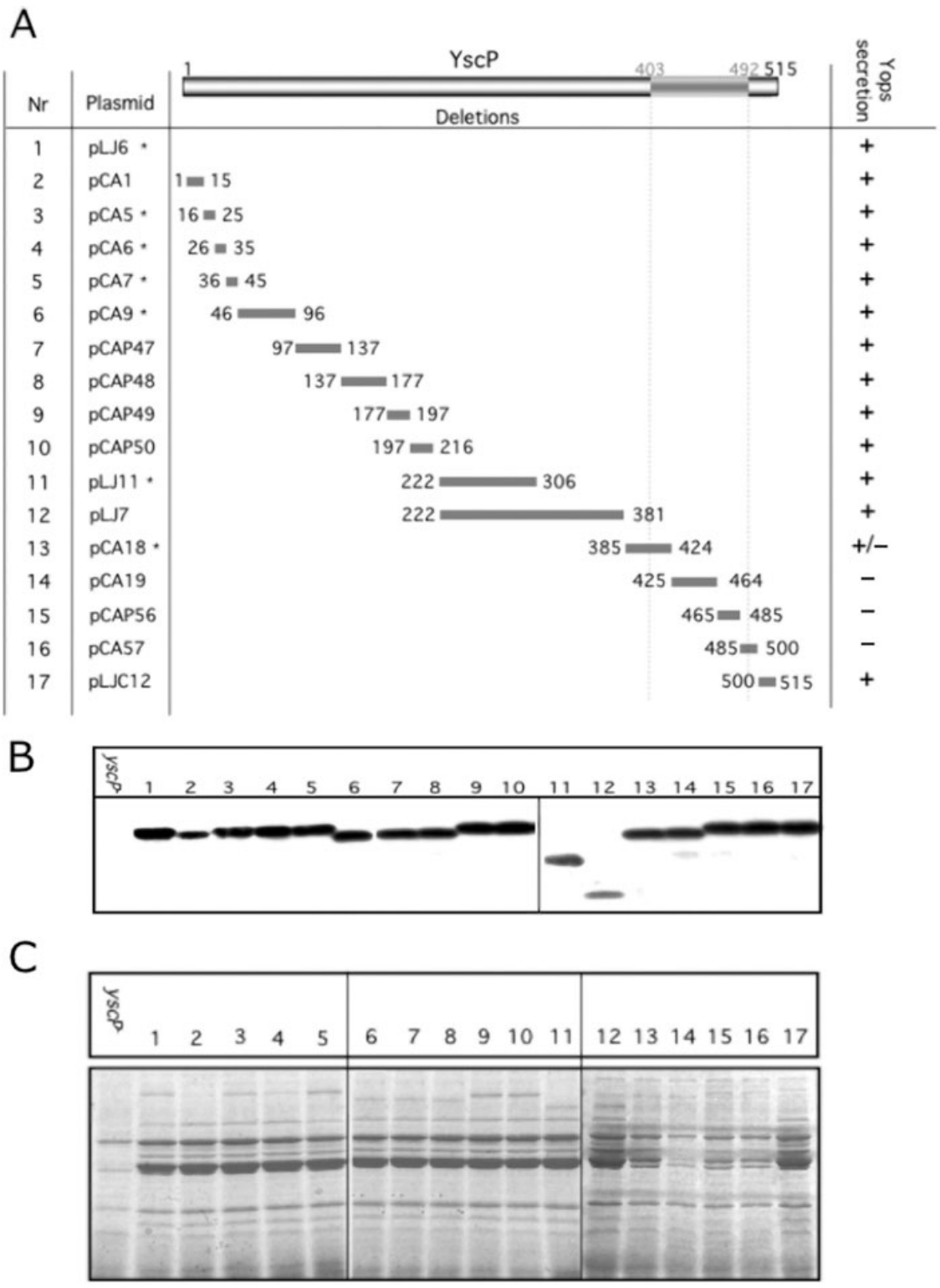

Fig. 1. A. Schematic representations of the *yscP* in frame deletions mutants together with their ability to secrete Yops. The highlighted box in YscP (aa 403–492) represents the T3S4 domain.
B. Western blot analysis (total cells; polyclonal antibody) of the various YscP proteins produced by *Y. enterocolitica* MRS40(pLJ4036), i.e the *yscP*$^{-}$ mutant (–, control); and by *Y. enterocolitica* MRS40(pLJ4036) carrying the plasmids (listed on the left) encoding the various *yscP*$^{+}$ genes.
C. Yop proteins secreted by the same *Y. enterocolitica* E40 strains as in B (Coomassie-stained SDS-PAGE). Note that MRS40(pLJ4036), the *yscP* knockout background is not completely negative for Yop secretion.

The YscP C-terminal region is conserved and defines a new family of proteins

YscP and its flagellar equivalent, FliK, have similar functions but their global identity at the primary sequence level is only within the 10% range. We identified the switch function in the C-terminus of YscP. In the model proposed for FliK, the domain that switches the substrate specificity is also localized in the C-terminus (Williams *et al*., 1996; Minamino *et al*., 2004). We therefore then wondered if the C-terminal regions of YscP and FliK were sharing similarities and if we could point out an equivalent region in proteins found in other injectisomes or T3S systems.

To begin with, we used the C-terminal domain of YscP (from aa 385 to the C-terminus) as query and performed PSI-BLAST searches (Altschul *et al*., 1997) on the non-redundant database (nr) at the National Center for Biological Information (NCBI) using an *E*-value inclusion threshold of 0.005. By iteration 4, searches converged to identify counterpart proteins of YscP in T3S systems from the YscP family: AscP, PscP, LscP and SctP. As suggested by the letter code, these proteins are encoded by genes that occupy the same locus as *yscP* in the operons encoding the different injectisomes. In addition, we found the VscP protein from *Vibrio harveyi* [GenBank identifier (gi) 41834182]. All these proteins turned out to have a conserved C-terminal domain (34% identity) preceded by variable regions. We called the conserved domain the T3S4 domain after Type III secretion substrate specificity switch.

We also found a suggestive match (*E*-value 0.19, 35% identity on a 117 aa overlap) with the flagellar hook-length control protein FliK from *Y. pestis* (gi 45442809). Integrating the *Y. pestis* FliK sequence within the position specific score matrix (PSSM) led to significantly detect all the members of the FliK family. One can note that the similarity between YscP and FliK proteins was directly found to be significant using a longer sequence of YscP as query (aa 363–515). The *Y. pestis* FliK region (aa 251–393) was also used as a query for reciprocal PSI-BLAST searches (same parameters). By iteration 2, LscP from *P. luminescens* was significantly retrieved ($E = 0.005$), whereas other members of the YscP family were retrieved by iteration 3 (*E*-value of 4×10^{-5} for *Y. enterocolitica* YscP). Proteins of the HrcP family were retrieved just below the threshold value after convergence by iteration 22 (e.g. *R. solanacearum* HpaP using the *Y. pestis* YscP sequence as query; *E*-value of 0.13, 18% sequence identity over 90 aa) or by iteration 14 (e.g. *R. solanacearum* HpaP using the *V. parahaemolyticus* LafE sequence as query; *E*-value of 0.023, 18% sequence identity over 90 aa).

Although marginal, the potential similarity between YscP/FliK and HrcP proteins was further supported at the 2D level by using hydrophobic cluster analysis (HCA) (Gaboriaud *et al*., 1987; Callebaut *et al*., 1997) (Fig. 2A and B and legend). The aligned sequences were also searched against databases using HMMER (Eddy, 1998), but such searches did not identify proteins other than those highlighted before. Interestingly the T3S4 domain is localized in the C-terminus in every member of the family, suggesting that this specific position might be relevant to the mechanism of length control (Fig. 3).

Finally, because it was anticipated that the T3S4 domain, detected in the YscP, FliK and HrcP families, would also be present in the Spa32 and InvJ family, we screened these last sequences using HCA for the presence of 2D markers of the T3S4 domain, which could have been missed by other search methods. This led to identify clear markers of the T3S4 domain in the Spa32/InvJ sequences (Fig. 2A and B, see also below), suggesting that these proteins could indeed share the T3S4 domain with the YscP, FliK and HrcP families.

Characterization of the T3S4 domain

The T3S4 domain defined in the preceding section between aa 385 and 500 of YscP, has all the characteristics of a globular domain, as visualized using HCA (Callebaut *et al*., 1997) (Fig. 2A). It contains approximately one-third of hydrophobic amino acids, organized in clusters, the lengths of which are typical of those of regular secondary structures. Based on the YscP sequence, the limits of the globular domain can be refined on both sides (Fig. 2A): (i) it starts at aa 403 as the preceding sequence (~aa 391–403) corresponds to a repeated fragment, the first copy of which can be found upstream in the YscP sequence (~aa 243–255) and it ends up at aa 492, where a long sequence devoid of hydrophobic amino acids starts. The latter sequence likely defines a hinge separating the switch domain from a small region, which might organize as an α-helix.

The T3S4 domain (arrow in Fig. 2A and boxed in Fig. 2B) has an α/β predicted fold, with a core region having almost no insertion-deletion. Seven hydrophobic clusters, as defined using HCA and numbered up to the alignment of Fig. 2A and B, delineate the predicted secondary structures, for which buried positions are highlighted by conservation of hydrophobic amino acids (boxed green in Fig. 2B). A conserved proline and a conserved glycine (P-x-L-G) between the predicted β-strands β1 and β2 seems to represent a signature of the T3S4 domain. No clear conservation is observed outside from the hydrophobic amino acids and loop markers, rendering a catalytic function unlikely.

Strikingly, in proteins from the YscP and FliK subgroups, the T3S4 domain is followed by a clear hinge region, particularly rich in acidic residues (represented in red in Fig. 2B). A hydrophobic cluster or a group of hydrophobic clusters (shaded grey on Fig. 2B) follows this hinge region

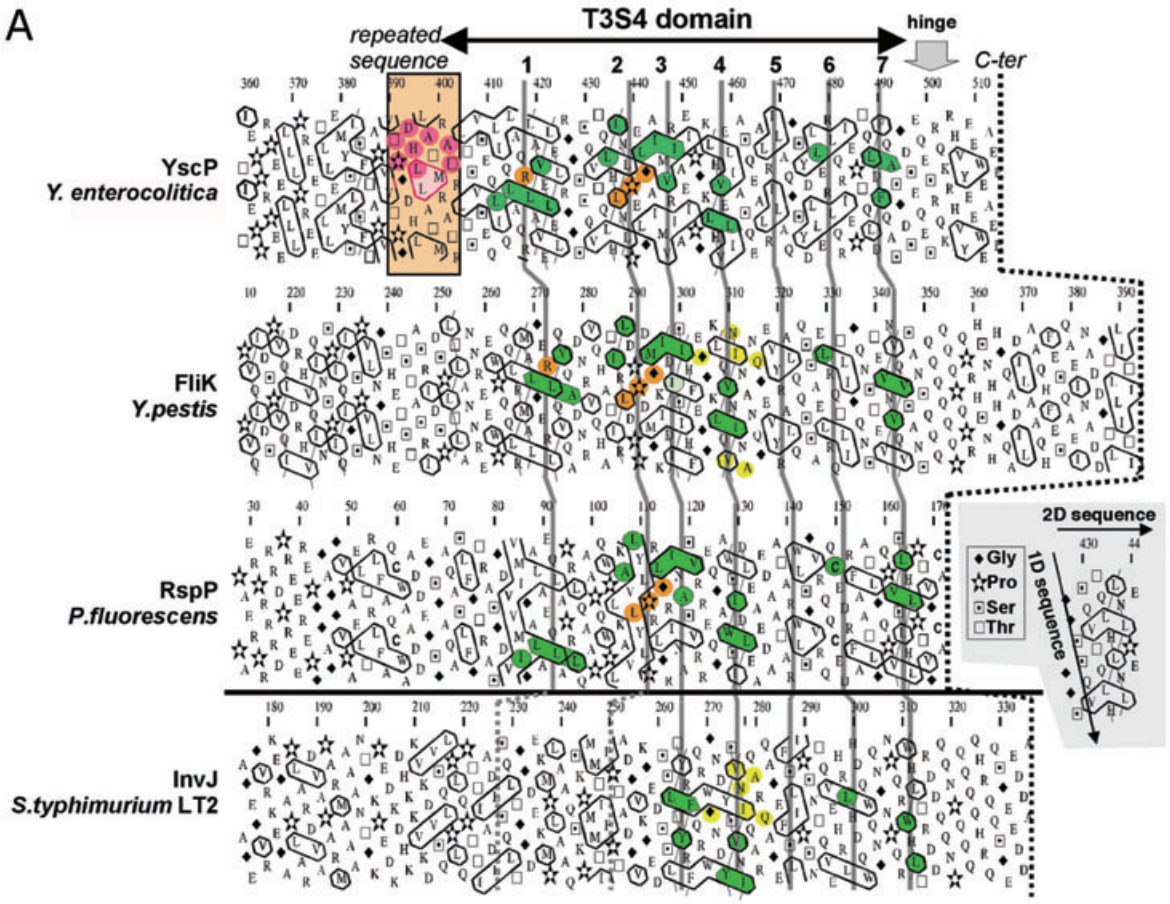

B

T3S4 domain

```
                                                    1                   2                   3                   4                   5                   6
Yersinia enterocolitica   YscP 404 RLTSVSEQLIQLAQRLAVELELRG----GSSQVTQLHLNLPELGAIMVRIAEIPGKLHVELIASQEALRILAQGSYDLLERLQ
Photorhabdus luminescens  LscP 287 ATSTISPLLEALIDKLSVEISIEL---TQQSRPATLHLTLPSLGALEIQLTNEHGKLQIEILANPAAQQLLKQARFELIERLQ
Photorahbdus luminescens  SctP 261 ATSTISPLLEVLIDKLSVEISIEL---TQQPRPATLHLTLPNLGALEIQLTSEHGKLQIEILANPAAQQLLKQARFELIERLQ
Aeromonas salmonicida     AscP 145 APAESNRELCQLLERLAVDIYQEL---GRPERPPLLRLTLPQLGDLSIRIAHHNGELQIEILATAQGELLLNQGRSDLVDRLQ
Pseudomonas aeruginosa    PscP 249 PLADIARLLDAVQGRIQVASAAES-------HAARLQVRLPQLGAVEVQVLHGHGQLQIEISASPGSLALLQQARGELLERLQ
Vibrio parahaemolyticus   VscP 324 PTREVNQLIQQLVDKVYVALPTAS-----NEKEVRLFLSEGQLKGGEIHIKLDSQGYSVTIRQEHALSIINQQARQDLAERLN

Yersinia pestis           FliK 259 REEWFQQLRMALGERLQVQADNR-------VQHATIRLDPPDMGKIDISIHFEGGKLQVNINANQGEVYRALQQSSAELRQTL
Salmonella thyphimurium   FliK 264 APLGSHEWQQTFSQQVMLFTRQG-------QQSAQLRLHPEELGQVHISLKLDDNQAQLQMVSPHSHVRAALEAALPMLRTQL
Escherichia coli          FliK 233 APLGSHEWQQSLSQHISLFTRQG-------QQSAELRLHPQDLGEVQISLKVDDNQAQIQMVSPHQHVRAALEAALPVLRTQL
Bacillus subtilis         FliK 290 TKTVADQVINAWKQMKYTPFGRS-------TGSFTIRLNPEHLGFVTIKLTNENGMFQSKIIASSQSAKELLEQHLPQLKQSL
Vibrio cholerae           FliK 532 VPLNKEMAADQLAERVQMMMSKN-------LKNIDIRLDPPELGRMHIRMNMQGDGATVHFTVANQHAREALEQTMPRLREML
Aeromonas salmonicida     LafE 230 PAHWGQQLVDVLKDKVELQVNQQ-------IKQAHIRLDPPELGRLELTVRVDGDRLNVQLNVTNPAVEDALIQSMEQLRMSL
Vibrio parahaemolyticus   LafE 226 AGKWGEQMMQVLHDRVTLQAQQS-------VQEAKIRLDPPDLGKLDLLVRVEGDRLSVQINANTAATREALMQVSERLRTEL

Pseudomonas fluorescens   RspP  78 RASGDVVMIGALAEQLAPRLQAA------PQWPLKAVLYLPRLGRINASVRREQGAWSIDLEAEDAATARWLSGVRQQCEDRF
Pseudomonas syringae      HrpP  95 FPVRAEQVPTQLIDELAQRLPDQ------PDGPLSFTLLMPSLGSVRVNANKTENRWSVQLGFARRDVLKRLSAHTGACRDSL
Ralstonia solanacearum    HpaP 100 EIGAGETMTEHLARLLSQFCASQAIRSGGECWEISLDLDPKILPETRLTLRLSPHTLSLRFEAGHPRSRHLLSEHGDTLRQRI
Secondary structure prediction     -----HHHHHHHHHHHHHHHH----------EEEE--------EEEEEE-----EEEEEE---HHHHHHHHHHHHHHHHHH
```

```
                                                    7                   hinge
Yersinia enterocolitica   YscP     RIEPTQ-LDFQASG---------DSEQESRQKRHVYEEWEAEE*  515 GI:7839593
Photorhabdus luminescens  LscP     LLYPTQTVELSLPE--------QTDSEHGSRQRRSVYEEWKKDA*  402 GI:27550059
Photorhabdus luminescens  SctP     LLYPTQTVELSLPE--------QTDSEHGSRQRRSVYEEWKKDA*  376 GI:37527631
Aeromonas salmonicida     AscP     RLYPGERVALDLFN--------QADSERGSRHKRSIYEEWDADA*  260 GI:38201227
Pseudomonas aeruginosa    PscP     RLHPEQPVQLTFNQ--------QQDSGQRSRQRRYLHEEWQAE*   369 GI:15596892
Vibrio parahaemolyticus   VscP     RMGFEQPLRVSISEQTSQHGHTQQDQQQSRQQRSVYEEWQPEADQ*446 GI:28898444

Yersinia pestis           FliK     IGQNSTEVNVQVSANSQQQQQQPQPRHSNHHGQADILAAQHFESQAEINADDGTLLITI*          393 GI:16121061
Salmonella thyphimurium   FliK     AESGIQLGQSSISSESFAGQQQSSSQQQS-SRAQHTDAFGAEDDIALAAPASLQAAARGNGAVDIFA*405 GI:16765312
Escherichia coli          FliK     AESGIQLGQSNISGESFSGQQQAASQQQQSQRTANHEPLAGEDDDTLPVPVSLQGRVTGNSGVDIFA*375 GI:16129890
Bacillus subtilis         FliK     PNMAVQIDRFTLPVQSGDQPIYGQLADEQKQQQEGQRQQRQKKQSNDFGDLLDEVSMVEMEEEE*   429 GI:16078690
Vibrio cholerae           FliK     AQQGVQLGDTSVQQQSAGQQQRYTGQEQSGFGQSARNERLNSEENLDTDIKLDLNVATKRDGLSYYA*674 GI:15642127
Aeromonas salmonicida     LafE     APHHVGGVEVNVGCGGEQGQQEKWQQQQIMAGRRQWQEDIEPTDSTMRDWLNTLV*              360 GI:22758823
Vibrio parahaemolyticus   LafE     QEQNFVHVDVNVGADQGQERHQQQMNDEDTTIFAARESSAFQSNTTTNYSEHWLNTQA*           359 GI:1518950

Pseudomonas fluorescens   RspP     AATLGQPVSLHLPTVGCA* 172 GI:15042139
Pseudomonas syringae      HrpP     SQALGQDVELDMHEDLSA* 189 GI:28868606
Ralstonia solanacearum    HpaP     HALLRQQVDVELEIW*    197  GI:17549083
Secondary structure prediction     H-------EEE---
```

Fig. 2. A. Comparison of the HCA plots of T3S4 domains of the YscP, FliK and HrcP families, highlighting conserved regular secondary structures. Protein sequences are shown on a duplicated alpha helical net on which the encircled hydrophobic amino acids (V, I, L, M, F, Y, W) form clusters. The positions of these clusters statistically match those of the regular secondary structures (alpha helices and beta strands). This analysis gives access to 2D signatures, which are much more conserved than 1D sequences and thus help sequence comparison at high levels of divergence. Guidelines to the use of HCA are given in the study by Gaboriaud *et al*. (1987) and by Callebaut *et al*. (1997) whereas recent publications can be found at the following URL (http://www.lmcp.jussieu.fr/~mornon/publications.html). The way to read the sequences and special symbols are indicated in the inset. Representative sequences of the three families are shown: YscP from *Y. enterocolitica* [GenBank identifier (gi) 17839593], FliK from *Y. pestis* (gi 16121061) and RspP from *P. fluorescens* (gi 15042139). Cluster similarities are indicated in green, sequence identities in orange. Amino acids shaded pink within the box in the YscP sequence ('repeated sequence') correspond to identities relative to a sequence fragment found upstream (aa 243–255). Vertical bars indicate cluster correspondences (labelled from 1 to 7). Clusters labelled 2, 3, 4 and 7 are highly representative of β-strands structures (Hennetin *et al*., 2003; K. Le Tuan *et al.* in preparation). The sequence of InvJ from *S. enterica* LT2 (gi 16766198) is shown at the bottom, below the YscP, FliK and RspP sequences, in order to illustrate the putative correspondence that can be identified using HCA with cognate T3S4 domains. In yellow are indicated some identity 'clusters' that can be identified relative to the FliK sequence, strengthening the putative relationship.
B. Representative multiple alignment of T3S4 domains, as deduced from PSI-BLAST analysis and adjusted manually, in particular considering Hydrophobic Cluster Analysis (HCA) (see before). Species and protein names are given on the left; GenBank identifiers (gi) are on the right. N- and C-termini amino acid positions are also indicated. Stars indicate the C-terminal ends of the sequences. The T3S4 domains are boxed, whereas acidic and polar amino acids (D, E, N, Q, S, T) C-terminal to the T3S4 domains are coloured in red, highlighting the presence of acidic/polar regions downstream the T3S4 domains in the YscP and FliK families. These forms 'hinge' regions separating T3S4 domains from short C-terminal globular sequences, evidenced by the presence of hydrophobic clusters (shaded grey). The SctP protein is specific of the subspecies *Iaumondii TTO1* of *Photorhabdus luminescens*. Conserved hydrophobic amino acids (V, I, L, F, M, Y, W) or amino acids that can substitute them (S, T, A, C) are boxed green, whereas other conserved positions are shaded using other colours. The secondary structure prediction, performed using JPred (Cuff and Barton, 1999), is shown beneath the alignment. H and E stand for helix and extended (β-strand) respectively.

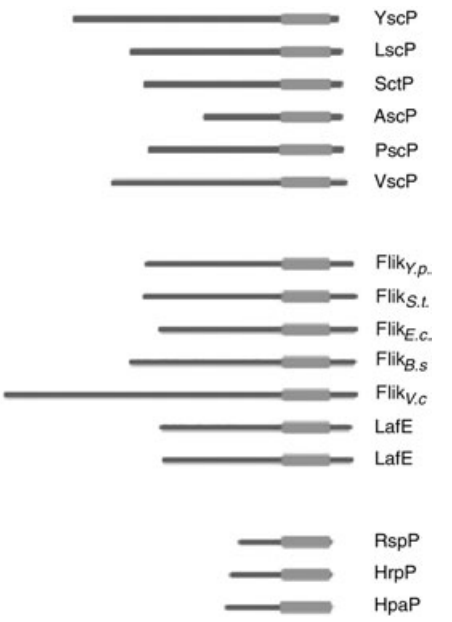

Fig. 3. Schematic representation of T3S4 domain-containing proteins equivalent to YscP from the different TTSS.

and ends the sequences in the YscP and FliK subgroups respectively. These additional secondary structure(s) (likely α-helices) might regulate the T3S4 domain function. However, deletion of this 15-residue tail from YscP had no major impact on the needle length (data not shown) and on Yop secretion (Fig. 1). In the group of proteins from plant pathogens, this tail is missing and the predicted last β-strand of the T3S4 domain ends the sequence.

Finally, additional secondary structures appeared to be present N-terminal to the first alignment block, suggesting that variable sequences might complete the T3S4 domain core.

Fold prediction methods [3DPSSM (Kelley *et al*., 2000), FUGUE (Shi *et al*., 2001)] did not highlight any known 3D structures, which might be compatible with the T3S4 domain structure.

The closest T3S4 domains are exchangeable

The overall structure of the T3S4 domain seems thus to be highly conserved among the different members of the YscP/FliK family. Not only the expected fold but also the size of the domain is the same, even though the full-length proteins are of different sizes (Fig. 3). This suggested that the T3S4 domains of different proteins could be exchanged. We tried to replace the T3S4 domain of YscP by the one of AscP (*Aeromonas salmonicida*) (Burr *et al*., 2003), PscP (*Pseudomonas aeruginosa*) and the one of FliK from *S. enterica* serovar Typhimurium and from *Yersinia pestis*. To do this, we first introduced two restriction sites on both sides of the region encoding the predicted T3S4 domains in the *yscP* gene cloned downstream from pBAD. The resulting YscP protein was still fully functional for both needle length control (data not shown) and Yop secretion (Fig. 4), suggesting that the proposed delineation of the T3S4 domain was correct and that both insertions were performed outside the domain. We then cloned the region encoding the T3S4 domain from the different proteins in the inserted sites and the recombinant plasmids were introduced in the *yscP*$^{-}$ strain. Secretion of Yops was triggered *in vitro* and monitored. The YscP hybrid proteins, in which the T3S4 domain was replaced by the T3S4 domain of AscP or PscP (40% and 38% sequence identity respectively), could restore a wild-type phenotype regarding Yop secretion. So it appears that T3S4 domains of AscP and PscP are capable of playing

the switch role of YscP although their sequence identity is limited. In contrast, the protein carrying the FliK T3S4 domain either from *S. enterica* ser Typhimurium or from *Y. pestis* could not complement the *yscP* mutant. Thus, T3S4 domains could be exchanged between proteins from the same family of injectisomes. But when it comes to exchange T3S4 domains between proteins involved in different systems such as flagellum and injectisome, the function cannot be performed any more.

We then analysed if the hybrid proteins YscP-AscP and YscP-PscP conferred needle length control. We observed by electron microscopy that the length of most needles was controlled but the control was leaky: the histograms of length distribution show a clear wt peak around 55 nm but some needles are longer (Fig. 4). Thus, it looks as though in hybrid proteins, the substrate specificity switch works but is not well controlled by the ruler.

Site-directed mutagenesis of the T3S4 domain

Based on the alignment performed using HCA and ClustalW combined, some residues appeared to be conserved. Most of them are the so-called topohydrophobic residues that are of great importance for the structure of domains and therefore their mutation would dramatically affect the structure. But there are also a few other positions conserved in all the T3S4 domains (R418, Q488), which are probably not as critical for the structure of the domain. We decided to mutate them by alanine replacement to perhaps identify residues essential for the function. These site-directed mutations were again engineered on the *yscP*$^{+}$ gene cloned in the pBADMycHisA vector, downstream from the arabinose promoter. The different constructs obtained were then transformed in the *yscP*$^{-}$ strain and secretion was monitored at 37°C after Ca^{2+} chelation. The mutants had a wild-type phenotype regarding Yop secretion (Fig. 5). Even though these two positions were conserved in all the T3S4 domains, they were not affected by an alanine replacement.

Considering that swapping the T3S4 domains between YscP, AscP and PscP yielded functional hybrids, we decided also to focus on positions conserved in the T3S4 domains of only this subgroup of proteins (Q472, E479, R480, Q482 and P486). None of the five single alanine replacements performed led to a Yop secretion mutant phenotype. The lack of effect of alanine substitutions strengthen the importance of the structure of the T3S4 domain for the function. Indeed no essential residues were highlighted beside the hydrophobic ones. Finally, we considered to mutate constitutive amino acids of the domain signature (P-x-L-G). So we performed alanine replacements of residues P440 and L442 although we were aware of the fact that a replacement of the proline could impact the local structure of the β-turn between the predicted β1 and β2 strands. The phenotype observed for the L442A mutant was wild-type for both functions (Fig. 6). In contrast, the P440A mutant secreted uniformly less Yops than wild-type bacteria. Hence, we also analysed needle length control in this mutant and found an intermediary phenotype (Fig. 6). Indeed a wt peak (55 nm) was observed but there were also needles completely deregulated, some being extra-longs. It seems thus that the domain still exerts its function in some individuals but not in others. The decreased efficiency may be attributed to a slight modification of T3S4 fold resulting from the replacement of the proline, usually crucial for the turn structure.

All the observations made are not only validating the predicted characteristics of the structure of the T3S4 domain but also pinpointing the importance of its overall structure for the function.

Discussion

We have previously reported that YscP acts as a molecular ruler and that the first 35 residues as well as the last 130 residues are required for the needle length control (Journet *et al*., 2003). We postulated from this observation that the two ends of YscP act as anchors. One end would be connected to the growing tip of the needle whereas the other end would be attached to the basal body. When YscP would be fully stretched, it would signal via its internal anchor to the secretion apparatus that would stop exporting YscF and the needle would stop growing (Journet *et al*., 2003). Here we show that the C-terminal domain, which is required for length control is also required for Yop secretion. Thus, the C-terminal domain is required for the two functions of YscP: control of Yop secretion and control of needle length. Such a dual function has previously been shown for FliK, which controls secretion of flagellin as well as the length of the hook of the flagellum (Williams *et al*., 1996; Minamino and Macnab, 2000; Minamino *et al*., 2004). To explain this phenotype, Williams *et al*. (Williams *et al*., 1996) suggested that

Fig. 4. Swapping of the T3S4 domains.
A. Coomassie stained SDS-PAGE of culture supernatants of *Y. enterocolitica* MRS40(pLJ4036) complemented with 1 pLJ6 (wild-type YscP, control); 2 pCA88 (introduction of a *Xba*I restriction site); 3 pCA89 (*Xba*I and *Bgl*II restriction sites); 4 pCA90 (T3S4 of AscP); 5 pCA91 (T3S4 of $FliK_{S.t.}$); 6 pCA92 (T3S4 of PscP); 7 pCA93 (T3S4 of $FliK_{Y.p.}$). The size of YscP is indicated by an arrow.
B. Histograms of the needle length measurements, and electron micrographs of *yscP*$^{-}$ + pCA90 (T3S4 of AscP) and *yscP*$^{-}$ + pCA91 (T3S4 of FliK). M, mean of the lengths; N, number of needles measured.

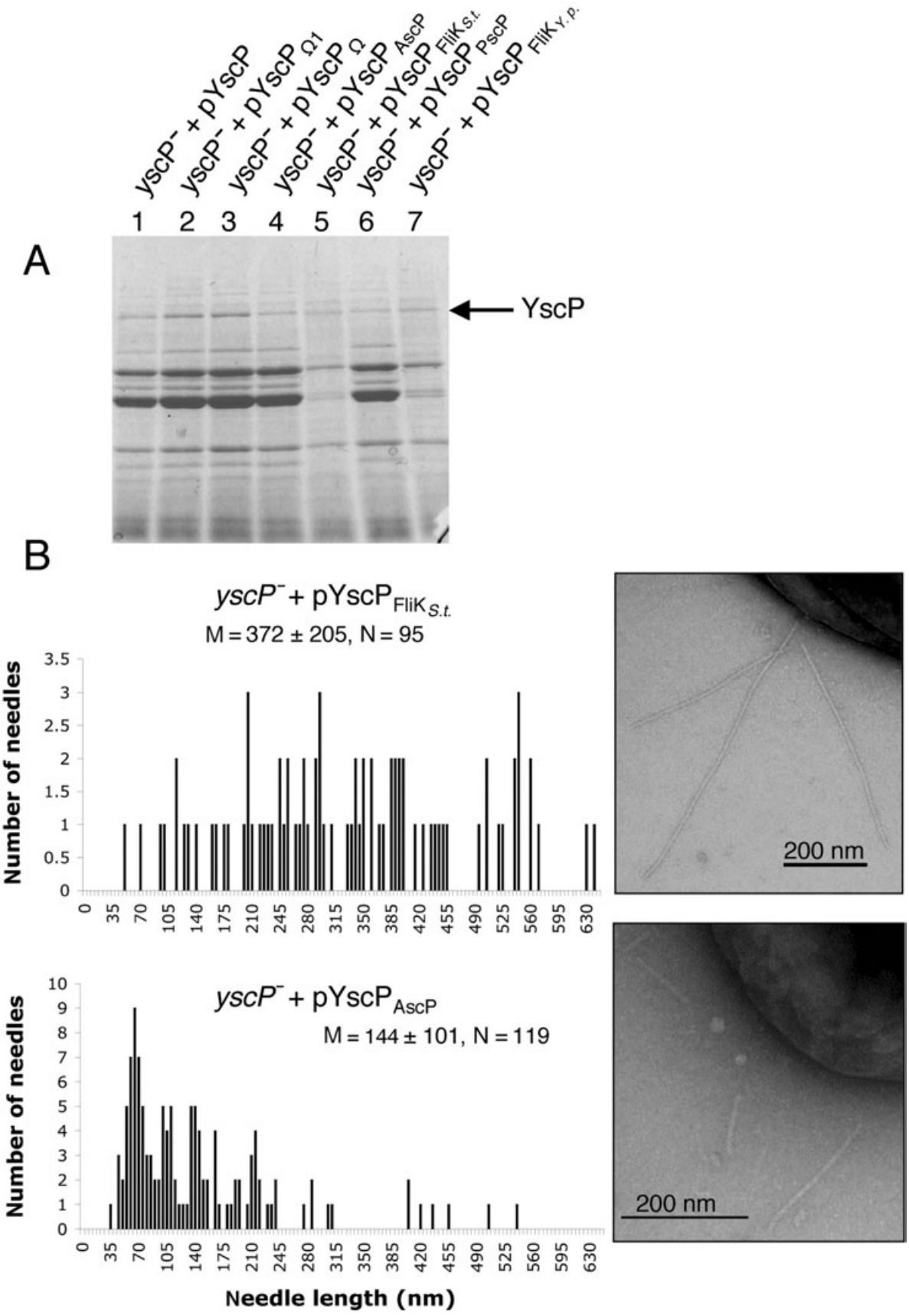
yscP⁻ + pYscP
yscP⁻ + pYscP Ω1
yscP⁻ + pYscP Ω
yscP⁻ + pYscP AscP
yscP⁻ + pYscP FliK S.t.
yscP⁻ + pYscP PscP
yscP⁻ + pYscP FliK Y.p.
1 2 3 4 5 6 7
A
YscP
B
yscP⁻ + pYscP FliK S.t.
M = 372 ± 205, N = 95
Number of needles
200 nm
yscP⁻ + pYscP AscP
M = 144 ± 101, N = 119
Number of needles
200 nm
Needle length (nm)

FliK would act on the basal body protein FlhB to switch the substrate specificity of the export apparatus. In other words, FliK would control the length of the hook by switching the export apparatus from hook subunit secretion to flagellin secretion. This interpretation was further supported by the isolation of suppressors of *fliK* mutations, which mapped in *flhB* (Minamino and Macnab, 2000; Fraser *et al*., 2003a). YscU from the basal body of the *Yersinia* Ysc injectisome is quite similar to FlhB, which prompted the group of H. Wolf-Watz to engineer *yscU* mutations, which were similar to the suppressive *flhB* mutations. As expected by the authors, these mutations turned out to be suppressive of *yscP* mutations (Edqvist *et al*., 2003) indicating that YscP presumably exerts the same switch function as FliK does. FliK consists of three regions: an N-terminal region, a proline-rich central region, and a C-terminal region highly conserved among FliK proteins from different species (Kawagishi *et al*., 1996; Williams *et al*., 1996). This C-terminal region is thought to be the region of FliK that interacts with FlhB (Suzuki and Iino, 1981; Williams *et al*., 1996; Minamino *et al*., 1999). We show here that this domain shares structural properties with the C-terminal domain of YscP, the domain which precisely controls Yop secretion. We can thus refine our model and postulate that the N-terminus of YscP is attached to the growing needle while the C-terminus would stay in the secretion apparatus and switch the substrate specificity from YscF to Yops by interacting with YscU.

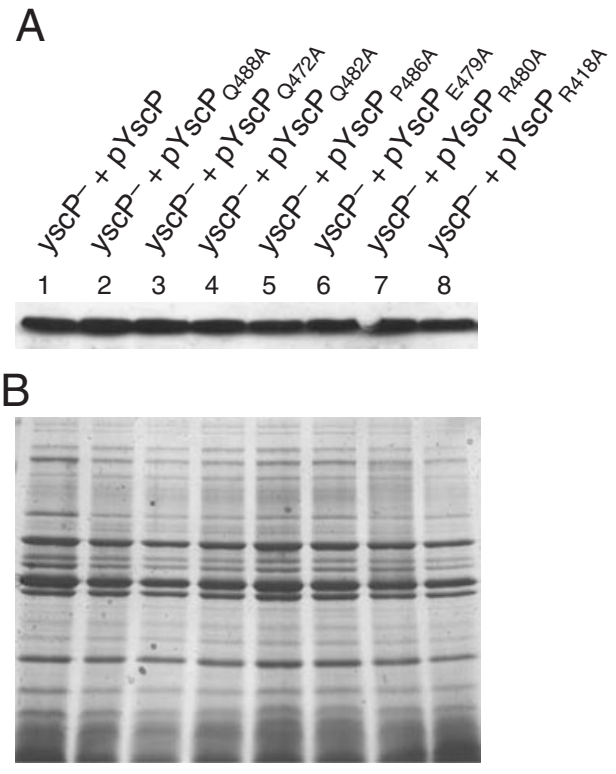

Fig. 5. Site-directed mutagenesis of T3S4.
A. Western blot analysis (total cells; polyclonal anti-YscP antibody) of 1 *yscP*$^-$ + pLJ6 (YscP wt); 2 *yscP*$^-$ + pCAP77; 3 *yscP*$^-$ + pCAP78; 4 *yscP*$^-$ + pCA79; 5 *yscP*$^-$ + pCAP80; 6 *yscP*$^-$ + pCAP81; 7 *yscP*$^-$ + pCAP82; 8 *yscP*$^-$ + pCAP85.
B. Yops proteins secreted by the same *Y. enterocolitica* E40 strains as in A (Coomassie stained SDS-PAGE).

Orthologues to YscP share less sequence similarity than any other component of injectisomes. Although YscP and FliK seem to perform the same function, they share very little similarity. However, the HCA performed here showed that the switch is a globular domain whose structure is conserved in orthologues, both in injectisomes and in flagella. In addition, according to fold prediction algorithms, this globular domain does not seem to adopt any known 3D structure. This domain that we called T3S4 thus defines a new family of proteins involved in length determination, which we propose to call the 'FliK/YscP' family. In good agreement with this conclusion, the T3S4 domain of AscP (from *A. salmonicida*) and the T3S4 domain from PscP (from *P. aeruginosa*) could replace the T3S4 domain of YscP and direct Yop secretion. However, the T3S4 domain from FliK was inactive when fused to the ruler part of YscP, showing that the interaction between the T3S4 and the secretion apparatus is rather specific. Interestingly, all the conserved residues between T3S4 domains appear to be hydrophobic, which suggests that the T3S4 domain has no catalytic activity. Proteins of the YscP/FliK family would thus not be directly responsible for the proteolytic cleavage of FlhB and YscU, which has been shown to occur when the substrate specificity changes (Fraser *et al*., 2003a; Lavander *et al*., 2003).

A recent biochemical analysis showed that FliK is monomeric in solution and has an elongated shape (Minamino *et al*., 2004). In addition, the C-terminal switch domain is more globular than full-length FliK. Our results are in perfect agreement with these data. Moreover, the authors cite unpublished results from T. Minamino and R. MacNab demonstrating that FliK interacts with the hook-capping protein FlgD and propose for FliK a model very similar to the one we proposed for YscP, namely that the N-terminal half of FliK within the central channel of the hook-basal body transmits the hook length information to the switch domain that then interacts with FlhB (Minamino *et al*., 2004). The study of YscP and FliK thus nicely converge to a similar general structure and a similar working model.

An interesting observation that arose from the experiments described in this paper is that the two phenotypes of *yscP* null mutants, loss of length control and failure to secrete Yops can be dissociated. Indeed, unlike mutants in the T3S4 domain, mutants that are deprived of the N-terminus of YscP do secrete Yops but fail to control length of the needle (Journet *et al*., 2003). One possible expla-

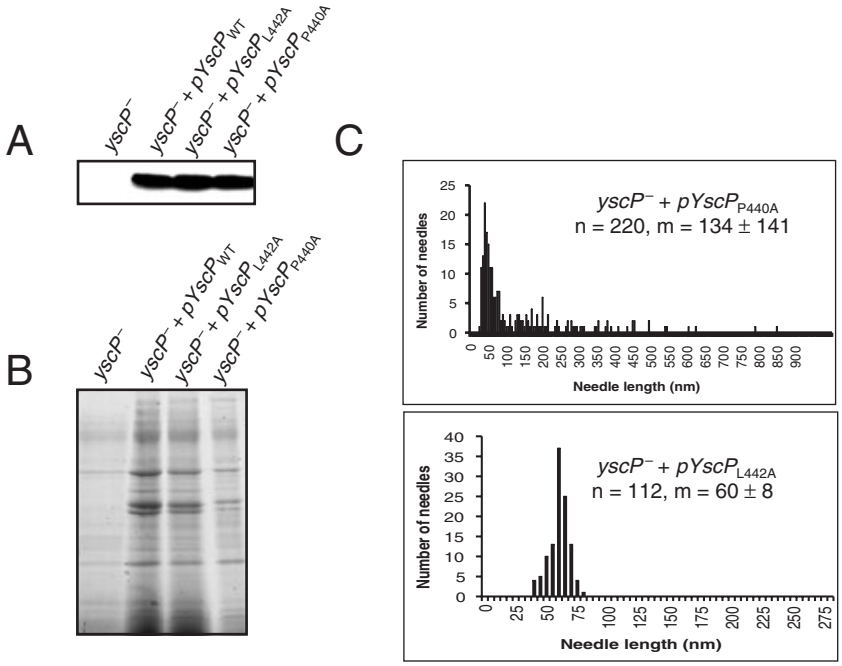

Fig. 6. Site-directed mutagenesis of the signature.
A. Western blot analysis (total cells; polyclonal anti-YscP antibody) of *yscP*⁻; *yscP*⁻ + pLJ6 (YscP wt); *yscP*⁻ + pCAP83 ($YscP_{L442\rightarrow A}$); *yscP*⁻ + pCAP86 ($YscP_{P440\rightarrow A}$).
B. Yops proteins secreted by the same *Y. enterocolitica* E40 strains as in A (Coomassie stained SDS-PAGE).
C. Histograms of the needle length measurement of the same strains as in A. Note the difference in scale of the *x*-axes.

nation would be that when the YscP constructs are deprived of one of their anchors the switch could operate at random, independently of the trigger given by the stretching of the ruler. In bacteria harbouring such constructs, the model would predict that the needle size would be variable but Yop secretion would occur from needles that have stopped growing. This is compatible with the observed phenotype but it could not be taken as a proof for the model unless one could demonstrate that only needles that have stopped growing do secrete Yops.

Although the model can account for the phenotype of mutants that do no longer tightly control the needle length but still secrete Yops, it predicts that mutants with the opposite phenotype (normal length but no Yop secretion) are unlikely to occur. Indeed, an arrest in the elongation of the needle implies that the secretion of YscF is switched off and thus that the switch is functional. None of the *yscP* mutants analysed to date displayed such a phenotype. In the flagellum also no *fliK* mutants controlling hook length but unable to initiate filament assembly were ever described (Williams *et al*., 1996).

According to our present study of the domain, a full understanding of its functions will probably have to await the determination of its 3D structure as well as that of its potential interacting partner YscU.

Experimental procedures

Sequence analysis

Similarity searches were performed using PSI-BLAST (Altschul *et al*., 1997) and HMMer(Eddy, 1998). The bidimensional HCA (Gaboriaud *et al*., 1987; Woodcock S., 1992; Callebaut *et al*., 1997) was used for refining the proposed similarities.

Secondary structure prediction was performed using Jpred (Cuff and Barton, 1999). FUGUE (Shi *et al*., 2001) and 3D-PSSM (Kelley *et al*., 2000) were used for fold recognition.

Induction of the yop *regulon and Yop secretion analysis*

Bacteria were routinely grown on Luria–Bertani agar plates and in liquid LB medium. For the induction of the *yop* regulon, *Y. enterocolitica* bacteria were inoculated to an OD_{600} of 0.1 and cultivated in brain–heart infusion (BHI; Remel) supplemented with 4 mg ml^{-1} glycerol, 20 mM $MgCl_2$ and 20 mM sodium oxalate (BHI-Ox) 2H at 22°C, then shifted to 37°C and incubated for 4 h. Expression of the different *yscP* genes cloned downstream from the pBAD promoter was induced by adding 0.2% arabinose to the culture just before the shift at 37°C, and again 2 h later. Ampicillin was used at a concentration of 200 μg ml^{-1} to select for the expression plasmids.

Proteins from the supernatant were precipitated overnight at 4°C with trichloroacetic acid 10% (w/v) final. Electrophoresis was carried out in 12% or 15% (w/v) polyacrylamide gels in the presence of SDS (SDS-PAGE). Proteins secreted by 3×10^8 bacteria were loaded per lane. For the total bacterial cells, the proteins from 10^7 bacteria were loaded per lane. After electrophoresis, proteins were stained with Coomassie brilliant blue (Pierce) or transferred by electroblotting to a nitrocellulose membrane. Immunoblotting was carried out using a polyclonal rabbit anti-YscP antibody (MIPA57).

Detection of immunoblots was performed with a secondary antibody conjugated to horseradish peroxidase (1:2000; Dako) before development with supersignal chemiluminescent substrate (Pierce).

Electron microscopy

Visualization of the needle-like structures at the cell surface of the bacteria was performed by electron microscopy as described by Hoiczyk and Blobel (Hoiczyk and Blobel, 2001). After 4 h of induction at 37°C, bacteria were harvested at 2000 *g* and resuspended gently in 20 mM Tris-HCl, pH 7.5. Droplets were applied for 1 min to freshly glow-discharged, formvar-carbon coated grids, and negatively stained with 2% (w/v) uranylacetate. Bacteria were visualized in a Philips Morgagni 268D electron microscope at a nominal magnification of ×44 000 or 27 000 and an acceleration voltage of

Table 1. Plasmids used in this work.

Plasmids	Encoded protein	Genotype or description	Source or reference
pYV			
pYV40		Wild-type virulence plasmid from strain *Y. enterocolitica* E40	Sory *et al.* (1995)
pLJ4036		pYV40 *yscP*$^-$	This work
Clones			
pBADMycHisA			Invitrogen
pCA1	YscP$_{\Delta 1-15}$	*pBADMycHisA – yscP*$_{\Delta 1-15}$	Journet *et al.* (2003)
pCA18	YscP$_{\Delta 385-424}$	*pBADMycHisA – yscP*$_{\Delta 385-424}$	Journet *et al.* (2003)
pCA5	YscP$_{\Delta 16-25}$	*pBADMycHisA – yscP*$_{\Delta 16-25}$	Journet *et al.* (2003)
pCA6	YscP$_{\Delta 26-35}$	*pBADMycHisA – yscP*$_{\Delta 26-35}$	Journet *et al.* (2003)
pCA7	YscP$_{\Delta 36-45}$	*pBADMycHisA – yscP*$_{\Delta 36-45}$	Journet *et al.* (2003)
pCA79	YscP$_{Q482\rightarrow A}$	Replacement of Q482 by alanine by inverse PCR on pLJ6 using oligonucleotides 3467 and 3468	This work
pCA83	YscP$_{L442\rightarrow A}$	Replacement of L442 by alanine by inverse PCR on pLJ6 using oligonucleotides 3460 and 3461	This work
pCA86	YscP$_{P440\rightarrow A}$	Replacement of P440 by alanine by inverse PCR on pLJ6 using oligonucleotides 3458 and 3459	
pCA88	YscP$_{\Omega 1}$	Introduction of a *Xba*I site between codons 405 and 406 of *yscP*$_{entero}$ by inverse PCR on pLJ6 using oligonucleotides 3478 and 3479	This work
pCA89	YscP$_{\Omega}$	Introduction of a *Bgl*II site between codons 495 and 496 of *yscP*$_{entero}$ by inverse PCR on pCA88 using oligonucleotides 3480 and 3481	This work
pCA9	YscP$_{\Delta 46-96}$	*pBADMycHisA – yscP*$_{\Delta 46-96}$	Journet *et al.* (2003)
pCA90	YscP$_{\Omega T3S4AscP}$	Insertion of aa 149 to aa 238 from AscP (*Aeromonas salmonicida*), amplified using oligonucleotides 3487 and 3488, into YscP$_{\Omega}$	This work
pCA91	YscP$_{\Omega T3S4FliK S.t.}$	Insertion of aa 268 to aa 353 from FliK (*Salmonella typhimurium* LT2), amplified using oligonucleotides 3476 and 3477, into YscP$_{\Omega}$	This work
pCA92	YscP$_{\Omega T3S4PscP}$	Insertion of aa 263 to aa 348 from PscP (*Pseudomonas aeruginosa*), amplified using oligonucleotides 3569 and 3570, into YscP$_{\Omega}$	This work
pCA93	YscP$_{\Omega T3S4FliK Y.p.}$	Insertion of aa 261 to aa 348 from FliK (*Yersinia pestis*), amplified using oligonucleotides 3567 and 3568, into YscP$_{\Omega}$	This work
pCAP19	YscP$_{\Delta 425-464}$	Deletion from pLJ6 using oligonucleotides 3244 and 3245	This work
pCAP47	YscP$_{\Delta 97-137}$	Deletion of codons 97–137 of *yscP*$_{entero}$ from pLJ6 by inverse PCR using phosphorylated oligonucleotides 3318 and 3319, followed by a ligation	This work
pCAP48	YscP$_{\Delta 137-177}$	Deletion of codons 137–177 of *yscP*$_{entero}$ from pLJ6 by inverse PCR using phosphorylated oligonucleotides 3320 and 3321, followed by a ligation	This work
pCAP49	YscP$_{\Delta 177-197}$	Deletion of codons 177–197 of *yscP*$_{entero}$ from pLJ6 by inverse PCR using phosphorylated oligonucleotides 3322 and 3323, followed by a ligation	This work
pCAP50	YscP$_{\Delta 197-216}$	Deletion of codons 197–216 of *yscP*$_{entero}$ from pLJ6 by inverse PCR using phosphorylated oligonucleotides 3338 and 3339, followed by a ligation	This work
pCAP56	YscP$_{\Delta 465-485}$	Deletion from pLJ6 using oligonucleotides 3340 and 3341	This work
pCA57	YscP$_{\Delta 485-500}$	Deletion from pLJ6 using oligonucleotides 3342 and 3343	This work
pCAP77	YscP$_{Q488\rightarrow A}$	Replacement of Q488 by alanine by inverse PCR on pLJ6 using oligonucleotides 3462 and 3464	This work
pCAP78	YscP$_{Q472\rightarrow A}$	Replacement of Q472 by alanine by inverse PCR on pLJ6 using oligonucleotides 3465 and 3466	This work
pCAP80	YscP$_{P486\rightarrow A}$	Replacement of P486 by alanine by inverse PCR on pLJ6 using oligonucleotides 3469 and 3470	This work
pCAP81	YscP$_{E479\rightarrow A}$	Replacement of E479 by alanine by inverse PCR on pLJ6 using oligonucleotides 3472 and 3473This work	
pCAP82	YscP$_{R480\rightarrow A}$	Replacement of R480 by alanine by inverse PCR on pLJ6 using oligonucleotides 3474 and 3475	This work
pCAP85	YscP$_{R418\rightarrow A}$	Replacement of R418 by alanine by inverse PCR on pLJ6 using oligonucleotides 3456 and 3457	This work
pLJ11	YscP$_{\Delta 222-306}$	*pBADMycHisA – yscP*$_{\Delta 222-306}$	Journet *et al.* (2003)
pLJ6	YscP$_{wt}$	*pBADMycHisA – yscP*$_{E40}$	Journet *et al.* (2003)
pLJ7	YscP$_{\Delta 222-381}$	*pBADMycHisA – yscP*$_{\Delta 222-381}$	Journet *et al.* (2003)
pLJC12	YscP$_{\Delta 501-515}$	Cloning of the YscP$_{\Delta 501-515}$ coding sequence, amplified by a PCR on pYV40 using oligonucleotides 3064 and 3072 (introducing *Nco*I and *Eco*RI sites respectively), in *Nco*I and *Eco*RI sites of pBADMycHisA	This work

Table 2. Oligonucleotides used in this work.

Codes	Oligonucleotides	Underlined sites
3064	GATCGAATTCTTACTCCTGTTCACTGTCAC	*Eco*RI site
3072	GATCCCATGGCCAATAAAATCACCACTCGT	*Nco*I site
3244	TTCTAGTTCTACCGCTAG	
3245	GAAGCTTTAAGAATTTTA	
3318	ATTATTCTGATGGTTGTGTTG	
3319	TTTTTAAAGGGGGTGACTTGT	
3320	CGCCAATGGCATGAGAGCATT	
3321	AATACCAAGCCGACTGTTCAG	
3322	TTGAACTGGCTGAACGGAATC	
3323	TGGTCTGTCGGTAGGGAAACT	
3338	CAAAAACGCCTTGCAGAAGAA	
3339	AATAACCTCTGCGCCGTCAGC	
3340	CTGACTGGCGATCAGTTCTAC	
3341	CCAACACAACTTGATTTTCAA	
3342	AATGCGTTGTAATCGCTCAAG	
3343	TCACGTCAGAAGCGCCACGTC	
3456	CTAGTTCTACCGCTAGTGCCTGTGCTAACTGTAT	
3457	ATACAGTTAGCACAGGCACTAGCGGTAGAACTAG	
3458	CAATTACACCTTAACTTAGCTGAATTGGGGGCTATTATG	
3459	CATAATAGCCCCCAATTCAGCTAAGTTAAGGTGTAATTG	
3460	CTTAACTTACCTGAAGCGGGGGCTATTATGGTT	
3461	AACCATAATAGCCCCCGCTTCAGGTAAGTTAAG	
3462	CGCATTGAGCCAACAGCACTTGATTTTCAAGCT	
3464	AGCTTGAAAATCAAGTGCTGTTGGCTCAATGCG	
3465	GCTTTAAGAATTTTAGCGGCGGGAAGTTATGACCTTCTT	
3466	AAGAAGGTCATAACTTCCCGCCGCTAAAATTCTTAAAGC	
3467	CTTCTTGAGCGATTAGCACGCATTGAGCCAACA	
3468	TGTTGGCTCAATGCGTGCTAATCGCTCAAGAAG	
3469	CGATTACAACGCATTGAGGCAACACAACTTGATTTTCAA	
3470	TTGAAAATCAAGTTGTGTTGCCTCAATGCGTTGTAATCG	
3472	AAGTTATGACCTTCTTGCGCGATTACAACGCATTG	
3473	CAATGCGTTGTAATCGCGCAAGAAGGTCATAACTT	
3474	AGTTATGACCTTCTTGAGGCATTACAACGCATTGAGCCA	
3475	TGGCTCAATGCGTTGTAATGCCTCAAGAAGGTCATAACT	
3476	GCCCTCTAGAAGCCATGAATGGCAG	*Xba*I site
3477	GCCCAGATCTGCTACTGATACTGCT	*Bgl*II site
3478	TGAGACTGATGTTCTAGACAGCCTCGTCGC	*Xba*I site
3479	GCGACGAGGCTGTCTAGAACATCAGTCTCA	*Xba*I site
3480	CTGTTCACTGTCAGATCTACCGCTAGCTTG	*Bgl*II site
3481	CAAGCTAGCGGTAGATCTGACAGTGAACAG	*Bgl*II site
3487	GCCCTCTAGAAGTAATCGGGAGCTG	*Xba*I site
3488	GCCCAGATCTGTTAAAGAGATCGAG	*Bgl*II site
3567	GCCCTCTAGAGAGTGGCCGCAACAA	*Xba*I site
3568	GCCCAGATCTAGCCGAAACCTGTAC	*Bgl*II site
3569	GCCCTCTAGACTCGCGCGCCTGCTC	*Xba*I site
3570	GCCCAGATCTCTGGTTGAAGGTGAG	*Bgl*II site

80 kV. Sizes were measured with the 'Soft Imaging System' software (Hamburg, Germany).

Construction of plasmids

The full list of plasmids used in this study is given in Table 1. DNA amplification for cloning purposes was made using the oligonucleotides listed in Table 2 and the Vent polymerase (Biolabs). Deletions were generated by inverse polymerase chain reaction, using the Pfu turbo polymerase (Stratagene). Both strands of each construct were sequenced using 3100-*Avant* genetic analyser (ABI Prism).

Acknowledgements

We thank M. Dürrenberger, G. Morson and U.M. Spornitz for use of electron microscopy facilities. We also thank J.M. Meyer for providing *Pseudomonas aeruginosa* PAO1 strain, K. Hughes for *Salmonella typhimurium* LT2 strain and J. Frey for *Aeromona salmonicida* JF2267. This work was supported by the Swiss National Science Foundation (Grant 32-65393.01).

References

Aizawa, S.I. (2001) Bacterial flagella and type III secretion systems. *FEMS Microbiol Lett* **202:** 157–164.

Allaoui, A., Woestyn, S., Sluiters, C., and Cornelis, G.R. (1994) YscU, a *Yersinia enterocolitica* inner membrane protein involved in Yop secretion. *J Bacteriol* **176:** 4534–4542.

Altschul, S.F., Madden, T.L., Schaffer, A.A., Zhang, J., Zhang, Z., Miller, W., and Lipman, D.J. (1997) Gapped

BLAST and PSI-BLAST: a new generation of protein database search programs. *Nucleic Acids Res* **25:** 3389–3402.
Anderson, D.M., and Schneewind, O. (1999) Type III machines of Gram-negative pathogens: injecting virulence factors into host cells and more. *Curr Opin Microbiol* **2:** 18–24.
Blocker, A., Gounon, P., Larquet, E., Niebuhr, K., Cabiaux, V., Parsot, C., and Sansonetti, P. (1999) The tripartite type III secreton of *Shigella flexneri* inserts IpaB and IpaC into host membranes. *J Cell Biol* **147:** 683–693.
Blocker, A., Komoriya, K., and Aizawa, S. (2003) Type III secretion systems and bacterial flagella: insights into their function from structural similarities. *Proc Natl Acad Sci USA* **100:** 3027–3030.
Burr, S.E., Wahli, T., Segner, H., Pugovkin, D., and Frey, J. (2003) Association of Type III secretion genes with virulence of *Aeromonas salmonicida* subsp. salmonicida. *Dis Aquat Organ* **57:** 167–171.
Callebaut, I., Labesse, G., Durand, P., Poupon, A., Canard, L., Chomilier, J., *et al.* (1997) Deciphering protein sequence information through hydrophobic cluster analysis (HCA): current status and perspectives. *Cell Mol Life Sci* **53:** 621–645.
Cornelis, G.R. (2002) *Yersinia* type III secretion: send in the effectors. *J Cell Biol* **158:** 401–408.
Cornelis, G.R., and Van Gijsegem, F. (2000) Assembly and function of type III secretory systems. *Annu Rev Microbiol* **54:** 735–774.
Cornelis, G.R., and Wolf-Watz, H. (1997) The *Yersinia* Yop virulon: a bacterial system for subverting eukaryotic cells. *Mol Microbiol* **23:** 861–867.
Cuff, J.A., and Barton, G.J. (1999) Evaluation and improvement of multiple sequence methods for protein secondary structure prediction. *Proteins* **34:** 508–519.
Dale, C., Young, S.A., Haydon, D.T., and Welburn, S.C. (2001) The insect endosymbiont *Sodalis glossinidius* utilizes a type III secretion system for cell invasion. *Proc Natl Acad Sci USA* **98:** 1883–1888.
Dale, C., Plague, G.R., Wang, B., Ochman, H., and Moran, N.A. (2002) Type III secretion systems and the evolution of mutualistic endosymbiosis. *Proc Natl Acad Sci USA* **99:** 12397–12402.
Eddy, S.R. (1998) Profile hidden Markov models. *Bioinformatics* **14:** 755–763.
Edqvist, P.J., Olsson, J., Lavander, M., Sundberg, L., Forsberg, A., Wolf-Watz, H., and Lloyd, S.A. (2003) YscP and YscU regulate substrate specificity of the *Yersinia* type III secretion system. *J Bacteriol* **185:** 2259–2266.
Fields, K.A., Plano, G.V., and Straley, S.C. (1994) A low-Ca2+ response (LCR) secretion (ysc) locus lies within the lcrB region of the LCR plasmid in *Yersinia pestis*. *J Bacteriol* **176:** 569–579.
Foultier, B., Troisfontaines, P., Müller, S., Opperdoes, F., and Cornelis, G.R. (2002) Characterization of the *ysa* pathogenicity locus in the chromosome of *Yersinia enterocolitica* and phylogeny analysis of type III secretion systems. *J Mol Evol* **55:** 37–51.
Fraser, G.M., Gonzalez-Pedrajo, B., Tame, J.R., and Macnab, R.M. (2003a) Interactions of FliJ with the *Salmonella* type III flagellar export apparatus. *J Bacteriol* **185:** 5546–5554.
Fraser, G.M., Hirano, T., Ferris, H.U., Devgan, L.L., Kihara, M., and Macnab, R.M. (2003b) Substrate specificity of type III flagellar protein export in *Salmonella* is controlled by subdomain interactions in FlhB. *Mol Microbiol* **48:** 1043–1057.
Gaboriaud, C., Bissery, V., Benchetrit, T., and Mornon, J.P. (1987) Hydrophobic cluster analysis: an efficient new way to compare and analyse amino acid sequences. *FEBS Lett* **224:** 149–155.
Galan, J.E., and Collmer, A. (1999) Type III secretion machines: bacterial devices for protein delivery into host cells. *Science* **284:** 1322–1328.
Hennetin, J., Le, T.K., Canard, L., Colloc'h, N., Mornon, J.P., and Callebaut, I. (2003) Non-intertwined binary patterns of hydrophobic/nonhydrophobic amino acids are considerably better markers of regular secondary structures than non-constrained patterns. *Proteins* **51:** 236–244.
Hoiczyk, E., and Blobel, G. (2001) Polymerization of a single protein of the pathogen *Yersinia enterocolitica* into needles punctures eukaryotic cells. *Proc Natl Acad Sci USA* **98:** 4669–4674.
Journet, L., Agrain, C., Broz, P., and Cornelis, G.R. (2003) The needle length of bacterial injectisomes is determined by a molecular ruler. *Science* **302:** 1757–1760.
Kawagishi, I., Homma, M., Williams, A.W., and Macnab, R.M. (1996) Characterization of the flagellar hook length control protein fliK of *Salmonella typhimurium* and *Escherichia coli*. *J Bacteriol* **178:** 2954–2959.
Kelley, L.A., MacCallum, R.M., and Sternberg, M.J. (2000) Enhanced genome annotation using structural profiles in the program 3D-PSSM. *J Mol Biol* **299:** 499–520.
Kimbrough, T.G., and Miller, S.I. (2000) Contribution of *Salmonella typhimurium* type III secretion components to needle complex formation. *Proc Natl Acad Sci USA* **97:** 11008–11013.
Knutton, S., Rosenshine, I., Pallen, M.J., Nisan, I., Neves, B.C., Bain, C., *et al.* (1998) A novel EspA-associated surface organelle of enteropathogenic *Escherichia coli* involved in protein translocation into epithelial cells. *EMBO J* **17:** 2166–2176.
Kubori, T., Matsushima, Y., Nakamura, D., Uralil, J., Lara-Tejero, M., Sukhan, A., *et al.* (1998) Supramolecular structure of the *Salmonella typhimurium* type III protein secretion system. *Science* **280:** 602–605.
Kubori, T., Sukhan, A., Aizawa, S.I., and Galan, J.E. (2000) Molecular characterization and assembly of the needle complex of the *Salmonella typhimurium* type III protein secretion system. *Proc Natl Acad Sci USA* **97:** 10225–10230.
Kutsukake, K., Minamino, T., and Yokoseki, T. (1994) Isolation and characterization of FliK-independent flagellation mutants from *Salmonella typhimurium*. *J Bacteriol* **176:** 7625–7629.
Lavander, M., Sundberg, L., Edqvist, P.J., Lloyd, S.A., Wolf-Watz, H., and Forsberg, A. (2003) Characterisation of the type III secretion protein YscU in *Yersinia pseudotuberculosis*. YscU cleavage – dispensable for TTSS but essential for survival. *Adv Exp Med Biol* **529:** 109–112.
Magdalena, J., Hachani, A., Chamekh, M., Jouihri, N., Gounon, P., Blocker, A., and Allaoui, A. (2002) Spa32 regulates a switch in substrate specificity of the type III

secreton of *Shigella flexneri* from needle components to Ipa proteins. *J Bacteriol* **184:** 3433–3441.

Makishima, S., Komoriya, K., Yamaguchi, S., and Aizawa, S.I. (2001) Length of the flagellar hook and the capacity of the type III export apparatus. *Science* **291:** 2411–2413.

Marlovits, T.C., Kubori, T., Sukhan, A., Thomas, D.R., Galan, J.E., and Unger, V.M. (2004) Structural insights into the assembly of the Type III secretion needle complex. *Science* **306:** 1040–1042.

Minamino, T., and Macnab, R.M. (2000) Domain structure of *Salmonella* FlhB, a flagellar export component responsible for substrate specificity switching. *J Bacteriol* **182:** 4906–4914.

Minamino, T., Gonzalez-Pedrajo, B., Yamaguchi, K., Aizawa, S.I., and Macnab, R.M. (1999) FliK, the protein responsible for flagellar hook length control in *Salmonella*, is exported during hook assembly. *Mol Microbiol* **34:** 295–304.

Minamino, T., Saijo-Hamano, Y., Furukawa, Y., Gonzalez-Pedrajo, B., Macnab, R.M., and Namba, K. (2004) Domain organization and function of *Salmonella* FliK, a flagellar hook-length control protein. *J Mol Biol* **341:** 491–502.

Patterson-Delafield, J., Martinez, R.J., Stocker, B.A., and Yamaguchi, S. (1973) A new fla gene in *Salmonella typhimurium* – flaR – and its mutant phenotype-superhooks. *Arch Mikrobiol* **90:** 107–120.

Plano, G.V., Day, J.B., and Ferracci, F. (2001) Type III export: new uses for an old pathway. *Mol Microbiol* **40:** 284–293.

Roine, E., Wei, W., Yuan, J., Nurmiaho-Lassila, E.L., Kalkkinen, N., Romantschuk, M., and He, S.Y. (1997) Hrp pilus: an hrp-dependent bacterial surface appendage produced by *Pseudomonas syringae* pv. *tomato* DC3000. *Proc Natl Acad Sci USA* **94:** 3459–3464.

Shi, J., Blundell, T.L., and Mizuguchi, K. (2001) FUGUE: sequence-structure homology recognition using environment-specific substitution tables and structure-dependent gap penalties. *J Mol Biol* **310:** 243–257.

Sory, M.P., Boland, A., Lambermont, I., and Cornelis, G.R. (1995) Identification of the YopE and YopH domains required for secretion and internalization into the cytosol of macrophages, using the cyaA gene fusion approach. *Proc Natl Acad Sci USA* **92:** 11998–12002.

Stainier, I., Bleves, S., Josenhans, C., Karmani, L., Kerbourch, C., Lambermont, I., *et al.* (2000) YscP, a *Yersinia* protein required for Yop secretion that is surface exposed, and released in low Ca2+. *Mol Microbiol* **37:** 1005–1018.

Sukhan, A., Kubori, T., and Galan, J.E. (2003) Synthesis and localization of the *Salmonella* SPI-1 type III secretion needle complex proteins PrgI and PrgJ. *J Bacteriol* **185:** 3480–3483.

Suzuki, T., and Iino, T. (1981) Role of the flaR gene in flagellar hook formation in *Salmonella* spp. *J Bacteriol* **148:** 973–979.

Tamano, K., Katayama, E., Toyotome, T., and Sasakawa, C. (2002) Shigella Spa32 is an essential secretory protein for functional type III secretion machinery and uniformity of its needle length. *J Bacteriol* **184:** 1244–1252.

Van Gijsegem, F., Gough, C., Zischek, C., Niqueux, E., Arlat, M., Genin, S., *et al.* (1995) The hrp gene locus of *Pseudomonas solanacearum*, which controls the production of a type III secretion system, encodes eight proteins related to components of the bacterial flagellar biogenesis complex. *Mol Microbiol* **15:** 1095–1114.

Van Gijsegem, F., Vasse, J., Camus, J.C., Marenda, M., and Boucher, C. (2000) Ralstonia solanacearum produces hrp-dependent pili that are required for PopA secretion but not for attachment of bacteria to plant cells. *Mol Microbiol* **36:** 249–260.

Viprey, V., Del Greco, A., Golinowski, W., Broughton, W.J., and Perret, X. (1998) Symbiotic implications of type III protein secretion machinery in *Rhizobium*. *Mol Microbiol* **28:** 1381–1389.

Williams, A.W., Yamaguchi, S., Togashi, F., Aizawa, S.I., Kawagishi, I., and Macnab, R.M. (1996) Mutations in fliK and flhB affecting flagellar hook and filament assembly in *Salmonella typhimurium*. *J Bacteriol* **178:** 2960–2970.

Woodcock, S., M.J., and Henrissat, B. (1992) Detection of secondary structure elements in proteins by hydrophobic cluster analysis. *Protein Eng* **5:** 629–635.

3-RESULTS

3.3- Secretion of YscP from *Yersinia enterocolitica* is essential to control the length of the injectisome needle but not to change the Type III secretion substrate specificity,

Agrain, C., Sorg, I., Paroz, C., and Cornelis, G.R.

Mol Microbiol 57: 1415-1427 (2005)

Summary

YscP, which acts both as a molecular ruler and as a substrate-specificity switch for type III secretion is also itself secreted by the injectisome. Therefore, we wondered whether its export is necessary for its functions and why YscP is secreted. By a systematic deletion analysis and by fusing different parts of the molecule to a reporter, two distinct secretion signals in YscP could be found: one in its N-term (aa 1-35) and one more central (aa 97-137). These two signals are functionally different from Yop secretion signals. When both secretion signals were removed, Yops could still be secreted but the needle length control was lost. In fact, the needle length control was already affected when only one signal was removed but the control could be improved by producing and thereby secreting more YscPs. The two signals exactly correspond to the N-term regions involved in needle length control. These data suggest a model in which YscP export is linked to needle length control.

The EM work (measurements and pictures) was done jointly with Dr. Isabel Sorg.

Molecular Microbiology (2005) **57**(5), 1415–1427 doi:10.1111/j.1365-2958.2005.04758.x

Secretion of YscP from *Yersinia enterocolitica* is essential to control the length of the injectisome needle but not to change the type III secretion substrate specificity

Céline Agrain, Isabel Sorg, Cécile Paroz and Guy R. Cornelis*
Biozentrum der Universität Basel, Basel, Switzerland.

Summary

The length of the needle of the *Yersinia* Ysc injectisome is determined by a protein called YscP. This protein, which acts both as a molecular ruler and as a substrate-specificity switch for type III secretion is itself secreted by the injectisome. In this report, we address the question why YscP is secreted. By a systematic deletion analysis and by fusing different parts of the molecule to the adenylate cyclase reporter, we identified two independent secretion signals. One of them is encompassed within the 35 N-terminal residues while the second one spans residues 97–137. These two signals are functionally different from Yop secretion signals. When both secretion signals were removed, Yops could still be secreted but the needle length control was lost. YscP possessing only one signal did not control needle length properly but the control was improved when more YscP was produced and secreted. YscP deprived of both signals could not control length, even when overproduced. We conclude from this that YscP needs to be secreted to exert its length control function but not its substrate-specificity switch function.

Introduction

Type III secretion (T3S) is a secretion pathway that is common to the flagellum of eubacteria and the injectisomes of many Gram-negative bacteria (Aizawa, 2001). The flagellum is a motility organelle made of a basal body embedded in the bacterial wall topped by an about 55-nm-long hook and a long flexible propelling filament (Macnab, 2003). The assembly of the hook and the filament occurs through sequential secretion by a built-in T3S export apparatus. The subunits travel inside the growing structure and polymerize at the end (Iino, 1969; Emerson *et al*., 1970). Injectisomes are stationary virulence nanomachines whose function is to secrete and translocate effector proteins across eukaryotic cell membranes (Cornelis and Wolf-Watz, 1997). These effectors, which are called Yops in *Yersinia* spp., interfere with host cell signalling and control (Cornelis, 2002; Navarro *et al*., 2005). Injectisomes consist of a basal body similar to that of the flagellum, topped by a stiff hollow needle (Kubori *et al*., 1998; Blocker *et al*., 1999; Kimbrough and Miller, 2000; Sekiya *et al*., 2001) made by the polymerization of a major subunit, YscF in *Yersinia* (Hoiczyk and Blobel, 2001). Like the flagellar hook, the needle has a definite length, around 58 nm for the Ysc injectisome of *Yersinia enterocolitica* E40 (Journet *et al*., 2003). This length is optimized with respect to the length of other proteins or lipopolysaccharide (LPS) present at the bacterial surface (Mota *et al*., 2005; West *et al*., 2005). During assembly, the T3S system of the injectisome exports the needle subunits till the needle has reached its final length. Secretion of the effectors and translocators can then be triggered by contact between the needle tip and an eukaryotic cell membrane (Mota *et al*., 2005).

Both nanomachines are thus endowed with the remarkable capacity to control the length of an external appendage – the needle and the hook – and to switch the substrate specificity for export when assembly is completed (needle) or partially completed (flagellum). Mutants deficient in FliK make extra-long hooks (called polyhooks) and no filament. Extragenic suppressive mutations restoring filament assembly on polyhook structures (polyhook-filament phenotype) have been mapped in *flhB*, a gene encoding a major component of the export apparatus (Suzuki and Iino, 1981; Kutsukake *et al*., 1994; Williams *et al*., 1996; Fraser *et al*., 2003). The study of these *fliK* suppressor mutations led to the proposal that the C-terminal domain of FlhB has two substrate specificity states and that a conformational change, mediated by FliK and accompanied by a proteolytic cleavage of FlhB, is responsible for the specificity-switching process allowing secretion of flagellin to occur once assembly of the hook is completed (Minamino and Macnab, 2000; Makishima *et al*., 2001; Fraser *et al*., 2003).

Accepted 22 June, 2005. *For correspondence. E-mail guy.cornelis @unibas.ch; Tel. (+41) 61 267 21 10; Fax (+41) 61 267 21 18.

The length of the injectisome needle is determined by Spa32 in *Shigella*, by InvJ in *Salmonella enterica* [*Salmonella* pathogenicity island 1 (SPI-1)] (Kubori *et al*., 2000; Magdalena *et al*., 2002; Tamano *et al*., 2002) and by YscP in *Yersinia* (Journet *et al*., 2003). The homologues of FlhB in injectisomes form the well-conserved YscU family (Allaoui *et al*., 1994). Introduction into YscU of the FlhB substitutions that suppress the *fliK* phenotype restores Yop secretion in *yscP* mutants (Edqvist *et al*., 2003). Moreover, like FlhB, YscU undergoes a proteolytic cleavage (Lavander *et al*., 2003). Thus, very much like FliK, YscP is thought to trigger a substrate-specificity switch, interacting with the basal-body component YscU to stop secretion of the YscF needle subunits and to start Yop secretion when contact is achieved. The switch domain, called T3S4 (for type 3 secretion substrate-specificity switch), spans residues 405–500 of YscP. It is a globular domain that appears to be conserved in the C-terminal part of all the length-measuring proteins in injectisomes as well as in the flagellum (Agrain *et al*., 2005).

Deletions and insertions between residues 36–96 and 222–306 of YscP lead to shorter and longer needles, respectively, with a linear correlation between the size of YscP and the needle length (Journet *et al*., 2003). This led to a model where YscP acts as a molecular ruler defining the needle length (Journet *et al*., 2003). According to the model, export of needle subunit proteins would be allowed until the needle reaches the length of the extended YscP ruler domain, after which the T3S4 domain of YscP would signal the secretion apparatus to stop exporting needle subunits. YscP is thus a protein with a dual function, ruler and substrate-specificity switch.

It is not clear yet whether FliK also acts as a molecular ruler. No systematic study similar to what was performed in YscP has been performed so far with FliK. However, mutations resulting in half- or three-quarter-length hooks have been mapped in proteins forming the basal body, suggesting that the switch complex could act as a measuring cup to control hook length (Makishima *et al*., 2001). The subunits would first accumulate in the cup before being all secreted. Once the cup is empty, FliK could interact with the newly exposed, cytoplasmic face of the secretion system and change its specificity from hook-type to filament-type secretion substrates (Makishima *et al*., 2001).

Although the cup model and the ruler model are clearly different, they have thus in common that FliK and YscP act as molecular switches by interacting with the export apparatus. The difference resides in the nature of the signal which is sensed. In the cup model, the signal would be the empty cup, while in the ruler model, it would be the stretching of the ruler part of the switch protein. Both YscP and FliK also have in common that they are secreted by the T3S system of the injectisome (Stainier *et al*., 2000) or the flagellum (Minamino *et al*., 1999) respectively.

In the present article, we characterize the secretion signal of YscP and we address the question why YscP needs to be secreted. We show that YscP is endowed with two different secretion signals which are both functionally different from the secretion signal of the Yops. By deleting both of them, we demonstrate that secretion of YscP is linked to its ruler function but not to its substrate-specificity switch function.

Results

Identification of two secretion signals in YscP

To identify putative secretion signals in YscP, we first generated large deletions that encompass the entire *yscP* gene cloned downstream from an arabinose-inducible promoter (pBAD) (Fig. 1A). The different plasmids were then introduced in *Y. enterocolitica* E40 (pLJ4036); a *yscP* null mutant strain and the mutant bacteria were tested for their capacity to secrete YscP. The translation and tran-

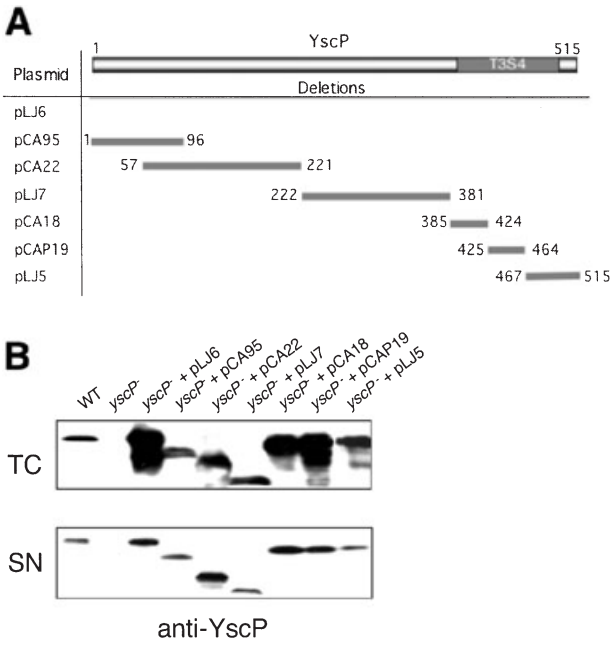

Fig. 1. Large deletions ranging from the N-terminus to the C-terminus of YscP do not affect its secretion.
A. Schematic representations of the in-frame deletions in YscP. The grey box in YscP (aa 403–492) represents the T3S4 domain.
B. Western blot analysis (anti-YscP, polyclonal antibody) of the total cells (TC) and culture supernatant (SN) fraction of *Y. enterocolitica* MRS40 (WT); *Y. enterocolitica* MRS40 (pLJ4036), i.e. the *yscP*$^-$ mutant (control); *Y. enterocolitica* MRS40 (pLJ4036) complemented with pLJ6 (YscP); pCA95 ($YscP_{97–515}$); pCA22 ($YscP_{\Delta57–221}$); pLJ7 ($YscP_{\Delta222–381}$); pCA18 ($YscP_{\Delta385–424}$); pCAP19 ($YscP_{\Delta425–464}$); pLJ5 ($YscP_{\Delta467–515}$).

scription start sites were provided by the pBAD vector. All the recombinant bacteria, incubated at 37°C in Ca^{2+}-deprived medium containing arabinose, synthesized YscP proteins of the expected size. The deletion of the first 96 residues of YscP was expected to prevent secretion of YscP as T3S substrates are normally recognized by their N-termini (Michiels *et al*., 1990; Sory and Cornelis, 1994; Schesser *et al*., 1996). Surprisingly, $YscP_{\Delta 1-96}$ was efficiently secreted (Fig. 1B). Other deletions covering the whole protein did not affect secretion of YscP either (Fig. 1B). To confirm that the secretion of these truncated YscPs occurred via the T3S pathway we transformed the constructed plasmids in an *yscN* mutant strain. This strain is defective in T3S as a result of the deletion of the ATPase of the system (Woestyn *et al*., 1994). Secretion was monitored as previously and none of the truncated YscPs was secreted (data not shown) showing that the YscP deletion mutants were indeed secreted by T3S. All these experiments suggested that YscP could have more than one secretion signal, each of them being sufficient for the protein to be secreted.

In order to localize these hypothetical signals, we then generated hybrid proteins by fusing portions of the *yscP* coding sequence to *cya*, encoding the adenylate cyclase (Cya) reporter protein (Sory and Cornelis, 1994). Fragments of *yscP* were cloned in frame, downstream from the *yopE* promoter and upstream from the *cya* gene, in plasmid pMSL56 (Table 1). *Y. enterocolitica* MRS40 [wild type (WT)] was transformed with recombinant plasmids and proteins secreted *in vitro* were analysed by SDS-PAGE. Hybrid proteins $YscP_{1-100}$-Cya and $YscP_{97-384}$-Cya were secreted whereas $YscP_{384-465}$-Cya and $YscP_{468-515}$-Cya were not (Fig. 2). These results were consistent with the hypothesis that YscP contains more than one secretion signal within the first half of the protein.

Delineation of the first secretion signal of YscP

The first secretion signal turned out to be comprised within the first 50 N-term residues as a new construct containing only $YscP_{1-50}$ and Cya was secreted (Fig. 3). To delineate more accurately this secretion signal, a systematic deletion analysis of $YscP_{1-50}$-Cya was performed. Deletion of the first 15 residues dramatically reduced the amount of intrabacterial protein suggesting that the N-term of the protein is required for stability of this hybrid protein. Therefore, we could not conclude about the secretion of this hybrid. Hybrid proteins deleted from residues 16–25 or residues 26–35 were efficiently synthesized but not secreted. A hybrid deleted from residues 36–45 was normally secreted (Fig. 3). These results indicate that the first YscP secretion signal is encoded within the first 35 amino acids and that this signal is sufficient to mediate the secretion of the Cya reporter.

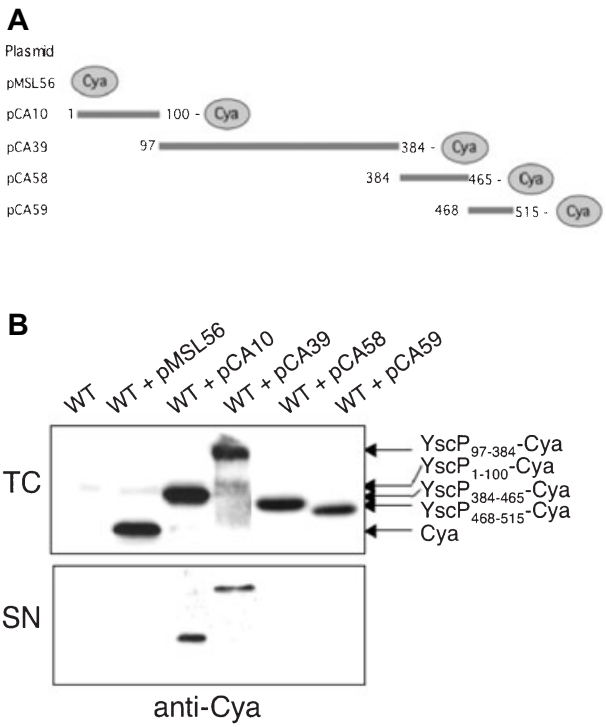

Fig. 2. A. Schematic representations of the different regions of YscP fused to Cya.
B. Western blot analysis (anti-Cya polyclonal antibody) of the total cells (TC) and culture supernatant (SN) fraction of *Y. enterocolitica* MRS40 (WT); *Y. enterocolitica* MRS40 complemented with pMSL56 (Cya); pCA10 ($YscP_{1-100}$-Cya); pCA39 ($YscP_{97-384}$-Cya); pCA58 ($YscP_{384-465}$-Cya); pCA59 ($YscP_{468-515}$-Cya).

Delineation of the second signal of YscP

To delineate the second YscP secretion signal, we also engineered systematic in-frame deletions within $YscP_{97-384}$-Cya. The constructs were introduced in *Y. enterocolitica* E40 WT and secretion was triggered by Ca^{2+}-chelation. Hybrid proteins with successive deletions ranging from amino acid 138–384 were efficiently secreted whereas one where amino acids 97–137 were removed was unable to mediate secretion of the Cya reporter (Fig. 4). The expression levels of all hybrids were equivalent, indicating that the absence of the protein from culture supernatants resulted from lack of secretion. The second signal is thus localized between residues 97 and 137 and like the first secretion signal, it is sufficient to mediate secretion.

The two secretion signals of YscP are functionally different from the Yop secretion signals

Yops secretion is severely reduced in *yscP* mutants (Stainier *et al*., 2000; Agrain *et al*., 2005), which is explained by the fact that YscP is required to switch the substrate specificity of the apparatus, from needle sub-

Table 1. Plasmids used in this work.

Plasmids	Encoded protein	Genotype or description	Source or reference
pYV plasmids			
pYV40		Wild-type virulence plasmid from strain *Y. enterocolitica* E40	Sory *et al*. (1995)
pLJ4036		pYV40 *yscP*$^-$	Agrain *et al*. (2005)
Expression plasmids			
pBADMycHisA			Invitrogen
pCA1	YscP$_{\Delta 1-15}$	pBADMycHisA – *yscP*$_{\Delta 1-15}$	Agrain *et al*. (2005)
pCA5	YscP$_{\Delta 16-25}$	pBADMycHisA – *yscP*$_{\Delta 16-25}$	Journet *et al*. (2003)
pCA6	YscP$_{\Delta 26-35}$	pBADMycHisA – *yscP*$_{\Delta 26-35}$	Journet *et al*. (2003)
pCA7	YscP$_{\Delta 36-45}$	pBADMycHisA – *yscP*$_{\Delta 36-45}$	Journet *et al*. (2003)
pCA9	YscP$_{\Delta 46-96}$	pBADMycHisA – *yscP*$_{\Delta 46-96}$	Journet *et al*. (2003)
pCA10	YscP$_{1-100}$-Cya	*yscP* fragment amplified with primers 3127 and 3128, digested by HindIII and BglII and cloned in the corresponding sites of pMSL56	This study
pCA12	YscP$_{1-50}$-Cya	*yscP* fragment amplified with primers 3127 and 3130, digested by HindIII and BglII and cloned in the corresponding sites of pMSL56	This study
pCA18	YscP$_{\Delta 385-424}$	pBADMycHisA – *yscP*$_{\Delta 385-424}$	Journet *et al*. (2003)
pCA20	YscP$_{\Delta 46-96+\Delta 222-306}$	pBADMycHisA – *yscP*$_{\Delta 46-96+\Delta 222-306}$	Journet *et al*. (2003)
pCA22	YscP$_{\Delta 57-221}$	Deletion of codons 57–221 of *yscP* from pLJ6 by inverse polymerase chain reaction (PCR) using primers 5′P-3239 and 5′P-3240, followed by a ligation	This study
pCA31	YscP$_{16-50}$-Cya	*yscP* fragment obtained by PCR on pYV with primers 3164 and 3130, digested by HindIII and BglII and cloned in the corresponding sites of pMSL56	This study
pCA33	YscP$_{1-50\ (\Delta 26-35)}$-Cya	Inverse PCR on pCA12 using primers 5′P-3068 and 5′P-3069 and ligation	This study
pCA34	YscP $_{1-50\ (\Delta 36-45)}$-Cya	Inverse PCR on pCA12 using primers 5′P-3070 and 5′P-3071 and ligation	This study
pCA37	YscP$_{138-384}$-Cya	*yscP* fragment amplified with primers 3334 and 3168, digested by HindIII and BglII and cloned in the corresponding sites of pMSL56	This study
pCA39	YscP$_{97-384}$-Cya	*yscP* fragment amplified with primers 3167 and 3168, digested by HindIII and BglII and cloned in the corresponding sites of pMSL56	This study
pCA58	YscP$_{384-465}$-Cya	*yscP* fragment amplified with primers 3166 and 3335, digested by HindIII and BglII and cloned in the corresponding sites of pMSL56	This study
pCA59	YscP$_{468-515}$-Cya	*yscP* fragment amplified with primers 3336 and 3169, digested by HindIII and BglII and cloned in the corresponding sites of pMSL56	This study
pCA76	YscP$_{\Delta 1-15-\Delta 97-137}$	*yscP* fragment obtained by PCR on pCA47 with primers 3167 and 3168, digested by NcoI and EcoRI and cloned in the corresponding sites of pBADMycHisA	This study
pCA95	YscP$_{\Delta 1-96}$	*yscP* fragment obtained by PCR on pYV with primers 3390 and 3345, digested by NcoI and EcoRI and cloned in the corresponding sites of pBADMycHisA	This study
pCAP19	YscP$_{\Delta 425-464}$	*pBADMycHisA – yscP*$_{\Delta 425-464}$	Agrain *et al*. (2005)
pCAP32	YscP$_{1-50\ (\Delta 16-25)}$-Cya	Inverse PCR on pCA12 using primers 5′P-3066 and 5′P-3067 and ligation	This study
pCAP47	YscP$_{\Delta 97-137}$	pBADMycHisA – yscP$_{\Delta 97-137}$	Agrain *et al*. (2005)
pCAP48	YscP$_{\Delta 137-177}$	pBADMycHisA – yscP$_{\Delta 137-177}$	Agrain *et al*. (2005)
pCAP49	YscP$_{\Delta 177-197}$	pBADMycHisA – yscP$_{\Delta 177-197}$	Agrain *et al*. (2005)
pCAP50	YscP$_{\Delta 197-216}$	pBADMycHisA – yscP$_{\Delta 197-216}$	Agrain *et al*. (2005)
pCAP51	YscP$_{97-384\ (\Delta 137-177)}$-Cya	Inverse PCR on pCA39 using primers 5′P-3320 and 5′P-3321 and ligation	This study
pCAP52	YscP$_{97-384\ (\Delta 177-197)}$-Cya	Inverse PCR on pCA39 using primers 5′P-3322 and 5′P-3323 and ligation	This study
pCAP53	YscP$_{97-384\ (\Delta 197-217)}$-Cya	Inverse PCR on pCA39 using primers 5′P-3337 and 5′P-3338 and ligation	This study
pCAP55	YscP$_{97-384\ (\Delta 222-381)}$-Cya	*yscP* fragment obtained by PCR on pLJ7 with primers 3167 and 3168, digested by HindIII and BglII and cloned in the corresponding sites of pMSL56	This study
pLJ5	YscP$_{\Delta 467-515}$	*pBADMycHisA – yscP*$_{\Delta 467-515}$	Journet *et al*. (2003)
pLJ6	YscP$_{WT}$	*pBADMycHisA – yscP*	Journet *et al*. (2003)
pLJ7	YscP$_{\Delta 222-381}$	*pBADMycHisA – yscP*$_{\Delta 222-381}$	Agrain *et al*. (2005)
pLJ19	YscP$_{\Delta 222-381}$	*pBADMycHisA – yscP*$_{\Delta 222-381}$	Journet *et al*. (2003)
pLJ20	YscP$_{\Delta 307-381}$	*pBADMycHisA – yscP*$_{\Delta 307-381}$	Journet *et al*. (2003)
pMSL56	Cya	pTM100-*yopE2-cya*	M.P. Sory and G.R. Cornelis (unpublished)

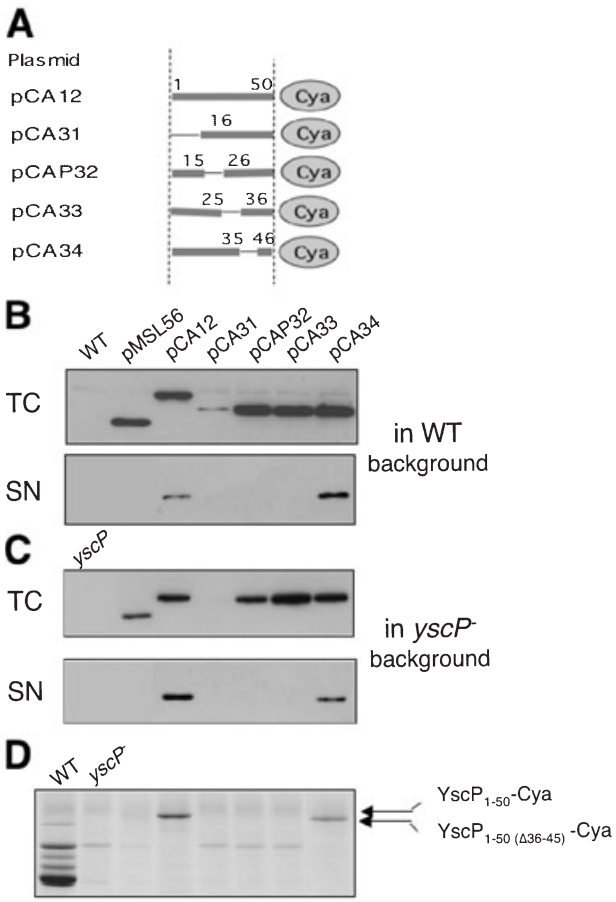

Fig. 3. Delineation of the first signal.
A. Schematic representations of the in-frame deletions in $YscP_{1–50}$ fused to Cya.
B. Western blot analysis (anti-Cya polyclonal antibody) of the total cells (TC) and culture supernatant (SN) fraction of *Y. enterocolitica* MRS40 (WT); *Y. enterocolitica* MRS40 complemented with pMSL56 (Cya); pCA12 ($YscP_{1–50}$-Cya); pCA31 ($YscP_{16–50}$–Cya); pCAP32 ($YscP_{1–50(Δ16–25)}$-Cya); pCA33 ($YscP_{1–50(Δ26–35)}$-Cya); pCA34 ($YscP_{1–50(Δ36–45)}$-Cya).
C. Western blot analysis (anti-Cya polyclonal antibody) of the total cells (TC) and culture supernatant (SN) fraction of *Y. enterocolitica* MRS40 (pLJ4036), i.e. the *yscP*⁻ mutant (control); *Y. enterocolitica* MRS40 (pLJ4036) complemented with pMSL56 (Cya, control); pCA12 ($YscP_{1–50}$-Cya); pCA31 ($YscP_{16–50}$-Cya); pCAP32 ($YscP_{1–50(Δ16–25)}$-Cya); pCA33 ($YscP_{1–50(Δ26–35)}$-Cya); pCA34 ($YscP_{1-50(D36-45)}$-Cya).
D. Yop proteins secreted by the same *Y. enterocolitica* strains as in (B) (Coomassie-stained SDS-PAGE).

units (YscF) to Yops. According to the switch concept (Kutsukake *et al*., 1994; Williams *et al*., 1996; Kutsukake, 1997; Minamino *et al*., 1999; Hirano *et al*., 2003), the secretion signal of YscP should be functionally different from the secretion signal of the Yops. To analyse the specificity of the secretion signals, we introduced the constructs encoding the hybrid Cya proteins in a *yscP*⁻ background and monitored secretion.

The *yscP*⁻ mutants expressing the different fusions were, as expected, defective both in Yops secretion (Fig. 3D) and in needle length control. Despite these defects, the hybrid proteins containing signal 1 ($YscP_{1–50}$ and $YscP_{1–50(Δ36–45)}$) were secreted by the *yscP*⁻ bacteria as well as by WT bacteria indicating that the secretion signal is different from a Yop secretion signal and that the machinery is capable of differentiating between YscP and the Yops.

The same results were observed when we tested hybrids endowed with the YscP secretion signal 2 (Fig. 4C).

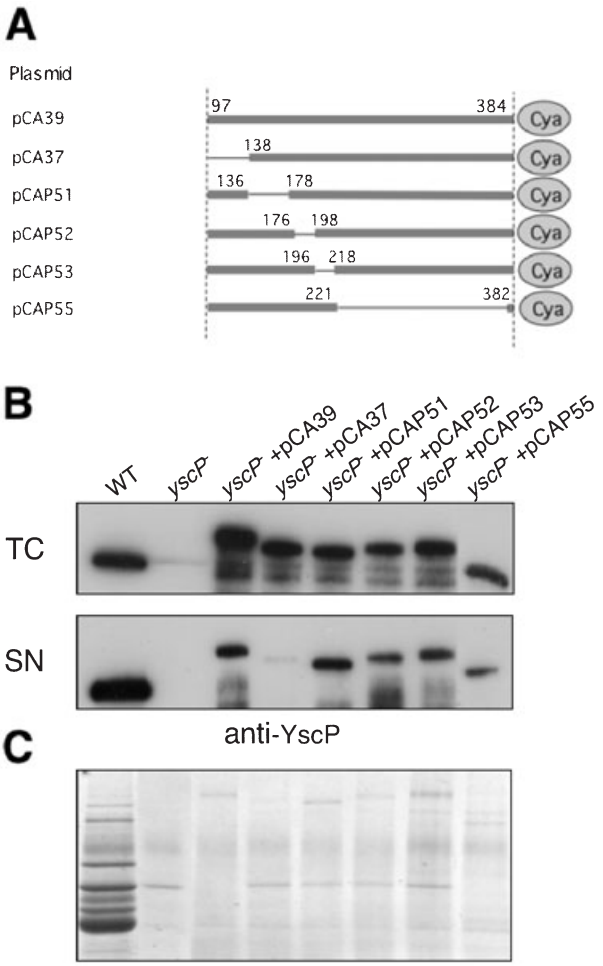

Fig. 4. Delineation of the second signal.
A. Schematic representations of the in-frame deletions in $YscP_{97–384}$ fused to Cya.
B. Western blot analysis (anti-YscP polyclonal antibody) of the total cells (TC) and culture supernatant (SN) fraction of *Y. enterocolitica* MRS40 (WT); *Y. enterocolitica* MRS40 (pLJ4036), i.e. the *yscP*⁻ mutant (control); *Y. enterocolitica* MRS40 (pLJ4036) complemented with pCA39 ($YscP_{97–384}$-Cya); pCA37 ($YscP_{138–384}$-Cya); pCAP51 ($YscP_{97–384(Δ137–177)}$-Cya); pCAP52 ($YscP_{97–384(Δ177–197)}$-Cya); pCAP53 ($YscP_{97–384(Δ197–217)}$-Cya); pCAP55 ($YscP_{97–384(Δ222–381)}$-Cya).
C. Yop proteins secreted by the same *Y. enterocolitica* strains as in (B) (Coomassie-stained SDS-PAGE)

The secretion signals of YscP are required for needle length control but not for switching on Yops secretion

Having now localized the two secretion signals of YscP, we wanted to assess the importance of the secretion of YscP for its functions. Thus, we deleted codons 1–35 plus 97–137 but the encoded protein was not expressed. The same happened when only codons 1–35 were deleted, indicating that the 1–35 deletion was the cause of the problem. Hence, we tried to delete internal parts of signal 1 plus signal 2 but there was a residual secretion of the mutants. Finally, as deletion 1–15 is known not to affect the stability of YscP (Agrain *et al.*, 2005), we deleted codons 1–15 plus 97–137. This construct was produced as well as WT YscP and was tested in parallel with $YscP_{\Delta 1–95}$ and $YscP_{\Delta 97–137}$. As expected, a deletion affecting the first signal only and the second signal only did not alter secretion of YscP but a deletion in both of them did (Fig. 5B). We inferred that deletion 1–15 of YscP was sufficient to destroy signal 1 although signal 1 is larger.

As regards to Yops secretion, bacteria expressing YscP depleted in one signal had a WT phenotype (Fig. 5A) (Agrain *et al.*, 2005). Bacteria expressing YscP affected in both signals secreted Yops almost normally showing that the T3S4 domain of YscP retains the ability to switch export specificity to some degree even if the protein is not secreted.

In contrast, as regards to needle length, bacteria producing YscP mutated in both signals or even in only one signal made needles of deregulated length (Fig. 5C). The control defect was maximal for mutant bacteria affected in both signals. For the Δsignal2 mutant a peak at approx-

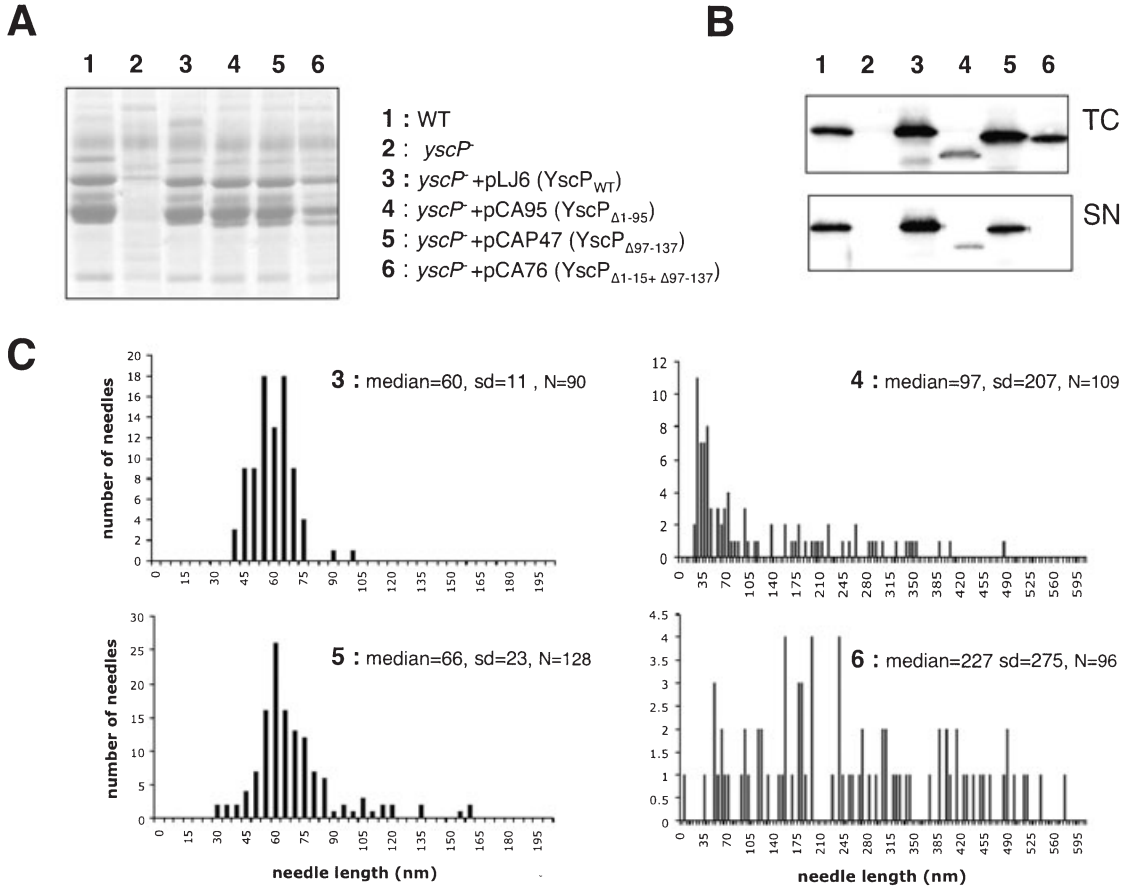

Fig. 5. Export of YscP is not necessary for Yops secretion but it is for needle length control.
A. Yop proteins secreted by the *Y. enterocolitica* strains MRS40 (WT); MRS40 (pLJ4036), i.e. the *yscP*⁻ mutant (control); *Y. enterocolitica* MRS40 (pLJ4036) complemented with pLJ6 ($YscP_{WT}$); pCA95 ($YscP_{\Delta 1–96}$); pCAP47 ($YscP_{\Delta 97–137}$); pCA76 ($YscP_{\Delta 1–15+\Delta 97–137}$) (Coomassie-stained SDS-PAGE).
B. Western blot analysis (anti-YscP polyclonal antibody) of the total cells (TC) and culture supernatant (SN) fraction of the *Y. enterocolitica* MRS40 (WT); *Y. enterocolitica* MRS40 (pLJ4036), i.e. the *yscP*⁻ mutant (control); *Y. enterocolitica* MRS40 (pLJ4036) complemented with pLJ6 ($YscP_{WT}$); pCA95 ($YscP_{\Delta 1–96}$); pCAP47 ($YscP_{\Delta 97–137}$); pCA76 ($YscP_{\Delta 1–15+\Delta 97–137}$).
C. Histograms of the needle length measurements. *Y. enterocolitica* MRS40 (pLJ4036) complemented with pLJ6 ($YscP_{WT}$, + control); pCA95 ($YscP_{\Delta 1–96}$); pCAP47 ($YscP_{\Delta 97–137}$) and pCA76 ($YscP_{\Delta 1–15+\Delta 97–137}$). Note the difference in scale of the *x*-axes between the histograms on the right and the ones on the left. Median (in nm); sd, standard deviation of the mean (in nm); N, number of needles measured.

imately WT needle length (around 60 nm) could still be observed even though it displayed a wider distribution (standard deviation of 23 nm). For mutant Δ1–96, the distribution was abnormally wide but there was nevertheless a peak between 30 and 45 nm. The smaller size of the peak could be explained by the fact that here not only the signal 1 is missing (aa 1–35) but also a part of the ruler (aa 36–96).

The measurements and related histograms suggest the first signal to be more important for needle length control than the second signal as the effect of its deletion is more pronounced. Taken together, these results reveal the importance of the secretion signals of YscP for the needle length control.

The regions flanking signal 2 are part of the ruler

The absence of needle length control in a mutant having a deletion in signal 2 (Δ97–137) led us to investigate more accurately the region spanning residues 97–222, which was not analysed in our previous study (Journet *et al.*, 2003). Six new deletions were engineered in pLJ6, our *yscP*$^+$-complementing plasmid, and all our mutants carrying deletions between residues 1 and 381 were analysed together for needle length. Except for the YscP$_{\Delta 97-137}$ mutant (Δsignal2), all mutants with deletions between residues 36 and 381 or insertions after residue 49 were able to control needle length (Fig. 6A) and led to shorter or longer needles respectively. Furthermore, when we plotted the needle lengths versus the number of YscP residues for all these mutants, we obtained a linear relationship (Journet *et al.*, 2003) (Fig. 6B) with an increment of 1.9 Å per YscP residue, enabling us to assign the ruler function to the two regions (36–96 and 138–381). Thus the ruler domain of YscP extends on both sides of secretion signal 2, up till the T3S4 domain (Journet *et al.*, 2003). This observation is in good agreement with the observation that insertion of supplementary residues after codon 49 (i.e. in between the two signals) leads to an increase of the needle length (Fig. 6A) (Journet *et al.*, 2003). In conclusion, on the N-term side, two short regions of YscP are required for length control and correspond exactly to the two secretion signals.

Increasing the amount of secreted YscP restores needle length control in a mutant lacking one secretion signal

As there is a correlation between the export of YscP and needle length control, we wondered whether increasing or decreasing the amount of YscP that is secreted would lead to a tighter or a looser control of needle length. To modulate the amount of YscP that is secreted, we induced synthesis of different constructs with concentrations of arabinose ranging from 0.02% to 0.5%. Production of the different truncated YscPs was proportional to the arabinose concentrations used for induction (Fig. 7A) and so was it for the secreted amount (Fig. 7A). The increase in the amount of secreted YscP was significant for constructs where only one signal was deleted. For the construct where both signals were affected, the increase in synthesis did not significantly modify the amount of secreted protein. We then measured the needle lengths under the different induction concentrations. Interestingly, the increase in the amount of secreted truncated YscP corresponded to a slight decrease in the needle length (Fig. 7B) and above all to a decrease in the standard deviation (Fig. 7B), meaning a better control of the needle length. For instance, *yscP* null bacteria complemented with pBAD-*yscP*$^+_{\Delta 1-15}$ made deregulated needles when synthesis was induced with only 0.02% of arabinose and the distribution of the needle length became sharper when the concentration of arabinose was increased to 0.2% and 0.5% (Fig. 7C). The same effect was observed by increasing the expression and thus the secretion of YscP$_{WT}$ and YscP$_{\Delta 97-137}$ (Fig. 7C). Increasing the synthesis of YscP$_{\Delta 1-15+\Delta 97-137}$ did not lead to a secretion of significant amounts of YscP; only at 0.5% arabinose a faint band could be detected. It also did not lead to any better control of the needle length (Fig. 7B). This suggests that secretion and needle length control are linked.

Discussion

The questions of how a single protein can determine the length of an extrabacterial organelle and why the length of this organelle is important are intellectually very challenging (Minamino and Pugsley, 2005). The objective of this work was to determine the reason why the length-measuring protein YscP is secreted. To address this question, we first needed to identify the secretion signal in order to engineer a non-secretable mutant. The exact nature of the signal recognized for export by the T3S pathway is an area of controversy for many years. Based on genetic analyses, several reports conclude that the secretion signal of *Yersinia* Yop effectors is an encrypted non-cleaved N-terminal sequence in the protein (Michiels *et al.*, 1990; Sory *et al.*, 1995; Schesser *et al.*, 1996; Lloyd *et al.*, 2001; 2002) while others conclude that it is embodied within the mRNA coding for the substrate (Anderson and Schneewind, 1997; 1999; Ramamurthi and Schneewind, 2003). In the flagellar field, a wealth of information is available regarding the structure of the extrabacterial components that are exported by T3S and these data suggest that for these proteins the T3S signal is a disordered N-terminal peptide structure (Namba, 2001). So far, there is only one report analysing the secretion signal of a needle-length controlling protein (Russmann *et al.*, 2002). It concerns InvJ, the protein, which controls the

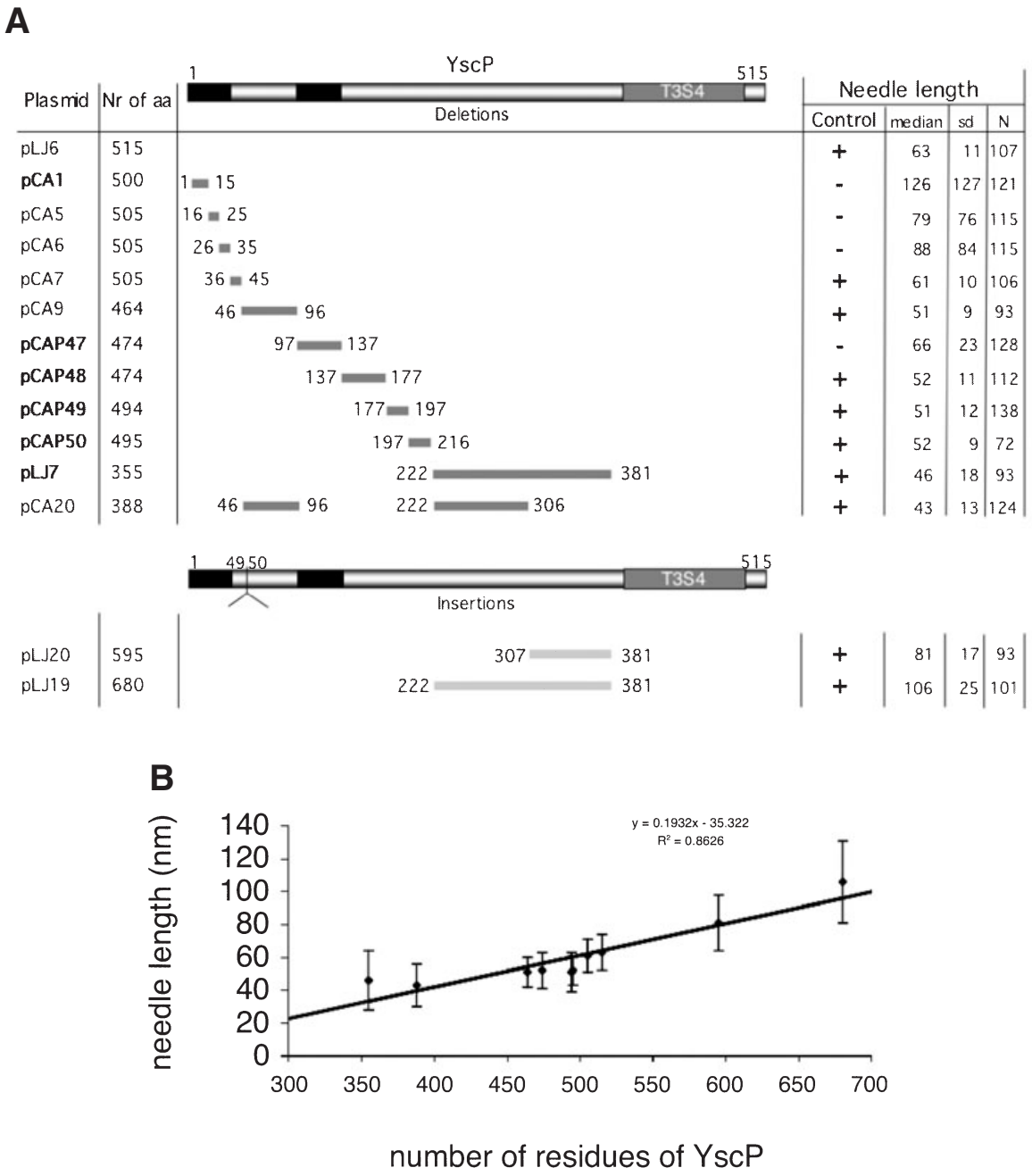

Fig. 6. A. Schematic representations of in-frame deletions that were generated in the first half of YscP (top) and in-frame insertions after residue 49 (bottom), together with their ability to control needle length. Total number of residues in YscP is given on the left. Median (in nm); sd, standard deviation (in nm); N, number of needles measured (on the right). In bold, deletions that were not yet analysed previously as regards to needle length control. The grey box in YscP (aa 403–492) represents the T3S4 domain and the two black boxes represent the two secretion signals of the protein.

B. Plot of the needle lengths versus the number of residues in YscP. Only YscP variants, which have retained the needle length control, are shown. The point for the smallest YscP protein deviates from the line more than the other variants. This may be explained by the fact that very small needles may escape detection.

Fig. 7. Increasing the export of YscP partially restores the needle length control.

A. Western blot analysis (anti-YscP polyclonal antibody) of the total cells (TC) and culture supernatant (SN) fraction of *Y. enterocolitica* MRS40 (pLJ4036) complemented with pLJ6 ($YscP_{WT}$); pCA1 ($YscP_{\Delta 1-15}$); pCA95 ($YscP_{\Delta 1-96}$), pCAP47 ($YscP_{\Delta 97-137}$); pCA76 ($YscP_{\Delta 1-15+\Delta 97-137}$). YscP synthesis was induced with increasing arabinose concentrations (0.02%, 0.1%, 0.2% and 0.5%).

B. Table summarizing the needle length measurements. N, number of needles measured.

C. Histograms of the needle length measurements. *Y. enterocolitica* MRS40 (pLJ4036) complemented with pLJ6 ($YscP_{WT}$); pCA1 ($YscP_{\Delta 1-15}$); pCAP47 ($YscP_{\Delta 97-137}$). YscP synthesis was induced with increasing arabinose concentrations (0.02%, 0.2% and 0.5%).

A

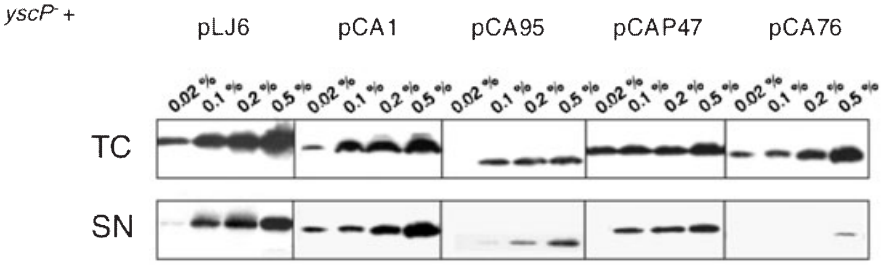

B

yscP- +	0.02 %	0.1 %	0.2 %	0.5 %
pLJ6 (pYscP)	median= 67 sd= **17** N=118	median= 61 sd=**11** N=104	median= 60 sd=**12** N=79	median= 58 sd= **10** N= 115
pCA1 ($pYscP_{\Delta 1-15}$)	median= 253 sd= **216** N=96	median= 148 sd= **146** N=110	median= 126 sd= **127** N=121	median= 86 sd= **72** N=107
pCA95 ($pYscP_{\Delta 1-96}$)	median= 387 sd= **291** N=96	median= 160 sd= **165** N=99	median= 97 sd= **162** N=108	median= 107 sd= **125** N=95
pCAP47 ($pYscP_{\Delta signal2}$)	median= 86 sd= **83** N=104	median= 72 sd= **24** N=99	median= 66 sd= **23** N=128	median= 61 sd= **12** N=51
pCA76 ($pYscP_{\Delta 1-15+\ \Delta 97-137}$)	median= 169 sd= **280** N=111	median= 196 sd= **212** N=103	median= 275 sd= **227** N=96	median= 198 sd= **203** N=96

C

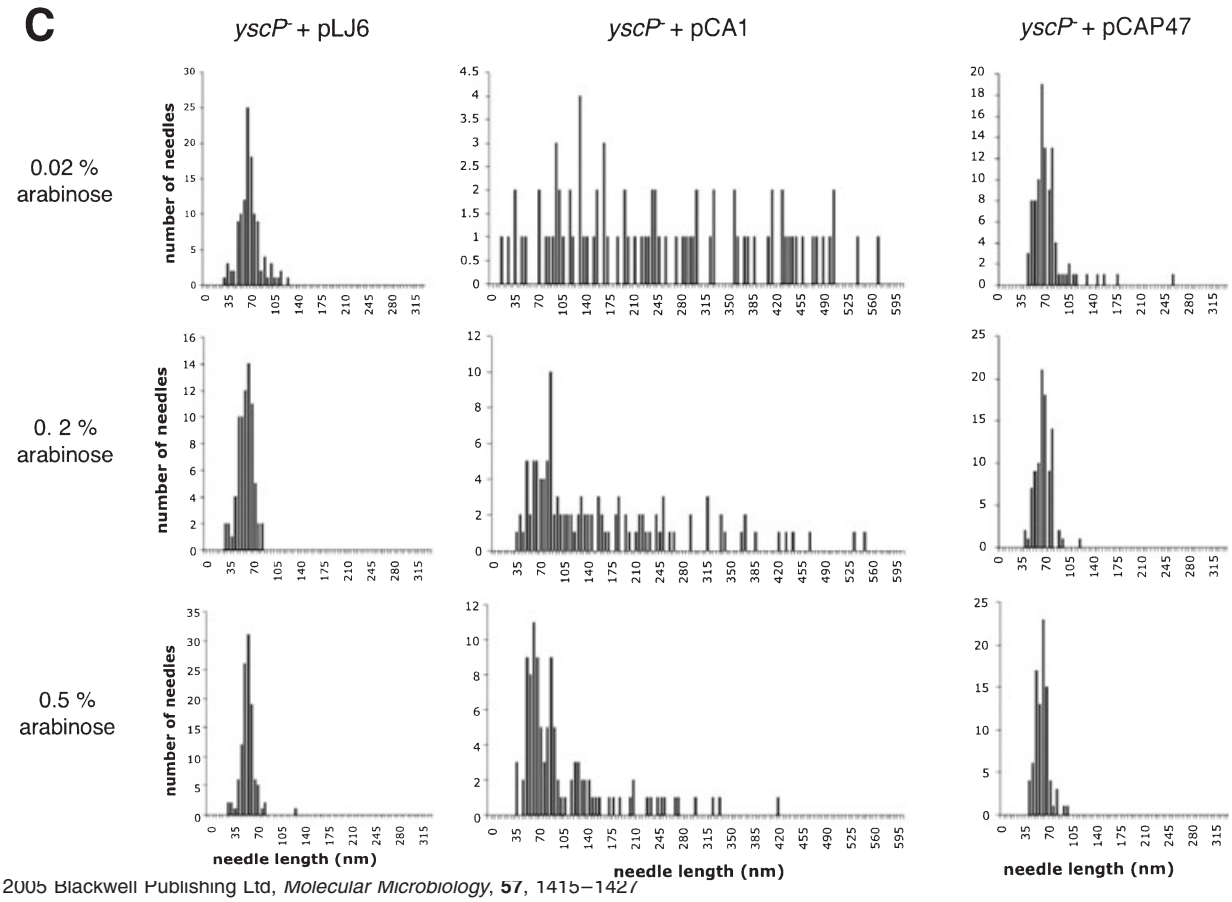

length of the needle of the SPI-1-encoded injectisome of *S. enterica*. Although it controls needle length as YscP does (Kubori *et al*., 2000), there is no significant sequence similarity with YscP and no proof yet that it works as a molecular ruler. The secretion signal of InvJ was found to consist only of amino acids 4–7 (Russmann *et al*., 2002).

In the present study, we generated overlapping deletions in YscP and we observed that all the deletion mutants were secreted normally. We reasoned that there could be two signals and to test this hypothesis, we fused different parts of YscP to the adenylate cyclase Cya (Ladant *et al*., 1989; Sory and Cornelis, 1994) taken as reporter. In agreement with the hypothesis, two different independent signals were identified, an N-terminal signal extending to residue 35 and an internal signal spanning residues 97–137. Both signals are longer than the ones found on Yop proteins. This situation is quite different from the one observed with InvJ (Russmann *et al*., 2002) and with FliK, which is not secreted if residues 1–10 are deleted (Minamino *et al*., 1999).

To our knowledge, the presence of two secretion signals is unprecedented in T3S, unless if one agrees that T3S chaperones assist secretion (Cheng *et al*., 1997) by forming a kind of tridimensional signal as suggested for YopE and its chaperone SycE (Birtalan *et al*., 2002). It is thus possible that the second signal of YscP constitutes a chaperone-binding domain but so far no chaperone could be identified for YscP. A mutant missing this hypothetical chaperone would be expected to have the same phenotype as a *yscP* mutant but no such mutant was reported so far. At this stage, one can thus not decide whether signal 2 is recognized directly or indirectly by the T3S translocon. It is, however, hard to conceive that the two secretion signals would be recognized by the same receptor.

The two signals of YscP were then removed in order to address the question of why YscP is secreted. This led to a complete loss of length control but not to a loss of Yop secretion. As far as length control is concerned, this is in agreement with observations made with InvJ. It was indeed found that InvJ secretion is essential for its function in needle length determination (Russmann *et al*., 2002). It is also in agreement with the observation that export of FliK during hook assembly is important for hook-length control (Minamino *et al*., 1999). Here we show that Yops can be secreted even if the needle length is not controlled. This means that YscP can switch the substrate specificity without being secreted itself. This is consistent with results presented recently by Aizawa and colleagues (Hirano *et al*., 2005) showing that FliK does not need to be exported to allow secretion of flagellin. We think that this observation fits with the model of a switch coupled to a ruler. Indeed, the ruler is exported via its N-terminus through the needle that it measures and its C-term operates as an intrabacterial switch. The model proposes that stretching of the ruler triggers the switch. However, the switch is very robust and can operate in a deregulated manner (no length control) when the ruler part is deleted.

Although the two signals seem to be redundant for secretion, they both are needed for a tight length control. Indeed, removal of signal 2 alone had a negative impact on length control: although some needles had a normal length, many were too long. The same was true for deletion of signal 1 and the impact was even more pronounced. These observations clearly indicate that YscP secretion is linked to the ruler function. In agreement with this idea, we could show that the more YscP is secreted, the tighter the control. The conclusion that the length control implies that the ruler is exported is in perfect agreement with the conclusions of Russmann *et al*. (2002) concerning InvJ and of Minamino *et al*. (1999) concerning FliK. It also fits well with the ruler model which implies the secretion of YscP (Journet *et al*., 2003). Even more, the localization of the two secretion signals in the N-terminal part of the protein implies that the N-terminus enters first into the channel which agrees with previous data showing that the substrate-specificity switch is localized in the C-terminus of the protein (Minamino *et al*., 2004; Agrain *et al*., 2005). The fact that the short region between the two signals acts as a ruler suggests that signal 2 does not enter the channel first. The most likely situation is that signal 1 leads the protein and that signal 2 acts as a helper to present signal 1 to the translocon. One could also imagine that one of the secretion signals acts as a binding domain involved in the interaction with another secreted protein like, e.g. YscF in the growing needle. In other words, YscP secretion might involve a piggybacking mechanism and secretion may be a consequence of its ruler function.

Finally, it is noteworthy that both secretion signals of YscP allow secretion of reporter proteins even in *yscP*$^-$ bacteria, which are unable to switch on Yops secretion. This means that these signals are functionally different from the Yop secretion signals and thus that there are different classes of T3S signals. One class of signals is recognized before the substrate-specificity switch while the other class is only recognized after. This idea was already implicit in the switch concept as developed for the assembly of the flagellum (Williams *et al*., 1996; Hirano *et al*., 2003) but it has never been demonstrated in the case of the injectisome. In the past, bioinformatics studies on the T3S signal have included YscP in the same analysis as Yops (Lloyd *et al*., 2002). It is now clear that there is hierarchy in T3S and that there are at least two classes of signals, maybe more. This should obviously be taken into account when trying to understand what selects substrates for T3S.

Experimental procedures

Induction of the yop regulon and Yop protein analysis

Bacteria were routinely grown on Luria–Bertani agar plates and in liquid Luria–Bertani medium. For the induction of the *yop* regulon, *Y. enterocolitica* bacteria were inoculated to an optical density at 600 nm (OD_{600}) of 0.1 and cultivated in brain–heart infusion (BHI; Remel) supplemented with 4 mg ml^{-1} glycerol, 20 mM $MgCl_2$ and 20 mM sodium oxalate (BHI-Ox) for 2 h at 22°C, then shifted to 37°C and incubated for 4 h. Expression of the different *yscP* genes cloned downstream from the pBAD promoter was induced by adding 0.2% arabinose to the culture just before the shift at 37°C, and again 2 h later. Ampicillin was used at a concentration of 200 μg ml^{-1} to select for the expression plasmids.

Proteins from the supernatant were precipitated overnight at 4°C with trichloroacetic acid 10% (w/v) final. Electrophoresis was carried out on 12% or 15% (w/v) polyacrylamide gels in the presence of SDS (SDS-PAGE). Proteins secreted by 3×10^8 bacteria were loaded per lane. For the total bacterial cells, the proteins from 10^7 bacteria were loaded per lane. After electrophoresis, proteins were stained with Coomassie brilliant blue (Pierce) or transferred by electroblotting to a nitrocellulose membrane. Immunoblotting was carried out using a polyclonal rabbit anti-YscP antibody (MIPA57) or using a polyclonal goat anti-Cya antibody (Santa Cruz).

Detection of immunoblots was performed with a secondary antibody conjugated to horseradish peroxidase (1:2000; Dako) before development with supersignal chemiluminescent substrate (Pierce).

Electron microscopy

Visualization of the needle-like structures at the cell surface of the bacteria was performed by electron microscopy as described by Hoiczyk and Blobel (2001). After 4 h of induction at 37°C, bacteria were harvested at 2000 *g* and resuspended gently in 20 mM Tris-HCl, pH 7.5. Droplets were applied for 1 min to freshly glow-discharged, formvar carbon-coated grids, and negatively stained with 2% (w/v) uranylacetate. Bacteria were visualized in a Philips Morgagni 268D electron microscope at a nominal magnification of 20 000× and an acceleration voltage of 80 kV. Sizes were measured with the 'Soft Imaging System' software (Hamburg, Germany).

Construction of plasmids

The list of plasmids used in this study is given in Table 1. DNA amplification for cloning purposes was made using the primers listed in Table S1 and the Vent polymerase (Biolabs). Deletions were generated by inverse polymerase chain reaction, using the Pfu turbo polymerase (Stratagene). Both strands of each construct were sequenced using 3100-*Avant* genetic analyser (ABI Prism).

Acknowledgements

We thank M. Dürrenberger, G. Morson and U.M. Spornitz for use of electron microscope facilities and Laure Journet for discussions. This work was supported by the Swiss National Science Foundation (Grant 32-65393.01).

References

Agrain, C., Callebaut, I., Journet, L., Sorg, I., Paroz, C., Mota, L.J., and Cornelis, G.R. (2005) Characterization of a type III secretion substrate specificity switch (T3S4) domain in YscP from *Yersinia enterocolitica*. *Mol Microbiol* **56:** 54–67.

Aizawa, S.I. (2001) Bacterial flagella and type III secretion systems. *FEMS Microbiol Lett* **202:** 157–164.

Allaoui, A., Woestyn, S., Sluiters, C., and Cornelis, G.R. (1994) YscU, a *Yersinia enterocolitica* inner membrane protein involved in Yop secretion. *J Bacteriol* **176:** 4534–4542.

Anderson, D.M., and Schneewind, O. (1997) A mRNA signal for the type III secretion of Yop proteins by *Yersinia enterocolitica*. *Science* **278:** 1140–1143.

Anderson, D.M., and Schneewind, O. (1999) *Yersinia enterocolitica* type III secretion: an mRNA signal that couples translation and secretion of YopQ. *Mol Microbiol* **31:** 1139–1148.

Birtalan, S.C., Phillips, R.M., and Ghosh, P. (2002) Three-dimensional secretion signals in chaperone-effector complexes of bacterial pathogens. *Mol Cell* **9:** 971–980.

Blocker, A., Gounon, P., Larquet, E., Niebuhr, K., Cabiaux, V., Parsot, C., and Sansonetti, P. (1999) The tripartite type III secreton of *Shigella flexneri* inserts IpaB and IpaC into host membranes. *J Cell Biol* **147:** 683–693.

Cheng, L.W., Anderson, D.M., and Schneewind, O. (1997) Two independent type III secretion mechanisms for YopE in *Yersinia enterocolitica*. *Mol Microbiol* **24:** 757–765.

Cornelis, G.R. (2002) The *Yersinia* Ysc-Yop 'type III' weaponry. *Nat Rev Mol Cell Biol* **3:** 742–752.

Cornelis, G.R., and Wolf-Watz, H. (1997) The *Yersinia* Yop virulon: a bacterial system for subverting eukaryotic cells. *Mol Microbiol* **23:** 861–867.

Edqvist, P.J., Olsson, J., Lavander, M., Sundberg, L., Forsberg, A., Wolf-Watz, H., and Lloyd, S.A. (2003) YscP and YscU regulate substrate specificity of the *Yersinia* type III secretion system. *J Bacteriol* **185:** 2259–2266.

Emerson, S.U., Tokuyasu, K., and Simon, M.I. (1970) Bacterial flagella: polarity of elongation. *Science* **169:** 190–192.

Fraser, G.M., Hirano, T., Ferris, H.U., Devgan, L.L., Kihara, M., and Macnab, R.M. (2003) Substrate specificity of type III flagellar protein export in *Salmonella* is controlled by subdomain interactions in FlhB. *Mol Microbiol* **48:** 1043–1057.

Hirano, T., Minamino, T., Namba, K., and Macnab, R.M. (2003) Substrate specificity classes and the recognition signal for *Salmonella* type III flagellar export. *J Bacteriol* **185:** 2485–2492.

Hirano, T., Shibata, S., Ohnishi, K., Tani, T., and Aizawa, S. (2005) N-terminal signal region of FliK is dispensable for length control of the flagellar hook. *Mol Microbiol* **56:** 346–360.

Hoiczyk, E., and Blobel, G. (2001) Polymerization of a single protein of the pathogen *Yersinia enterocolitica* into needles punctures eukaryotic cells. *Proc Natl Acad Sci USA* **98:** 4669–4674.

Iino, T. (1969) Polarity of flagellar growth in *salmonella*. *J Gen Microbiol* **56:** 227–239.

Journet, L., Agrain, C., Broz, P., and Cornelis, G.R. (2003) The needle length of bacterial injectisomes is determined by a molecular ruler. *Science* **302:** 1757–1760.

Kimbrough, T.G., and Miller, S.I. (2000) Contribution of *Salmonella typhimurium* type III secretion components to needle complex formation. *Proc Natl Acad Sci USA* **97:** 11008–11013.

Kubori, T., Matsushima, Y., Nakamura, D., Uralil, J., Lara-Tejero, M., Sukhan, A., *et al.* (1998) Supramolecular structure of the *Salmonella typhimurium* type III protein secretion system. *Science* **280:** 602–605.

Kubori, T., Sukhan, A., Aizawa, S.I., and Galan, J.E. (2000) Molecular characterization and assembly of the needle complex of the *Salmonella typhimurium* type III protein secretion system. *Proc Natl Acad Sci USA* **97:** 10225–10230.

Kutsukake, K. (1997) Hook-length control of the export-switching machinery involves a double-locked gate in *Salmonella typhimurium* flagellar morphogenesis. *J Bacteriol* **179:** 1268–1273.

Kutsukake, K., Minamino, T., and Yokoseki, T. (1994) Isolation and characterization of FliK-independent flagellation mutants from *Salmonella typhimurium*. *J Bacteriol* **176:** 7625–7629.

Ladant, D., Michelson, S., Sarfati, R., Gilles, A.M., Predeleanu, R., and Barzu, O. (1989) Characterization of the calmodulin-binding and of the catalytic domains of *Bordetella pertussis* adenylate cyclase. *J Biol Chem* **264:** 4015–4020.

Lavander, M., Sundberg, L., Edqvist, P.J., Lloyd, S.A., Wolf-Watz, H., and Forsberg, A. (2003) Characterisation of the type III secretion protein YscU in *Yersinia pseudotuberculosis*. YscU cleavage – dispensable for TTSS but essential for survival. *Adv Exp Med Biol* **529:** 109–112.

Lloyd, S.A., Norman, M., Rosqvist, R., and Wolf-Watz, H. (2001) *Yersinia* YopE is targeted for type III secretion by N-terminal, not mRNA, signals. *Mol Microbiol* **39:** 520–531.

Lloyd, S.A., Sjostrom, M., Andersson, S., and Wolf-Watz, H. (2002) Molecular characterization of type III secretion signals via analysis of synthetic N-terminal amino acid sequences. *Mol Microbiol* **43:** 51–59.

Macnab, R.M. (2003) How bacteria assemble flagella. *Annu Rev Microbiol* **57:** 77–100.

Magdalena, J., Hachani, A., Chamekh, M., Jouihri, N., Gounon, P., Blocker, A., and Allaoui, A. (2002) Spa32 regulates a switch in substrate specificity of the type III secreton of *Shigella flexneri* from needle components to Ipa proteins. *J Bacteriol* **184:** 3433–3441.

Makishima, S., Komoriya, K., Yamaguchi, S., and Aizawa, S.I. (2001) Length of the flagellar hook and the capacity of the type III export apparatus. *Science* **291:** 2411–2413.

Michiels, T., Wattiau, P., Brasseur, R., Ruysschaert, J.M., and Cornelis, G. (1990) Secretion of Yop proteins by Yersiniae. *Infect Immun* **58:** 2840–2849.

Minamino, T., and Macnab, R.M. (2000) Domain structure of *Salmonella* FlhB, a flagellar export component responsible for substrate specificity switching. *J Bacteriol* **182:** 4906–4914.

Minamino, T., and Pugsley, A.P. (2005) Measure for measure in the control of type III secretion hook and needle length. *Mol Microbiol* **56:** 303–308.

Minamino, T., Gonzalez-Pedrajo, B., Yamaguchi, K., Aizawa, S.I., and Macnab, R.M. (1999) FliK, the protein responsible for flagellar hook length control in *Salmonella*, is exported during hook assembly. *Mol Microbiol* **34:** 295–304.

Minamino, T., Saijo-Hamano, Y., Furukawa, Y., Gonzalez-Pedrajo, B., Macnab, R.M., and Namba, K. (2004) Domain organization and function of *Salmonella* FliK, a flagellar hook-length control protein. *J Mol Biol* **341:** 491–502.

Mota, L.J., Journet, L., Sorg, I., Agrain, C., and Cornelis, G.R. (2005) Bacterial injectisomes: needle length does matter. *Science* **307:** 1278.

Namba, K. (2001) Roles of partly unfolded conformations in macromolecular self-assembly. *Genes Cells* **6:** 1–12.

Navarro, L., Alto, N.M., and Dixon, J.E. (2005) Functions of the *Yersinia* effector proteins in inhibiting host immune responses. *Curr Opin Microbiol* **8:** 21–27.

Ramamurthi, K.S., and Schneewind, O. (2003) Substrate recognition by the *Yersinia* type iii protein secretion machinery. *Mol Microbiol* **50:** 1095–1102.

Russmann, H., Kubori, T., Sauer, J., and Galan, J.E. (2002) Molecular and functional analysis of the type III secretion signal of the *Salmonella enterica* InvJ protein. *Mol Microbiol* **46:** 769–779.

Schesser, K., Frithz-Lindsten, E., and Wolf-Watz, H. (1996) Delineation and mutational analysis of the *Yersinia pseudotuberculosis* YopE domains which mediate translocation across bacterial and eukaryotic cellular membranes. *J Bacteriol* **178:** 7227–7233.

Sekiya, K., Ohishi, M., Ogino, T., Tamano, K., Sasakawa, C., and Abe, A. (2001) Supermolecular structure of the enteropathogenic *Escherichia coli* type III secretion system and its direct interaction with the EspA-sheath-like structure. *Proc Natl Acad Sci USA* **98:** 11638–11643.

Sory, M.P., and Cornelis, G.R. (1994) Translocation of a hybrid YopE-adenylate cyclase from *Yersinia enterocolitica* into HeLa cells. *Mol Microbiol* **14:** 583–594.

Sory, M.P., Boland, A., Lambermont, I., and Cornelis, G.R. (1995) Identification of the YopE and YopH domains required for secretion and internalization into the cytosol of macrophages, using the *cyaA* gene fusion approach. *Proc Natl Acad Sci USA* **92:** 11998–12002.

Stainier, I., Bleves, S., Josenhans, C., Karmani, L., Kerbourch, C., Lambermont, I., *et al.* (2000) YscP, a *Yersinia* protein required for Yop secretion that is surface exposed, and released in low Ca^{2+}. *Mol Microbiol* **37:** 1005–1018.

Suzuki, T., and Iino, T. (1981) Role of the *flaR* gene in flagellar hook formation in *Salmonella* spp. *J Bacteriol* **148:** 973–979.

Tamano, K., Katayama, E., Toyotome, T., and Sasakawa, C. (2002) *Shigella* Spa32 is an essential secretory protein for functional type III secretion machinery and uniformity of its needle length. *J Bacteriol* **184:** 1244–1252.

West, N.P., Sansonetti, P., Mounier, J., Exley, R.M., Parsot, C., Guadagnini, S., *et al.* (2005) Optimization of virulence functions through glucosylation of *Shigella* LPS. *Science* **307:** 1313–1317.

Williams, A.W., Yamaguchi, S., Togashi, F., Aizawa, S.I., Kawagishi, I., and Macnab, R.M. (1996) Mutations in fliK

and flhB affecting flagellar hook and filament assembly in *Salmonella typhimurium*. *J Bacteriol* **178:** 2960–2970.
Woestyn, S., Allaoui, A., Wattiau, P., and Cornelis, G.R. (1994) YscN, the putative energizer of the *Yersinia* Yop secretion machinery. *J Bacteriol* **176:** 1561–1569.

Supplementary material

The following supplementary material is available for this article online:

Table S1. Oligonucleotides used in this work.

3- RESULTS

3.4- Bacterial injectisomes: needle length does matter,

Mota, L.J., Journet, L., Sorg, I., Agrain, C., and Cornelis, G.R.

Science 307: 1278 (2005)

Summary

Why does the needle have a determined length? To adress this question, we studied the effect of needle length variations on the efficacy of translocation of Yop effector proteins into J774 mouse macrophages. To monitor the amount of YopP translocated inside the host cell, we quantified the degree of apoptosis induced on infected macrophages by different *Y. enterocolitica* strains expressing YscP proteins of different sizes. In relation to the WT strain, the level of apoptosis was reduced about 2-fold when macrophages were infected with a strain expressing short needles, but was identical to WT when the infection was done with a strain expressing long needles. Reducing the size of YadA, an adhesin protruding at the bacterial surface, suppressed the negative effect of shortening the needle. Furthermore, increasing YadA increased the deficiency in bacteria carrying short needles. This demonstrates that increasing the distance between the needle and the host cell reduces the efficacy of translocation. Our results suggest that the different structures at the bacterial surface and the nature of its interaction with host receptors might have shaped a precise injectisome needle size during evolution and the need of its strict control for optimal function of T3S.

Statement of my work

My contribution to this paper was restricted to provide some constructions and to participate in the clonings.

Bacterial Injectisomes: Needle Length Does Matter

Luís Jaime Mota, Laure Journet, Isabel Sorg, Céline Agrain, Guy R. Cornelis*

Type III secretion (T3S) allows Gram-negative pathogenic bacteria adhering to the membrane of a eukaryotic cell to paralyze or reprogram this cell by injecting proteins into its cytosol (*1*). Many T3S nanomachines (injectisomes) possess a stiff needlelike structure of a defined length (*2*). The needle is thought to function as the conduit for protein translocation. In *Yersinia* bacteria, including *Y. pestis*, the needle length is defined by the protein ruler YscP (*3*), and the proteins injected upon host cell contact, called Yops, are involved in, among other things, caspase activation and macrophage apoptosis (*4*).

To address the question of why the needle length is controlled, we replaced *yscP* (515 codons) on the 70-kb virulence plasmid of *Y. enterocolitica* E40 by either a truncated (388 codons) or an enlarged (680 codons) allele. We incubated the modified bacteria in conditions that artificially induce *Yersinia* T3S (*4*) and observed no clear difference in Yop secretion in relation to wild-type bacteria (fig. S1). We compared *Yersinia* that make short ($YscP_{388}$, needle length L = 45 ± 13 nm) and long ($YscP_{680}$, L = 88 ± 23 nm) needles to wild-type bacteria (L = 55 ± 11 nm) (fig. S2) for their capacity to inject the apoptosis-inducing YopP into J774A.1 macrophages, by assaying caspase activation in infected cells. Bacteria making long needles were as efficient as the wild type, but those making short needles were not (Fig. 1A). This suggested that the needle must span a minimal distance, presumably determined by the *Y. enterocolitica* adhesins YadA and invasin (Inv).

Although YadA protrudes ~28 nm from the bacterial outer membrane (*5*), Inv is only 18 nm long (*6*). YadA (455 amino acids) has a lollipop-shaped structure with an oval head on top of a coiled-coil rod (*5*). Variations in coiled-coil domain length result in longer or shorter YadAs (*5*), modulating the distance between the bacterium and host-cell lipid membranes. We altered YadA length by deletion or duplication of residues 230 to 319 within the coiled-coil rod, yielding shorter ($YadA_{365}$, estimated length of 15 nm) and longer ($YadA_{545}$, ~40 nm) adhesins. We disrupted *inv* and *yadA* in *Yersinia* carrying $yscP_{388}$, $yscP_{wt}$, and $yscP_{680}$ and introduced plasmids encoding $YadA_{wt}$, $YadA_{365}$, and $YadA_{545}$. The YadA variants were as functional as $YadA_{wt}$ in promoting cell attachment (fig. S3). Caspase activity in *Yersinia*-infected macrophages revealed that shortening YadA suppressed the defect of short needles, whereas lengthening YadA enhanced the deficiency (Fig. 1A). Accordingly, lengthening YadA reduced the efficacy of wild-type needles but not of long needles (Fig. 1A). We monitored the translocation of YopO into J774A.1 by using an adenylate cyclase (Cya) reporter assay (Fig. 1B), confirming that short needles lead to a defect in Yop injection.

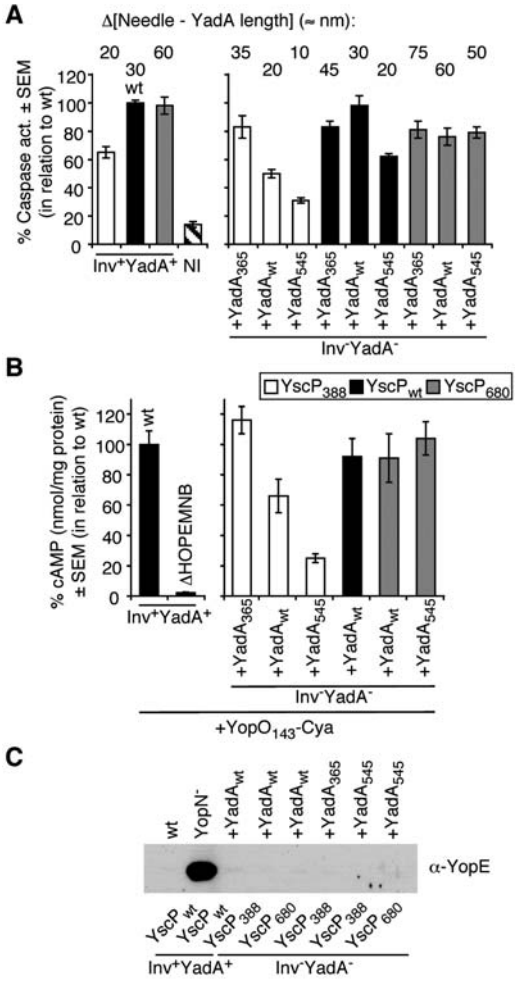

Fig. 1. (**A**) Caspase activity (act.) on *Y. enterocolitica* E40-infected macrophages. Results are the mean ± SEM from five independent experiments, each done in triplicate. The numbers on top indicate how far the needle sticks out (in nm) relative to YadA. NI, not infected; wt, wild-type. (**B**) $YopO_{143}$-Cya translocation into macrophages. ΔHOPEMNB is a negative control, not expressing the YopB translocator (*4*). Data are the mean ± SEM from three independent experiments, each done in triplicate. cAMP, cyclic adenosine monophosphate. (**C**) Immunoblot of cultured supernatant proteins from *Y. enterocolitica* E40–infected macrophages. YopN– is a positive control; in a *yopN* mutant, Yop translocation is independent of contact (*4*).

Thus, increasing the distance between the needle tip and the host cell by shortening the needle or by lengthening YadA reduces translocation; i.e., the needle needs to have a minimal length to be fully functional. We tested if bacteria with impaired translocation efficiency secreted Yops into the medium when incubated with J774A.1. Regardless of the length of the needle or YadA, we could not detect YopE in this fraction (Fig. 1C), indicating that there was no leakage and suggesting that contact between the needle tip and the host cell membrane is necessary to trigger T3S. It is thus likely that needle length has evolved to match specific structures at the bacterial and host cell surfaces.

References and Notes

1. J. E. Galán, A. Collmer, *Science* **284**, 1322 (1999).
2. T. C. Marlovits *et al.*, *Science* **306**, 1040 (2004).
3. L. Journet, C. Agrain, P. Broz, G. R. Cornelis, *Science* **302**, 1757 (2003).
4. G. R. Cornelis, *Nature Rev. Mol. Cell Biol.* **3**, 742 (2002).
5. E. Hoiczyk, A. Roggenkamp, M. Reichenbecher, A. Lupas, J. Heesemann, *EMBO J.* **19**, 5989 (2000).
6. Z. A. Hamburger, M. S. Brown, R. R. Isberg, P. J. Bjorkman, *Science* **286**, 291 (1999).
7. We thank M. Dürrenberger, G. Morson, and U. M. Spornitz for use of electron microscope facilities; J. A. Bengoechea and U. Jenal for discussions; K. T. Hughes and J. Pieters for critical reading; and the Swiss National Science Foundation for grant no. 32-65393.01.

Supporting Online Material
www.sciencemag.org/cgi/content/full/307/5713/1278/DC1
Materials and Methods
Figs. S1 to S3
References and Notes

18 November 2004; accepted 16 December 2004
10.1126/science.1107679

Biozentrum, Universität Basel, 4056 Basel, Switzerland.

*To whom correspondence should be addressed. E-mail: guy.cornelis@unibas.ch

Supporting Online Material

Materials and Methods

This work was done with *Yersinia enterocolitica* E40 (pYV40) [$yscP_{wt}$] and its isogenic derivatives E40 (pLJ4022) [$yscP_{388}$], E40 (pLJM4001) [$yscP_{680}$], E40 inv^- (pLJM4029) [$yscP_{wt}$ $yadA^-$], E40 inv^- (pLJM4031) [$yscP_{388}$ $yadA^-$], E40 inv^- (pLJM4032) [$yscP_{680}$ $yadA^-$] and plasmids pLJM32 [$yadA_{wt}$], pLJM33 [$yadA_{365}$], and pLJM34 [$yadA_{545}$].

DNA and proteins analyses were performed using standard methods (*S1*).

Before use, *Y. enterocolitica* strains were pre-grown overnight with continuous shaking (120 rpm) in Brain Heart Infusion (BHI) at 22°C. For infection, bacteria were then diluted to an optical density at 600 nm (OD_{600}) of 0.1 in fresh BHI and cultured for 3 hours at 37°C in a shaking water bath (120 rpm). To grow the bacteria in conditions that artificially induce Yop secretion (*in vitro* Yop secretion), *Y. enterocolitica* bacteria were inoculated at an OD_{600} of 0.1, cultivated in BHI supplemented with 20 mM sodium oxalate, 4 mg/ml glucose, and 20 mM $MgCl_2$ for 2 hours at 22°C with shaking, and then transferred to a shaking water bath for 4 hours at 37°C.

Murine monocyte-macrophage J774A.1 cells (ATCC TIB67) were cultured in RPMI 1640 (Invitrogen) supplemented with 10% (v/v) foetal bovine serum (FBS; Invitrogen), 2 mM L-glutamine (Invitrogen), 1 mM sodium pyruvate (Invitrogen) and 0.02 mM □-mercaptoethanol (Sigma); human epithelial HeLa cells were cultured in Dulbecco modified Eagle medium (Invitrogen) supplemented with 10% (v/v) foetal bovine serum (Invitrogen) and 1 mM sodium pyruvate (Invitrogen). Cells were cultured at 37°C in humidified atmosphere containing 5% CO_2. Cells were seeded the day before the experiment, and then

infected with the relevant *Y. enterocolitica* strains at a multiplicity of infection (MOI) of 50. Extracellular bacteria were killed 2 hours after infection by adding gentamicin (100 μg/ml). For measurement of caspase activity, 5 hours after infection, J774A.1 macrophages were washed once with ice-cold phosphate-buffered saline (PBS), and lysed as described (*S2*). Caspase activity was determined by incubation of cell lysates (containing 15 μg of total protein) with 50 μM of the fluorogenic substrate acetyl-Asp-Glu-Val-Asp-aminomethylcoumarin (Ac-DEVD-AMC) (Alexis Biochemicals) as previously reported (*S2*). The release of fluorescent AMC was measured by fluorometry (end point method) using a Wallac Victor^2 1420 Multilabel Counter (Perkin Elmer).

To monitor translocation of $YopO_{143}$-Cya, J774A.1 macrophages were infected for 2 hours, and cyclic AMP (cAMP) was extracted and assayed by using the cAMP Biotrak Enzymeimmunoassay (EIA) System (Amersham Biosciences) as previously reported (*S3*).

For the analysis of Yop proteins in cell culture supernatants of J774, the cells were washed extensively in RPMI 1640 without FBS before infection. After a 2 hours infection, the culture supernatants were collected, centrifuged to remove non-adherent bacteria, and proteins were precipitated with methanol/chloroform and then analyzed by SDS-PAGE followed by Immunoblot with polyclonal serum against YopE.

Analysis of needles by electron microscopy and genetic manipulations were performed as described before (*S4*).

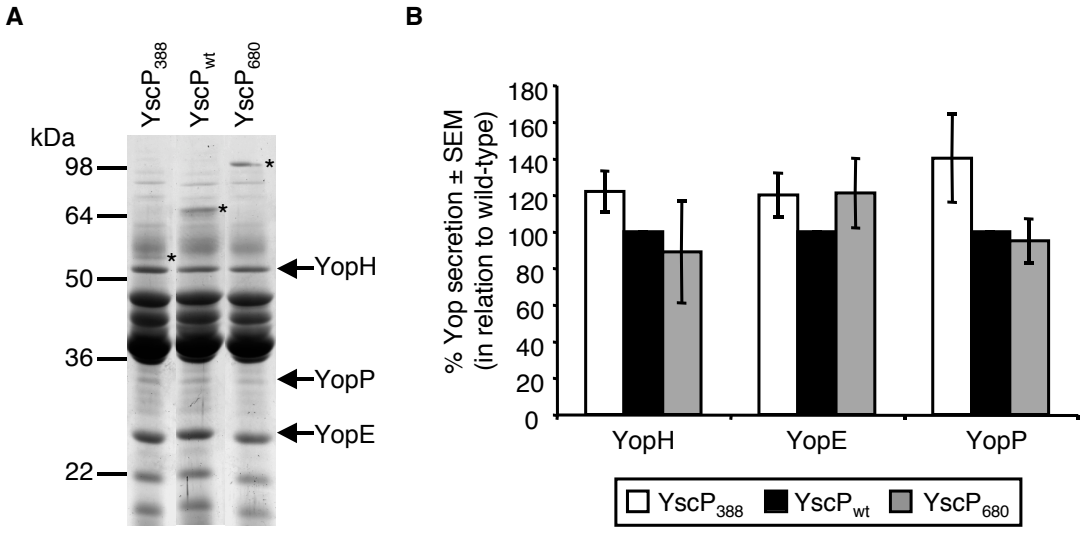

Fig. S1. *In vitro* Yop secretion by *Y. enterocolitica* E40 expressing different YscP proteins. (A) Proteins in the supernatant were analyzed by SDS-PAGE and Coomassie blue staining. Arrows point out the position of YopH, YopP, and YopE, and asterisks indicate the secreted YscP proteins. (B) The amount of secreted YopH, YopP, and YopE was estimated by densitometric analysis. Results are presented as percentage of secretion in relation to the amount observed in wild-type bacteria ($YscP_{wt}$) and are the mean ± standard error of the mean (SEM) of five different gels, from five independent experiments.

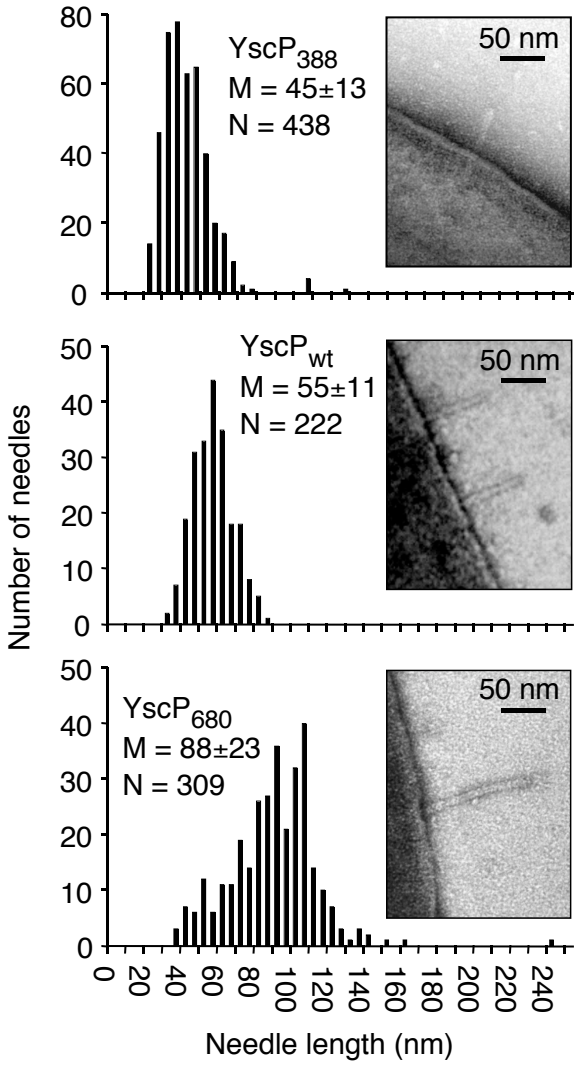

Fig. S2. Histograms of needle length measurements, and electron micrographs of *Y. enterocolitica* E40 making short ($YscP_{388}$), normal ($YscP_{wt}$) or long ($YscP_{680}$) needles. M, mean of the lengths (cm); N, number of needles measured.

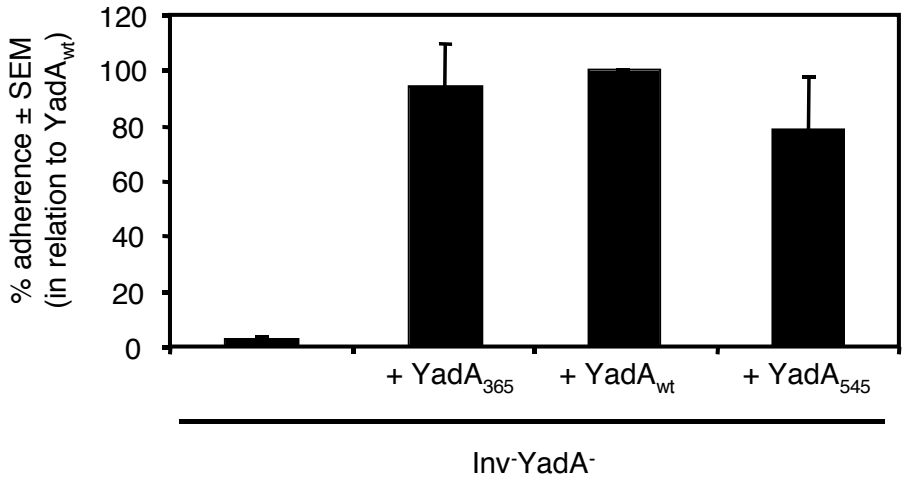

Fig. S3. Adherence to human epithelial HeLa cells of *Y. enterocolitica* E40 Inv$^-$ carrying the indicated YadA proteins. Adherence was monitored by Triton X100 lysis of HeLa cells infected for 2 hours with *Y. enterocolitica* and bacteria were titrated by plating the cell lysates. Results are presented as percentage of adherence in relation to the values obtained with bacteria expressing YadA$_{WT}$ and are the mean ± standard error of the mean (SEM) of three independent experiments, each done in triplicate.

References

S1. J. Sambrook, D. W. Russel, *Molecular Cloning: a laboratory manual* (Cold Spring Harbor Laboratory Press, Cold Spring Harbor, New York, ed 3rd, 2001).

S2. G. Denecker *et al*., *J. Biol. Chem*. **276**, 19706 (2001).

S3. M. P. Sory, G. R. Cornelis, *Mol. Microbiol.*, **14**, 583 (1994).

S4. L. Journet, C. Agrain, P. Broz, G. R. Cornelis, *Science* **302**, 1757 (2003).

Supporting Online Material

www.sciencemag.org

Materials and Methods

Figs. S1, S2, S3

References

3. RESULTS

3.5. Unpublished results

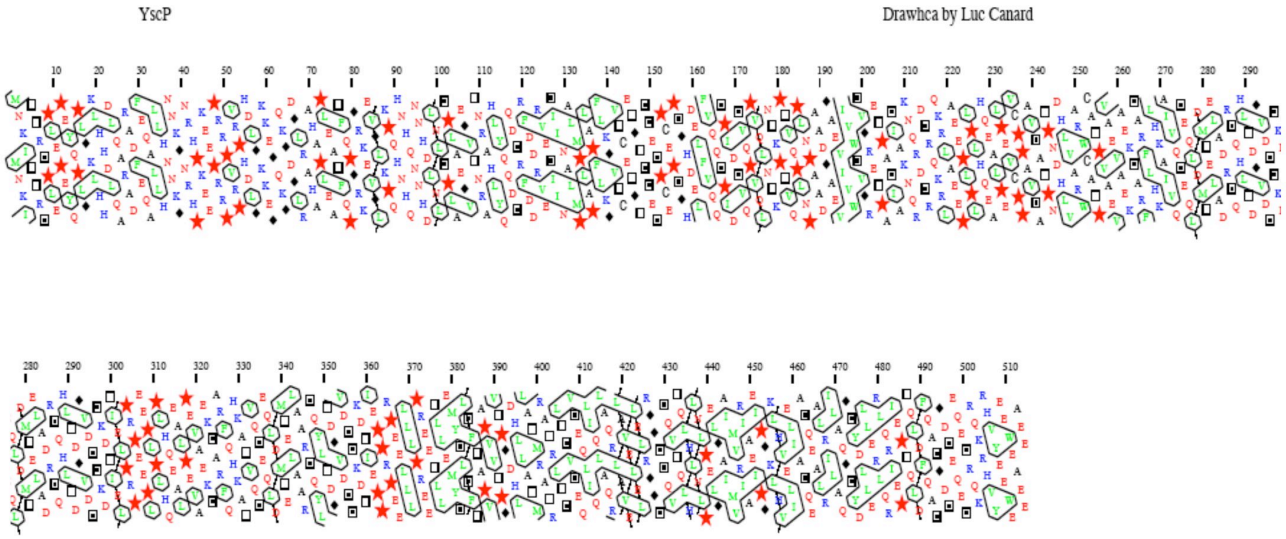

Fig. 12: **HCA of YscP**

Guidelines for the use of HCA are given in the study by Gaboriaud et al., 1987 and by Callebaut et al., 1997. The way to read the sequence and also the specials symbols are also described there.

3.5.1. Physico-chemical properties of YscP

3.5.1.1. HCA- Hydrophobic Cluster Analysis of completeYscP

The Hydrophobic Cluster Analysis (HCA) pattern of YscP is quite original as it shows large regions deprived of any secondary structure, notably $YscP_{36-97}$, $YscP_{141-188}$, $YscP_{201-243}$, $YscP_{305-334}$. Indeed, as shown on Fig.12, these regions display only a few small hydrophobic clusters with many proline, known as a structure disruptor. Interestingly, these regions were shown to be ruler regions. Thus, the absence of folding of these regions is fitting well with the structural property required by their function.

Some other regions like the C-term domain, described in detain by Agrain et al. (2005) appear to have, on the contrary, a well-defined folding. It is the case of the regions ranging from aa1 to aa35 and from aa98 to aa140, constituted mainly by alpha-helices. These two regions correspond exactly to the two export signals found in YscP. Another large structured region can be found in-between aa244 and aa304. However this region has not been assigned any particular function so far.

Altogether the structure predictions obtained from the HCA analysis, reflect quite well the functional observations.

3.5.1.1. Stability of truncated YscPs

The expression of truncated forms of YscP can be quite difficult according to the fragment that has to be expressed and the deleted pieces. In fact, some of the YscP fragments could even not be produced. By listing all the different mutants that are not expressed and pointing out their exact location along the predicted structure, it appears that the instable mutants are encoding fragments of YscP starting with a non-folded region. However, whenever the fragment to express starts with a region displaying a putative secondary structure there is no major difficulty. For example, a deletion of the first 35 or 50 amino acids is not expressed whereas a deletion of the first 96 is. The deletion of both export signals, which would have left only the ruler regions combined to the C-term, can also not be expressed. This could explain why in order to construct a non-secreted mutant we had to remove only part of the 1st signal. This lack of expression is not specific to *Yersinia,* as the same was observed in *Escherichia coli.* It is probably related to the stability of the resulting polypeptides.

3.5.1.3. Structural properties of YscP

- **Purification of YscP wt**

To produce and purify YscP, a pBAD vector encoding a recombinant YscP carrying a N-terminal His tag (pLJ14) was used. His-YscP was fully functional in a complementation test. *Escherichia coli* TOP10 cells were transformed with pLJ14, and cell lysates were prepared from the resulting transformants in the presence of protease inhibitors and in a phosphate buffer (pH=7.4) containing 0.5M NaCl. After ultracentrifugation, the soluble fraction was loaded onto a Ni-NTA affinity chromatography. The elution was performed with an increasing concentration of imidazole. His-YscP started to elute from the column with 100 mM imidazole. Nevertheless, most of the recombining protein eluted with 300 mM imidazole. The corresponding fractions were not pure but the amount of protein obtained was 5,6 mg.

- **Analytical ultracentrifugation of His-FliK**

(in collaboration with Prof. T. Kiefhaber's group)

To further examine the state of His-YscP, sedimentation velocity measurements were carried out. The apparent sedimentation coefficient g (s p) was 2.8 S. As only one distinct peak was observed it is likely that it is a monomer. This result is very different from what would have been obtained with a globular protein of the same size, which would have given a 4.5 S coefficient. All these results are not trustworthy since large aggregates were observed and shown by the obtained pattern. However, for His-FliK, the apparent sedimentation coefficient g(s p) observed was 2.1 S (Minamino et al, 2004), which is comparable to what we obtained. It was also shown to be monomeric.

- **3-D structure determination**

(in collaboration with Dr. Caroline Peneff, Prof. T. Schirmer)

In order to solve the structure of YscP, which is rather large (54 KDa) and constituted of unstructured, proline-rich regions, it was decided to proceed only with pieces of the protein.

- **Purification of YscP$_{\Delta 57\text{-}384}$-His**

(in collaboration with Dr. Caroline Peneff)

The region, which was the best candidate to think of is the C-term of YscP, because it has a globular, well-conserved structure, as shown before.

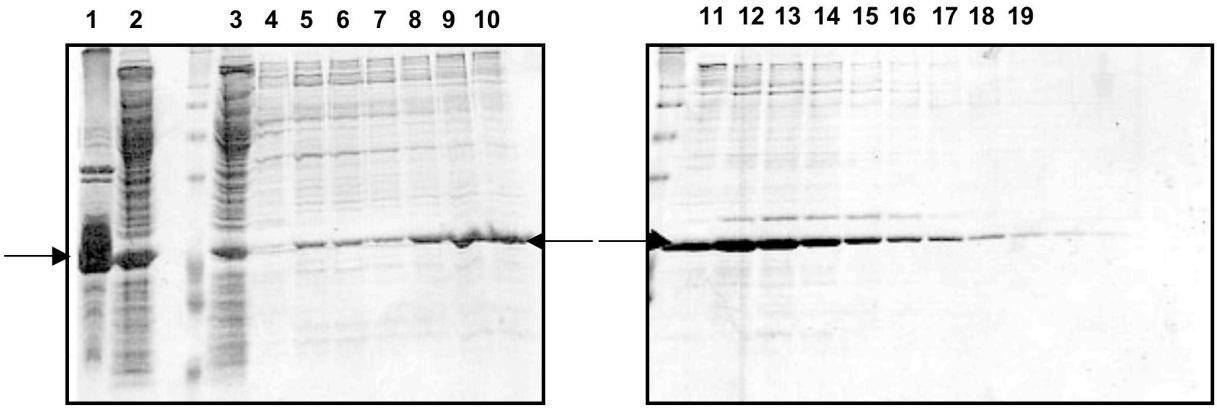

Fig. 13: **Ni-NTA chromatography of YscP$_{\delta 57\text{-}384}$-His**. Coomassie stained SDS-PAGE of elution fractions. The fraction 1 correspond to the insoluble fraction ; fraction 2, soluble fraction; 3, flowthrough; 4-7, elution with 10 mM imidazole; 8-13, elution with 50 mM imidazole; 14-19, elution with 75 mM imidazole. The arrows indicate YscP$_{\delta 57\text{-}384}$-His.

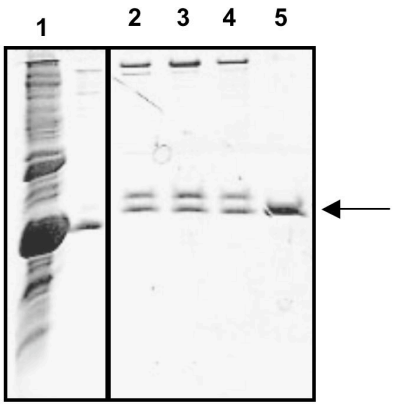

Fig. 14: **Anionic exchange chromatography of YscP$_{\delta 57\text{-}384}$ -His**. Coomassie stained SDS-PAGE of elution fractions. The fraction 1 correspond to the insoluble fraction ; fraction 2-4, elution with 350 mM NaCl; 5, elution with 500 mM NaCl. The arrow indicate YscP$_{\delta 57\text{-}384}$-His.

Thus, the ideal situation would have been to produce the C-term of YscP alone. Different constructs encoding different fragments containing the C-term of YscP were cloned. However none of them could be expressed. In contrast, the production of the first 56 aa of YscP in combination with the C-terminal region was efficient. Therefore, *E.coli* TOP10 cells were transformed with pCA11, a pET22+-based plasmid encoding a C-terminally His-tagged truncated YscP with a deletion from aa57 to 384. This construct has an extra 19aa tail (including the 6 histidines) at the C-term of the protein, a pI of 5,8 and a MW of 23,8 KDa.

$YscP_{\Delta 57\text{-}384}$-His has been shown to be functional in complementation tests for Yops secretion but not for needle length control. The truncated protein is exported.

When it was overproduced in *E. coli*, a major band was detected by Coomassie staining of SDS-PAGE of whole cell extracts. It had an apparent molecular mass of 24 Kda, consistent with its deduced mass. After sonication and centrifugation, the protein is found mostly but not exclusively in the insoluble fraction. Several attempts were made to increase the soluble fraction. Different incubation time (2H, 4H, 6H, overnight), IPTG concentrations (from 0,02 mM to 1 mM), temperature (20°C, 30°C, 37°C) were tested but none of these conditions led to a significant improvement of the solubility of the recombinant protein. However, as there was a small soluble fraction, by starting a bigger volume of culture it was possible to obtain an amount sufficient for further purification.

The soluble fraction in a phosphate buffer with 5 mM imidazole, 0,3 M NaCl was first purified by Ni-NTA affinity chromatography. The recombinant protein did not bind efficiently to the column. Indeed, the flowthrough contained a large amount of the recombinant protein, which also eluted further in all the first fractions (elution with 10 mM to 50 mM imidazole)(Fig.13). Furthermore, the eluted fractions where the protein was found were not pure (Fig.13). The yield was of about 15 mg from 600 mL of culture.

Then, $YscP_{\Delta 57\text{-}384}$-His was further purified by anionic exchange chromatography (ResourceQ). The recombinant protein eluted at high salt concentration (500 mM NaCl) and was quite pure (Fig. 14). However, only 1 mg, in total, could be retrieved.

To establish that purified $YscP_{\Delta 57\text{-}384}$-His was a single species, we carried out analytical gel filtration chromatography with a Superdex™ 75 HR. Apparently, the purified $YscP_{\Delta 57\text{-}384}$-His was not homogeneous. Indeed, two different forms were obtained.

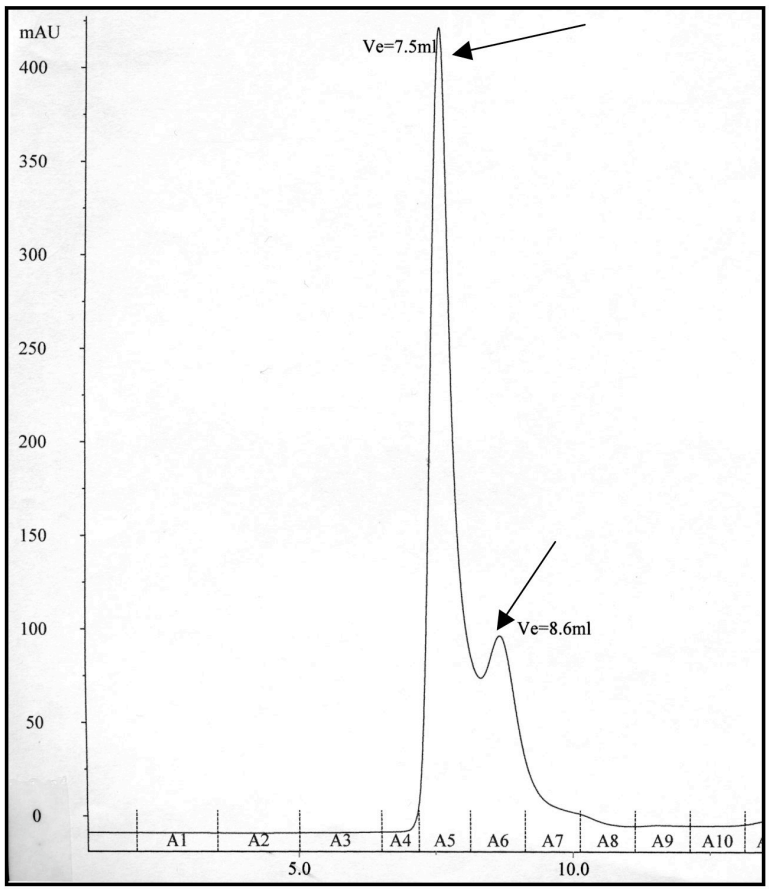

Fig. 15: **Analytical gel filtration chromatography of YscP$_{\delta 57\text{-}384}$-His**. Arrows indicate elution positions.

$YscP_{\Delta 57\text{-}384}$-His eluted from the column at a volume of 7,5 mL and at 8,6 mL (Fig. 15). The former correspond to the void volume and thus, to an apparent molecular mass larger than 100 Kda which could be aggregates or oligomers. The latter corresponds to an apparent molecular mass of 70 Kda. The protein composition of all elution fractions was verified by SDS-PAGE. As its deduced molecular mass is about 24Kda, $YscP_{\_57\text{-}384}$-His is either forming aggregates or displays hydrodynamic properties of an oligomer.

- **Cristallization of $YscP_{\Delta 57\text{-}384}$-His**

  (in collaboration with Dr. Caroline Peneff)

Cristallization assays of the 70 Kda species at a concentration of 12,5 mg/mL were performed. Unfortunately, precipitation was too fast and also too important.

- **Purification of $YscP_{T3S4}$**

  (in collaboration with Dr.Hwain Shin)

After numerous attempts, the C-term of YscP alone could finally be produced by using pCA99, a pBADMycHisA plasmid encoding $YscP_{367\text{-}515}$. As the anionic exchange chromatography had allowed the obtention of pure fractions in the purification of $YscP_{\Delta 57\text{-}384}$-His, we decided to start by this. Indeed, it could be a good mean to purify the C-term without adding any amino acids. The need for really high salt concentration to elute the recombinant protein from the column could be due to the charged tail of YscP.

A

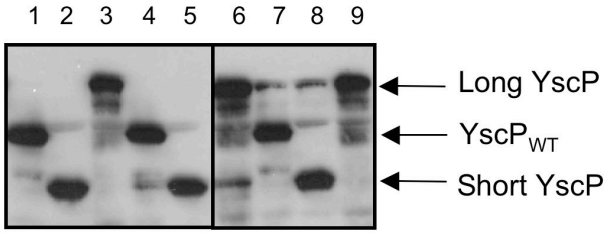

B

	Strain	Plasmid	Needle length (nm)	Standard deviation (nm)
1	*yscP*$^-$	WT	61	12
2	*yscP*$^-$	short	55	11
3	*yscP*$^-$	Long	94	25
4	short	WT	51	13
5	short	short	43	10
6	short	Long	64	20
7	long	WT	58	12
8	long	short	47	11
9	long	Long	84	33

C

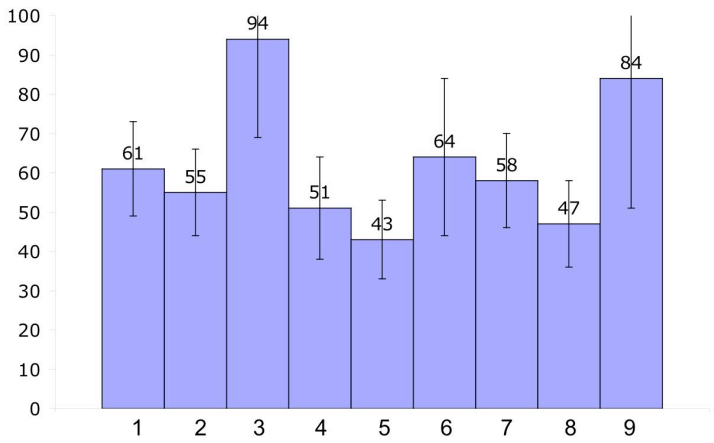

Fig. 16: **Co-expression of long and short YscPs**

A. Western blot analysis (total cells; polyclonal antibody) of the various YscP proteins proteins produced by *Y. enterocolitica yscP*$^-$ mutant carrying pLJ6 (YscP$_{WT}$)(1), pCA20 (YscP$_{short}$)(2), pLJ19 (YscP$_{long}$)(3); by YscP$_{\Delta 46\text{-}96+222\text{-}381}$ (4-6) and by YscP$_{\Omega 222\text{-}381}$ (7-9) carrying the same plasmids.

B. Table of the needle length measurements of the same strains as in A.

C. Histogram representing the results as in B.

3.5.2. Co-expression of long and small YscPs

(in collaboration with Dr. Isabel Sorg)

To find out how many YscP are involved in the determination of the length of one injectisome's needle, we decided to co-express simultaneously long and short YscPs and to see which kind of needle would be obtained.

To this purpose, four different strains were used, WT, *yscP*$^{-}$, *yscP*$_{\Delta 46\text{-}96+222\text{-}381}$, *yscP*$_{\Omega 222\text{-}381}$, encoding WT YscP (515 aa), no YscP, short YscP (388 aa) and long YscP (680 aa), respectively. Three different pBADMycHisA plamids, pLJ6, pCA20, pLJ19, encoding WT YscP, short YscP and long YscP, respectively, were transformed in the previously mentionned strain to produce the different possible combinations of YscPs. The gene encoded on the pBAD plasmid was expressed by adding 0,1% or 0,5% arabinose in the media while the gene encoded on the pYV plasmid was under the control of its native promoter. Transformed bacteria were incubated in conditions that artificially induce *Yersinia* T3S and examined by electron microscopy. The expression and secretion of the different YscPs were analyzed by Western-blot (Fig.16A). The protein encoded on the pBAD plasmid was overexpressed as compared to the one encoded on the pYV. Even with only 0,1% arabinose, it was at least 5 times more abundant in the cell and thereby also more secreted. As we have assessed the impact of variations in the YscP expression level on needle length, it is hard to relieve on the results obtained in these conditions.

As shown in Fig. 16B and C, the phenotype resulting from the co-expression of two different YscPs was always dictated by the form of YscP encoded on the pBAD plasmid and this with 0,1% arabinose as well as with 0,5% arabinose.

The other problem which complicates any possible interpretation of the results is the fact that it is impossible to distinguish between two populations of needles having overlapping distributions, and one population with a median corresponding to an intermediate length.

Altogether these preliminary results and observations led us to the conclusion that the strategy should be modified. Firstly, both short and long YscPs to be co-expressed should be dependant on the same promoter and encoded on a plasmid with the same copy number to ensure an identical level of expression. Then, the long and the short YscPs should have needle length distribution not overlapping to facilitate the interpretation of the results. Therefore, the engineering of a longer YscP is in progress.

A

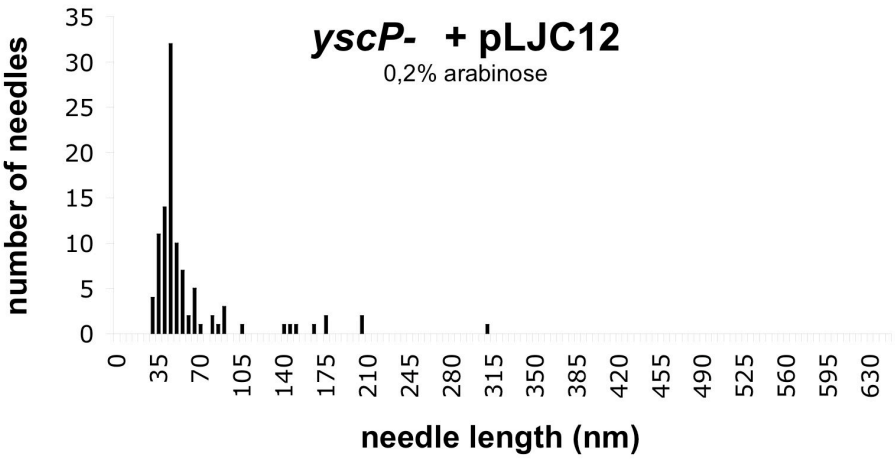

B

	Average	Median	Standard
WT	55 nm	55 nm	12 nm
yscP- + pLJC12 0.2 % arabinose	61 nm	45 nm	44 nm
	48 nm	45 nm	13 nm
yscP- + pLJC12 0.5 % arabinose	50 nm	46 nm	18 nm
	47 nm	46 nm	9 nm

Fig. 17 : **The tail of YscP**

A. Histogram of the needle length measurements of *yscP*- complemented with pLJC12 (YscPΔ500-515). YscP synthesis was induced with 0,2% arabinose.

B. Table summarizing the needle length measurements of *Y. enterocolitica* WT and *yscP*- complemented with pLJC12 (YscPΔ500-515). In grey are indicated the values obtained when only the regulated needles where taken into account.

3.5.3. The tail of YscP

While aligning the primary sequence of YscP and its counterpart in other virulence-associated TTSS, one small region appears to be highly conserved. This 10 amino acids region, which consensus sequence is RxVYEEW, is located at the extreme C-term. The HCA analysis highlights the existence of a similar short C-term globular sequence, evidenced by the presence of hydrophobic clusters (shaded grey), not only in YscP and its counterparts but also in every FliK proteins (Agrain et al., 2005). The remarkable conservation of this small cluster suggests that a function is associated with this structure. This cluster is separated from the T3S4 domains by a small acidic and polar region, rich in D, E, Q, S and T, forming a “hinge” region (Agrain et al., 2005). In YscP, the “hinge” domain is ranging from aa 496 to aa 506 and the following hydrophobic cluster from aa 507 to aa 511.

To assign a function to this region, $YscP_{\Delta 500\text{-}515}$ (pLJC12) was tested for its capacity to complement an *yscP* null mutant. As for Yops secretion, the mutant is capable to restore WT level of Yops secretion (Agrain et al., 2005). As for needle length control the first observation is that it is not as well controlled as in a WT (sd=44nm). Few needles (10%) seem to have escape length control. This could be due to the fact that the deletion is quite close from the T3S4 domain known to be essential for needle length control. A second observation is quite surprising and concerns the observed median, which is not only smaller than WT but also smaller than expected from a deletion of 15 aa in the ruler region (which would have given needles of 52 nm).

As a small hydrophobic cluster preceded by a hinge region could possibly be a regulator, we also tested its capacity to sense calcium. Yops secretion was observed in secreting permissive conditions but not in non-permissive ones suggesting that this mutant do not display a Ca^{2+}-blind phenotype.

3.5.4. Yops secretion is not abolished in *yscP*$^-$

In contrast to what was shown before (Stainier et al., 2000), we observed that in an *yscP*$^-$ mutant, Yops secretion is not completely abolished. Indeed, we observed a residual Yops secretion even in the *yscP* null mutant (Agrain et al., 2005), which was engineered to ensure that this leakiness was not due to the part of YscP still

		YopE-DHFR (pMAF15)	YscP-DHFR (pCA15)	YscX-DHFR (pCA45)
In WT	Secretion of YscF	+	+	+
	Needles	nd	WT needles + deregulated needles	WT needles
	Yop secretion	+	+/-	+
In the corres-ponding mutant	Secretion of YscF	+	-	-
	Needles	WT needles	-	-
	Yop secretion	-	-	-

Fig. 18:

Table summarizing the phenotypes observed when producing YopE-DHFR, YscP-DHFR and YscX-DHFR in *Y. enterocolitica* WT and in ΔHOPEMT, *yscP*$^{-}$ and *yscX*$^{-}$, respectively. nd= not determined.

present in the previous *yscP*$^-$ mutant (*yscP*$_{\Delta 97\text{-}465}$)(Journet et al., 2003). In a Coomassie-stained SDS-PAGE of *yscP*$^-$ culture supernatant, 3 bands are always visible and could be identified as YopM, YopN and YopE. Why these three Yop proteins are secreted in the absence of the substrate-specificity switch is not known.

3.5.5. Hierarchy of secretion

3.5.5.1. YscP is one of the first protein in the channel

To adress the following question “Is the secretion of YscP essential for its function ?”, we needed a non-secreted YscP mutant. However none of the deletion mutants engineered at the beginning was affected in the secretion of YscP. Therefore, it was decided to fuse YscP to DHFR which is thought to plug the channel, thereby preventing the release of the hybrid protein in the supernatant. The engineered pBADMycHisA plasmid encoding YscP fused to DHFR (pCA15) was transformed in *yscP*$^-$. As expected the hybrid protein was not found in the supernatant fraction. No Yop secretion was observed and interestingly, no needles could be seen at the bacterial surface (Fig. 18). In fact, YscF was not found in the supernatant. In contrast, the production of YopE-DHFR (pMAF8) in a ΔHOPEMT strain, which also blocks Yops secretion, did not prevent the secretion of YscF and the needles assembly. These results suggest that YscP is probably one of the first protein to enter the channel, even before YscF, which is in perfect agreement with the function it exerts. It is also fitting with the idea of YscP being an early substrate (Agrain et al., 2005b).

The production of the hybrid protein YscP-DHFR in a WT strain still allowed Yop secretion although reduced as compared to WT. The distribution of the needle lengths observed at the bacterial surface was wide. The average length was 297 nm with a standard deviation of 302 nm. By getting a closer look at this distribution, two different populations could be found. Half of the needles were of deregulated length and half of them were WT needles. A peak at WT length was clearly visible on the histogram. Furthermore, when needles larger than 110 nm were discarded, the average length fell to 51 nm with a standard deviation of 17 nm. The obtention of these two different populations is quite surprising as we would have rather expect to see only WT needles (YscP WT is present) but less than in a WT strain (YscP-DHFR is also present and plugging some of the injectisomes).

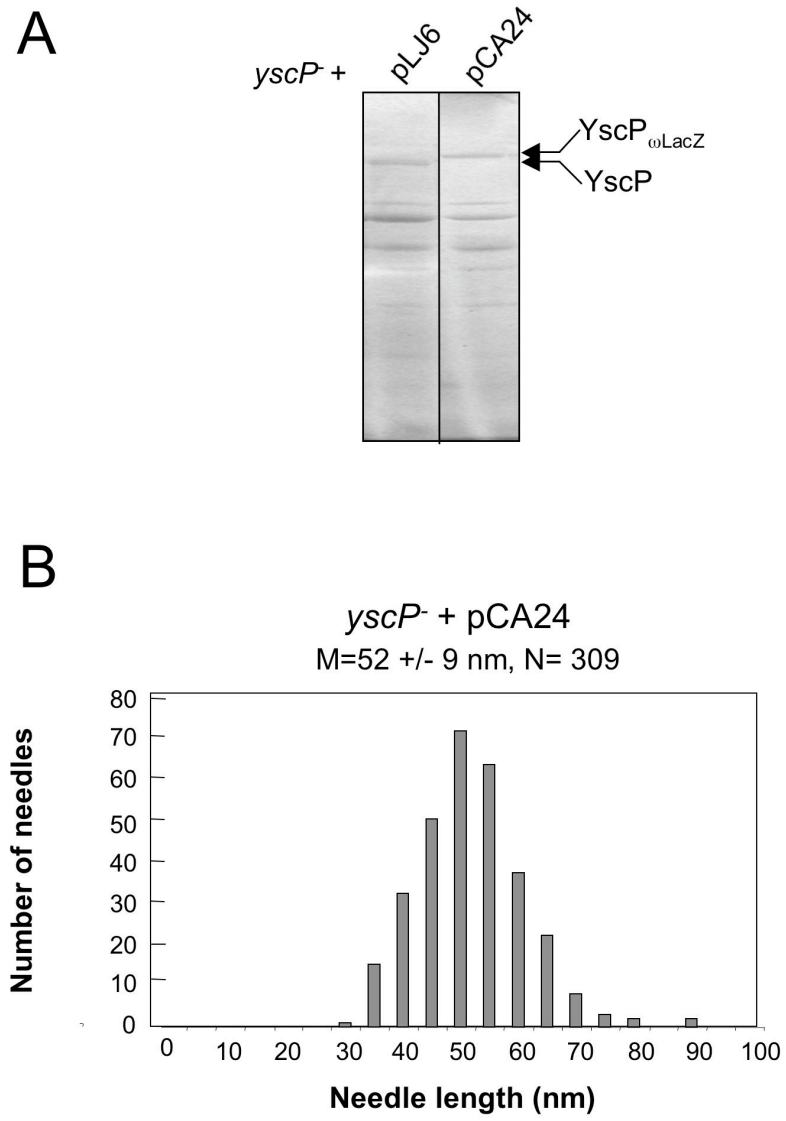

Fig. 19: **Insertion of a LacZ fragment in the ruler region of YscP**

A. Coomassie stained SDS-PAGE of culture supernatants of *Y. enterocolitica yscP*$^-$ complemented with pLJ6 (YscP WT) and pCA24 (YscP-LacZ). The size of YscP and of YscP with the LacZ insertion are indicated by arrows.

B. Histograms of the needle length measurements of *yscP*$^-$ + pCA24. M, mean of the lengths; N, number of needles measured.

3.5.5.2. Construction of other Ysc-DHFR fusions

Fusing proteins to be exported to DHFR, producing them and monitoring which proteins could be exported before the plugging of the injectisome could be a strategy to study the hierarchy of secretion. To this purpose, different hybrid proteins were constructed: YscX-DHFR (pCA45), YscO-DHFR (pCA62), YscF-DHFR (pCA61).

3.5.5.3. YscX-DHFR (Fig.18)

In an *yscX* mutant, no Yop secretion is observed and there is no needles at the bacterial surface. When pCA45, a pBADMycHisA plasmid encoding the YscX-DHFR fusion, is introduced and expressed in this *yscX* mutant, the obtained phenotype is the same. On the contrary, the production of YscX-DHFR in a WT strain is altering neither Yop secretion nor YscP's export. Moreover, needles also are of WT length with an average of 59 nm and a standard deviation of 11 nm (N=160). First, this suggests that the presence of a few WT YscX is sufficient for a proper functioning of the machinery. It also raises the possibility that YscX, although exerting an early role, is probably not exported so early. Otherwise, by producing the plugging YscX-DHFR in a WT strain, one would expect an impact on some injectisomes. One could also envision that the DHFR C-term fusion is rendering YscX not functional and preventing its targeting to the translocon. This could explain the similarity of phenotype in the *yscX* mutant, transformed or not with pCA45, and the WT phenotype observed in a WT background, where YscX WT is also present.

3.5.6. Does the nature of the insertion in the ruler matter?

Or can we insert anything, in the ruler, to get a longer YscP and thereby, produce longer needles? To adress this question, a 102 bp of *lacZ* was amplified and cloned in the *Not*I/*Xba*I sites of pCA23 (Journet et al., 2003). The resulting plasmid (pCA24) was introduced in an *yscP*$^{-}$ mutant. The longer YscP retains Yop secretion and needle length control but does not program longer needles. The needles displayed at the bacterial cell surface have an average length of 52 nm with a standard deviation of 9 nm (N=309)(Fig. 19). The insertion of *lacZ*' does not affect the functions of YscP (Yop secretion and needle length control) but does also not result in elongated needles, in contrast to what was observed when inserting fragments of the same nature. To support this conclusion, more constructs should be engineered and tested. Different kind of proteins, different structures, and longer insertions could thus be considered.

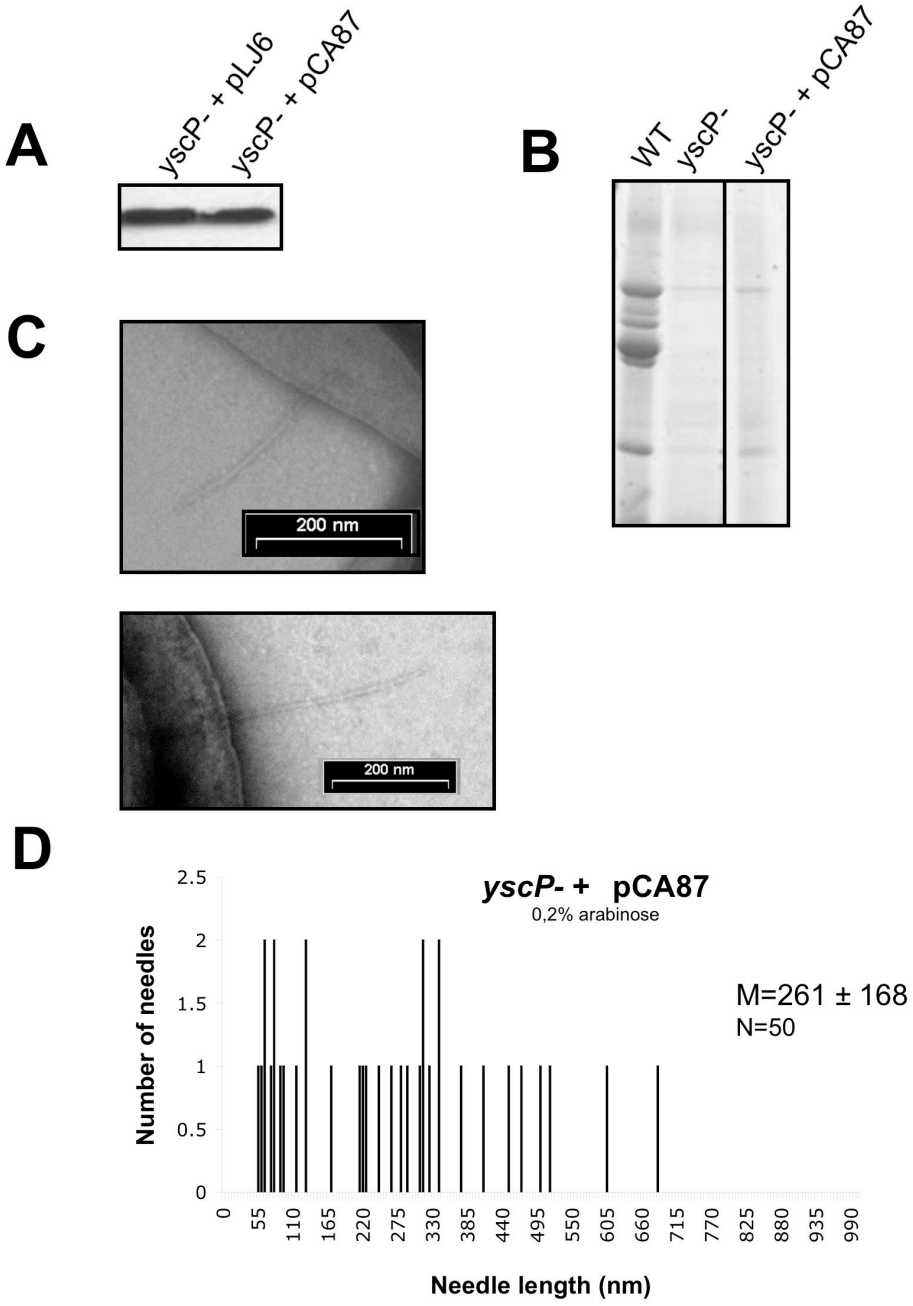

Fig. 20:

A. Western blot analysis (anti-YscP, polyclonal antibody) of the total cells fraction of *Y.enterocolitica yscP*$^-$ mutant complemented with pLJ6 (YscP) and pCA87.

B. In vitro secretion of *Y.enterocolitica* WT, *yscP*$^-$ and *yscP*$^-$ complemented with pCA87.

C. Electron micrographs of *yscP*$^-$ + pCA87

D. Histogram of the needle length measurements. M =mean of the length, N=number of needles measured.

3.5.7. YscP is not cleaved

To ensure that YscP is not cleaved while secreted, the culture supernatant of *Y. enterocolitica* WT in secretion-permissive conditions was loaded on a SDS-PAGE and the secreted proteins were visualized by Coomassie staining. Then the band corresponding to YscP was cut and submitted to a mass spectrometry analysis (Paul Jenö). The results confirmed that the exported YscP is the full-length protein and that both its N- and C-term are intact.

3.5.8. A multiple aa substitution in T3S4 can affect both YscP functions

A small region appears to be quite conserved in the T3S4 domain of the YscP sub-family: L477, L478, E479, R480, L481 and Q482. Single alanine replacements of E479, R480 and Q482 did not show any effect (Agrain et al., 2005). One multiple alanine-replacement (residues 477 to 482→ A) was performed to mutate this region. This multiple site-directed mutation was engineered on the *yscP*$^{+}$ gene cloned in the pBADMycHisA, downstream from the arabinose promoter (pCA87). The construct obtained was then transformed in the *yscP*$^{-}$ strain and Yop secretion was triggered by chelating Ca^{2+} ions and raising temperature. The mutated YscP could neither complement the defect in Yop secretion nor the length control failure (Fig. 20). This region, which is part of a predicted α-helix (Agrain et al., 2005), seems to be important for the substrate-specificity switch and thereby, needle length control.

3.5.9. The feedback inhibition is not affecting YscP even when depending on a YopE promoter

In an *yscP*$^{-}$ mutant, *yop* genes are hardly expressed since there is a feedback inhibition. Surprisingly, a sequence encoding the YscP export signal fused to a reporter gene and cloned downstream from a *yopE* promoter is very efficiently expressed. This tends to suggest that the feedback inhibition is not exerted on the promoter.

4- SUMMARY

Summary

The *Yersinia* injectisome needle has a constant length of around 60nm. Mutants affected in the *yscP* gene display abnormally long needles, suggesting that needle length is genetically controlled and that YscP is involved in this process.

First, both N- and C-term of YscP were shown to be required for proper needle length control. In contrast, the central part could be shortened or lengthened without loss of function, but giving a needle length strictly proportional to the number of residues of YscP. This led us to assign the function of a ruler to YscP.

In addition to its role in the determination of the needles length, YscP is required for Yop secretion. The C-term part of YscP, required for proper needle length control, was shown to be also crucial for Yop secretion. Thus it is probably involved in the substrate-specificity switch of the machinery, from the needle component YscF to Yops. The study of this region by Hydrophobic Cluster Analysis led to a characterization of a new domain that we called T3S4 (Type 3 Secretion Substrate-Specificity Switch) and which can be found in all counterparts of YscP in other injectisomes but also in flagellum. The conservation of the T3S4 structure suggests a similar function for all these proteins. The T3S4 domains found in injectisomes happened to be partially exchangeable. The overall structure of the domain seems to be the critical point. This is further supported by the fact that single alanine-replacement of the few conserved amino acids not affecting the structure, did not impact the functions.

Since YscP is secreted by the injectisome, we analyzed whether its export is necessary for its functions. Two original export signals were found in YscP: one in the N-term (aa 1-35) and one more central (aa 97-137). These two signals exactly correspond to the N-term regions involved in needle length control. When YscP is deprived from its export signals, it still switches the substrate specificity but it cannot control needle length any more. These data suggest a model in which YscP export is linked to needle length control.

Having evolved such a complex process for length control stresses the necessity of a certain length. Indeed, the length has evolved to match specific structures at the bacterial and host cell surfaces.

5- CONCLUSION

CONCLUSION

Why is the hook/needle length determined?

Having evolved such length determination processes stresses the necessity of a certain length. As the needle seems to need contacting the host cell to trigger T3S, it is likely that its length has evolved to match specific structures at the bacterial and host cell surfaces [78]. As for the hook it probably also needs to be of a particular length. If it were too short, it would not generate a sufficient bend angle and if it were too long, it would not be able to transmit torque efficiently to the filament [75]. The process of hook and needle length control is therefore not only one of intrinsic interest, but is functionally important for the behaviour of the cell.

How is YscP determining needle length?

Similarly to the mutants in FliK, InvJ and Spa32, three length controlling proteins identified, an *yscP* mutant in *Yersinia enterocolitica* exhibits needles of deregulated length at its surface and absence of Yop secretion [68].

To elucidate the role of YscP in needle length control, internal in-frame mutants were analyzed. Deletions or insertions in the central part of YscP lead to needles of controlled length (with a narrow distribution) but shorter or longer, respectively. On the contrary, mutating the N- or C-term of YscP affects needle length control. The central part of YscP seems to act as a ruler, determining the standard length while the two extremities of YscP are the controllers, ensuring that the length is uniform.

These observations, together with the fact that YscP is itself secreted suggested the following model for the needle assembly [79]:

- YscP takes place in the channel, one of its extremities anchored to the basal body and the other one to the tip of the nascent needle, in a similar fashion than gpH in the lambda tail.
- YscF is secreted and polymerizes. As the needle elongates, YscP is being stretched.
- When the needle reaches its mature length, YscP is fully stretched and signals via its internal anchor to stop secreting YscF and start secreting Yops.
- YscP is itself exported.
- Upon contact with a target cell, Yops secretion starts.

Is YscP a molecular ruler ?

Besides the observation that deletions or insertions in the ruler part of YscP lead to shorter or longer needles, respectively, several arguments are supporting the idea that YscP could be a ruler. It has an original predicted secondary structure with unstructured regions that would allow it to remain in a non-compacted form to exert its function. The elongated structure of YscP has been confirmed by the preliminary results obtained while studying its physico-chemical properties.

It is also important to mention the unusual observation that some mutants, in which half of the protein is deleted, are still fully functional. This would support the existence of ruler regions in the protein which sole role would be measuring. The structure/function distribution of the protein would also not contradict a ruler function. Indeed the length controlling regions are set at the extremities while the ruler region is in-between. The only part of the protein contradicting this statement is the region ranging from aa97-aa137, located right in the middle of the ruler region, and which is also involved in the length control [80].

What are the commonalities between phage tail rulers and needle rulers?

The ruler model resembles the one proposed for gpH or gp29 controlling the length of bacteriophage tails but is unprecedented in bacteria. The tail structures resemble the needle in morphology, size and even function. Like GpH, YscP appears to be a multifunctional protein. It is not only serving as a length standard but it is also involved in the needle length control and in the substrate-specificity switch.

The structure/function analysis of tail rulers shows that in these cases, only one extremity is needed to control tail length, the other can be considered as a part of the length standard. This is in contrast with the results obtained by mutating YscP where none of the two extremities could be removed without losing length control.

While listing the differences between YscP and phage tail rulers, it is also important to mention that the secondary structure of both phage tail rulers and YscP are quite different. Indeed, whereas the former is mainly alpha-helical, the latter is only composed of a few alpha-helices.

One other major difference is that the tails do not assemble in the absence of the gpH whereas needles are of undetermined length in the absence of YscP. This observation would rather reflect a similarity between YscP and the growth-terminating proteins gpU or gp3 in the bacteriophage. In fact, the T3S4 domain could be considered as a growth-terminator.

What are the commonalities between the tail length determination and the needle length determination mechanisms?

The overall functioning of the needle length determination mechanism appears to be more complex than the one of tail length determination.

This complexity is probably generated by the fact that the needle assembles at the bacterial surface with all the actors being produced in the bacteria and addressed to the machinery. In contrast, in the phage tail, all actors access directly the assembly site.

Whereas in the phage tail there are two major distinct length determinants, one setting the length standard (gpH or gp29) and the other terminating the assembly (gpU or gp3), in the needle there seems to be only one protein involved in both functions. Indeed, YscP combines the capacity to set and control the needle length and to terminate their assembly by switching the substrate-specficity via its C-term. However, this is not so surprising as it is hard to conceive how both functions could be completely distinct. In fact, no mutant in which there are regulated needles and no Yops secretion has ever been isolated reinforcing the idea that to have a needle of controlled length you need the substrate-switch to occur.

The termination of hooks or needles involves multiple factors, more than the tail termination. Whereas the phage tail termination needs a pause in the assembly combined to the action of a growth-terminating protein, the needle length termination needs a pause in the assembly and at least the T3S4 domain of length-controlling proteins, the cytoplasmic region of the YscU family of proteins and the substrate-specificity switch.

What are the commonalities between YscP and FliK?

From a structural point of view YscP and FliK share common features ; both have a high proline content and are thought to be quite elongated [81] with the exception of their C-term which is thought to be globular. The phenotypes of *yscP*$^-$ and *fliK*$^-$ are also quite similar. In both mutants, the needle/hook length is deregulated and the substrate-specificity switch do not occur.

Although there is no significant homology between them at the level of the primary sequence, bioinformatics tools have underscored the presence of the same domain, called T3S4 (Type Three Secretion Substrate-Specificity Switch) in the C-term of both proteins [82,83]. This domain has the same size, even though the size of the full-length protein differs (515 aa for YscP and 405 aa for FliK in *Salmonella typhimurium* LT2). It has also been shown in both cases to be necessary for the substrate-specificity switch, from rod-/hook-type

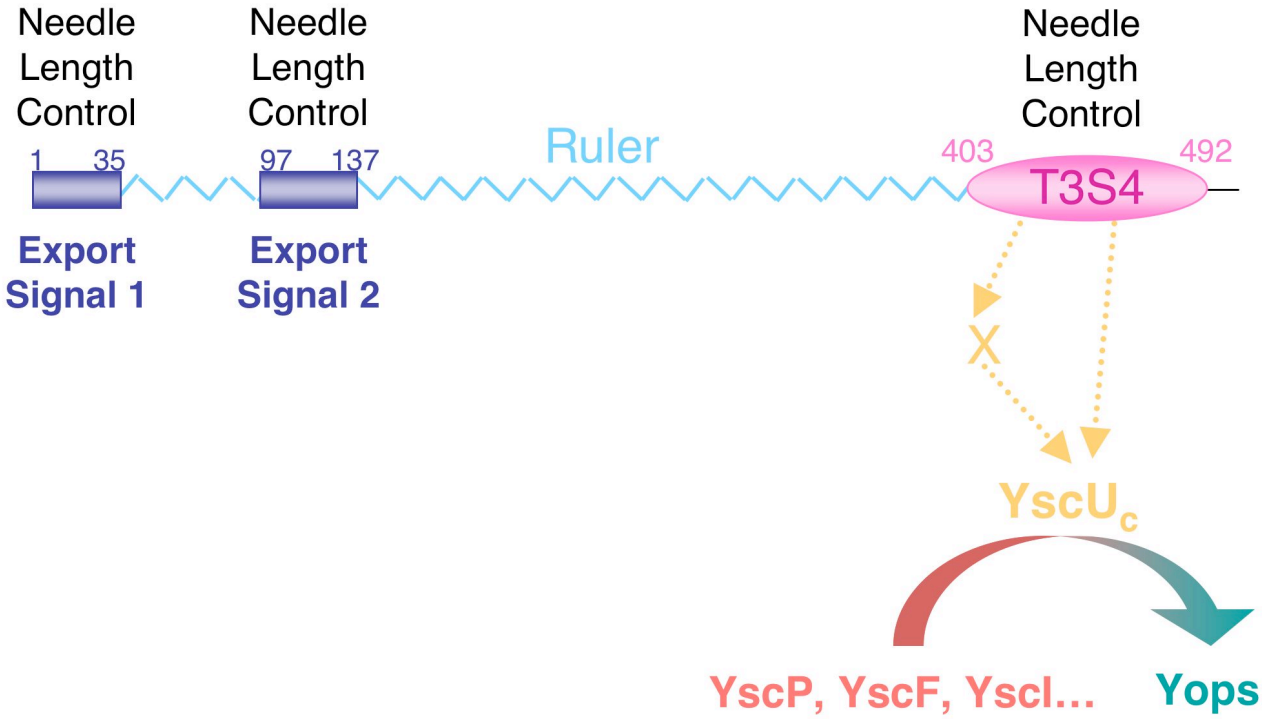

Fig. 21: Schematic drawing summarizing the structure-function analysis of YscP

to filament-type substrates in the former, and from needle subunits to Yops in the latter [42,82] (Fig. 21), thereby terminating hook/needle assembly. Although the importance of the overall structure of the T3S4 domain for its function has been highlighted, the swapping of $FliK_{T3S4}$ and $YscP_{T3S4}$ led to a loss of both functions [82]. This observation suggests that something more than an overall identical structure is needed; it has to be able to communicate with its partner.

The similar characteristics and results obtained from YscP and FliK suggest a similar function. Thus, its is likely that the function of ruler assigned to YscP can also be applied to FliK. The fact that for a long time deletions in FliK only led to polyhooks structure and not shorter hooks is not an argument against its function as a ruler. But it rather stresses the importance of where the mutations take place. Indeed, as observed for YscP, not the whole protein is serving as a ruler. Some regions are also involved in the control of the needle length, which is responsible for the narrow distribution. Moreover, recently, insertions of increasing size in some central regions of FliK lead to a proportionnal increase of hook size (Hughes, K ., and Aizawa, S.I., personal communication), which further supports that FliK could act as a ruler. A precise delineation of the ruler regions and the ones involved in the hook length control has not been performed yet.

While mentioning the commonalities between FliK and YscP it is worth mentioning that both are proteins found in the supernatant. Furthermore, in both cases, its the N-term which has been shown to be responsible for the export. But when studying more deeply their export a difference can be pinpointed. Whereas deleting the first 10 residues of FliK is enough to abolish its export, the deletion of the first 96 residues of YscP does not affect its secretion. In fact, YscP was found to have two “export signals” (1-35 and 97-137), one of them being sufficient for the protein to be exported [80].

FliKN was shown to bind to FlhBc [81]. This strong binding is likely to represent the recognition of FliK, an export substrate, by the machinery. The binding properties observed were similar to the one of an early substrate. One can envision that YscP is also recognized by YscU, the homologue of FlhB, via one of its export signals. Moreover our data also suggest that YscP is an early substrate; it is one of the first proteins to enter the channel.

What are the commonalities between the cup model and the ruler model?

The two proposed models share a common mechanism that can be defined as follows: first, a measurement is operated, and once the proper measure is attained, the assembly is terminated by a substrate-specificity switch. Eventually the length-controlling proteins are released. The sticking point concerns what is measured and what is measuring. While in the cup model the C-ring would act as a quantized cup measuring the hook subunits (FlgE), in the ruler model, a stretched YscP would measure the needles.

Other length determinants?

As mentioned above, the common point to both length determination models is the substrate-specificity switch, which has a major role in determining length by terminating the assembly. Not only the length-controlling proteins (YscP/FliK) are involved in this switch but also proteins from the well-conserved YscU/FlhB family.

Concerning its role in the substrate-specificity switch, all the observations made so far argue for the function of the T3S4 domain of the length-controlling proteins in a structurally regulated manner. Whether this feature serves in an interaction with the other switching protein (FlhB or YscU), whose function is also strongly governed by its structural properties, is not demonstrated yet. The study of *fliK* suppressors mutations found in *flhB* revealed a lack of allele specificity, underlining the improbability of a direct amino-acid/amino-acid interaction [41]. Biochemical in vitro attempts to confirm the interaction between FlhBc and FliKc have failed so far [81]. Altogether these results are either reinforcing the idea of a transient and dynamic interaction, mediated by a conformational flexibility and adaptability of the two partners, or suggesting the presence of a third intermediary protein.

Mutations in FlhBc, although abolishing filament assembly i.e substrate specificity switch, still display a number of WT hooks among others, which are longer but not polyhook structures. So, apparently the hook assembly can terminate even though the substrate switch never occurs. The same was observed in gp3 or gpU, the growth-terminating proteins of the bacteriophage tails. The explanation provided in these cases is that once the tail is completed, the assembly process is pausing. This pause would not be dependent on the presence of the terminator protein.

Such a slowing down in the assembly could explain not only the *flhBc*$^-$ phenotype but also the peak at WT hook length observed in the *fliK*$^-$ mutant in which most of the structures are polyhooks. In a double mutant *flhBc*$^-$ *flgK*$^-$, the hook length is far more deregulated than in *flhBc*$^-$ and the average length is longer, despite the presence of FliK. Hence, FlgK seems to be another hook length determinant. Normally, the hook capping protein FlgD, an absolute requirement for hook assembly, is displaced by FlgK. In the absence of FlgK, FlgD remains at the hook tip. Therefore, one could imagine that, if the export of the hook protein is still permitted, hook elongation would continue. However the substrate-specificity switch is stopping the secretion of hook proteins and turning on the secretion of the late substrates. Consistent with this, WT hooks are observed in *flgK*$^-$ even though they fail to initiate filament assembly. Therefore the function of termination cannot be exclusively assigned to FlgK. The phenotype observed in the double mutant is rather due to the combination of a weak switch because of FlhB and the absence of the hook-terminating substrate FlgK. Thus, the failure is greater than that caused by either defect alone.

Why are FliK and YscP secreted?

The reason why the length controlling proteins have to be exported is a matter of discussion. Is there any particular need for their export or is it just a trash issue? It is important here to highlight that the use of the word secretion in all the papers published on the subject refers to the fact that the protein is found in the extracellular media. Whether it is meant to be directed to the extracellular compartment or it is just a consequence of its function is not really clear yet.

Non-exported FliK mutant proteins still retain the switching function i.e. the ability to switch secretion after hook completion [84] when they are overexpressed. Overexpression probably enables access to the partner for a few of them [84]. However, the distribution of hook length, as compared to WT, is broader, suggesting that the control has been lost. Indeed, some hooks still have a WT length but the vast majority of them are longer than 75 nm [84]. The observation that the secretion of the length controlling proteins is necessary for a strict length control but not for the substrate-specificity switch has also been shown for YscP [80]. The data obtained are the same, only the conclusion drawn from them differs. Indeed, while we consider the whole distribution of needle length, in the FliK analysis they have decided to focus on those hooks which size is still controlled even if they comprised only 1/4 of the population. Deletion of both signals does not prevent the substrate-specificity

switch but is sufficient to abolish the needle length control [80]. These results suggest the importance of the export of YscP for its role in needle length control which is further supported by the fact that increasing its export lead to an enhancement of needle length control [80]. Increasing the copy number of partially functional YscP with a part of one or the other signal, would increase the probability of their access to the secretion apparatus. Whether both regions involved in the export are actually real “export signals” remains unclear. One of them could very well be a domain of interaction with another protein and in this case, its export would only be the result of a piggybacking mechanism (Agrain et al., 2005b) One could also envision that these so-called “export signals” are directing YscP to its place in the injectisome or hook-basal body lumen, where it can exert its function and then, the release in the extracellular media would only occur later on.

What are the weaknesses of the cup model?

The main drawback of the cup model is that it restricts the role of FliK to terminate hook length. However, as mentioned previously, FliK has just been found to be also a tape-measuring protein. The cup model as it stands cannot explain this. Furthermore, none of the experiments that could actually directly validate the role of quantizing cup for the C-ring filled with hook subunits have been performed.

The fact that a variation in the level of expression and export of the length-controlling proteins is modulating the hooks length is also not fitting with this model.

What are the weaknesses and strengths of the ruler model?

This last argument can also be upbraided to the ruler model as it was proposed and urges us to envision a more dynamic ruler model (See below).

Another problem to be solved concerns the location of YscP during needle assembly. This is still a matter of discussion, all the more so as it was shown by immunogold that YscP might be bacterial surface-associated [68](Broz P., unpublished data). This would rather support a location outside the needle. However it would be hard to conceive how it would communicate with components close to the inner membrane if located outside.

On the contrary, some new arguments have come to strengthen the ruler model. Indeed, an in vitro interaction between FliK and the hook-capping protein, FlgD, has been found [81]. This preliminary result, if confirmed, could be a clue that FliK is actually a physical intermediate between the distal end of the hook and the basal body.

What could be a new model? What are its weaknesses?

To take into account the effect of the levels of YscPs exported, a more dynamic version of the ruler model could be proposed. Needle sub-units (YscF) would be secreted and polymerize at the tip (or the bottom?) of the elongating needle. Every x YscF an YscP molecule elongated would be stretched. If the needle has not reached its proper length YscP would be released and new YscF could come. If the correct length is attained then YscP would somehow sense it (via its N-term) signal, via its C-term, to YscU (whether directly or indirectly) to switch the export specificity. Finally, YscP would also be released.

A dynamic functioning would require a number of exported YscPs higher than two. If the number of YscP per injectisome is equivalent to the number of FliK exported per flagellum which has been shown to be 1 or 2, such a mechanism would be hard to envision.

Another point to investigate is the observation that in non-permissive conditions, WT needles are assembled even though YscP is not detected in the supernatant.

6- OUTLOOKS

Outlooks

The deciphering of the needle length control mechanism would need to find its partners, to further investigate their exact role and to establish the chronological events.

Here are some questions directly arousing from the present study and which would be relevant to address:

- **Location of YscP** during the assembly? OUTSIDE or INSIDE the needle? Cell-surface associated or in the basal body lumen ?
- How many YscP are needed to control the length of one needle?
- When is YscP released?
- What are the **interacting partners of YscP**? Is it interacting with the equivalents in Yersinia of the C-ring components FliG, FliM, FliN? Is it interacting with a protein (the counterpart of FlgD) located in the vicinity of the tip of the needle? Is it communicating with YscU directly (interaction) or via an intermediary?
- How is YscP regulated? And the other early substrates? Are there common feature?
- How does the export apparatus recognize the early substrates?
- Is there any hierarchy among these early substrates?

7- REFERENCES

1. Kellenberger E: **Assembly in biological systems**. *Ciba Found Symp* 1972, **7**:189-206.
2. Hendrix RW: **Tail length determination in double-stranded DNA bacteriophages**. *Curr Top Microbiol Immunol* 1988, **136**:21-29.
3. Katsura I: **Mechanism of length determination in bacteriophage lambda tails**. *Adv Biophys* 1990, **26**:1-18.
4. Katsura I, Hendrix RW: **Length determination in bacteriophage lambda tails**. *Cell* 1984, **39**:691-698.
5. Katsura I: **Determination of bacteriophage lambda tail length by a protein ruler**. *Nature* 1987, **327**:73-75.
6. Casjens SR, Hendrix RW: **Locations and amounts of major structural proteins in bacteriophage lambda**. *J Mol Biol* 1974, **88**:535-545.
7. Rossmann MG, Mesyanzhinov VV, Arisaka F, Leiman PG: **The bacteriophage T4 DNA injection machine**. *Curr Opin Struct Biol* 2004, **14**:171-180.
8. Ishimoto LK, Ishimoto KS, Cascino A, Cipollaro M, Eiserling FA: **The structure of three bacteriophage T4 genes required for tail-tube assembly**. *Virology* 1988, **164**:81-90.
9. Abuladze NK, Gingery M, Tsai J, Eiserling FA: **Tail length determination in bacteriophage T4**. *Virology* 1994, **199**:301-310.
10. Vianelli A, Wang GR, Gingery M, Duda RL, Eiserling FA, Goldberg EB: **Bacteriophage T4 self-assembly: localization of gp3 and its role in determining tail length**. *J Bacteriol* 2000, **182**:680-688.
11. Zhao L KS, Chaidirek C, Arisaka F., Related Articles L: **P15 and P3, the tail completion proteins of bacteriophage T4, both form hexameric rings**. *J Bacteriol*. 2003, **185**:1693-1700.
12. Pedulla ML, Ford ME, Houtz JM, Karthikeyan T, Wadsworth C, Lewis JA, Jacobs-Sera D, Falbo J, Gross J, Pannunzio NR, et al.: **Origins of highly mosaic mycobacteriophage genomes**. *Cell* 2003, **113**:171-182.
13. Duda RL, Gingery M, Eiserling FA: **Potential length determiner and DNA injection protein is extruded from bacteriophage T4 tail tubes in vitro**. *Virology* 1986, **151**:296-314.
14. Sadewasser DA KL: **Identification of bacteriophage T4D gene 29 product, a baseplate hub component, as a folylpolyglutamate synthetase**. *Biochem Biophys Res Commun* 1983, **15**:1119-1124.
15. Macnab RM: **How bacteria assemble flagella**. *Annu Rev Microbiol* 2003, **57**:77-100.
16. Yamaguchi S, Fujita H, Ishihara A, Aizawa S, Macnab RM: **Subdivision of flagellar genes of Salmonella typhimurium into regions responsible for assembly, rotation, and switching**. *J Bacteriol* 1986, **166**:187-193.
17. Homma M, Kutsukake K, Hasebe M, Iino T, Macnab RM: **FlgB, FlgC, FlgF and FlgG. A family of structurally related proteins in the flagellar basal body of Salmonella typhimurium**. *J Mol Biol* 1990, **211**:465-477.
18. Muller V, Jones CJ, Kawagishi I, Aizawa S, Macnab RM: **Characterization of the fliE genes of Escherichia coli and Salmonella typhimurium and identification of the FliE protein as a component of the flagellar hook-basal body complex**. *J Bacteriol* 1992, **174**:2298-2304.
19. Minamino T, Yamaguchi S, Macnab RM: **Interaction between FliE and FlgB, a proximal rod component of the flagellar basal body of Salmonella**. *J Bacteriol* 2000, **182**:3029-3036.
20. Francis NR, Sosinsky GE, Thomas D, DeRosier DJ: **Isolation, characterization and structure of bacterial flagellar motors containing the switch complex**. *J Mol Biol* 1994, **235**:1261-1270.

21. Khan S, Zhao R, Reese TS: **Architectural features of the Salmonella typhimurium flagellar motor switch revealed by disrupted C-rings**. *J Struct Biol* 1998, **122**:311-319.
22. Francis NR, Irikura VM, Yamaguchi S, DeRosier DJ, Macnab RM: **Localization of the Salmonella typhimurium flagellar switch protein FliG to the cytoplasmic M-ring face of the basal body**. *Proc Natl Acad Sci U S A* 1992, **89**:6304-6308.
23. Zhao R, Schuster SC, Khan S: **Structural effects of mutations in Salmonella typhimurium flagellar switch complex**. *J Mol Biol* 1995, **251**:400-412.
24. Zhao R, Amsler CD, Matsumura P, Khan S: **FliG and FliM distribution in the Salmonella typhimurium cell and flagellar basal bodies**. *J Bacteriol* 1996, **178**:258-265.
25. Sockett H, Yamaguchi S, Kihara M, Irikura VM, Macnab RM: **Molecular analysis of the flagellar switch protein FliM of Salmonella typhimurium**. *J Bacteriol* 1992, **174**:793-806.
26. Mathews MA, Tang HL, Blair DF: **Domain analysis of the FliM protein of Escherichia coli**. *J Bacteriol* 1998, **180**:5580-5590.
27. Kubori T, Yamaguchi S, Aizawa S: **Assembly of the switch complex onto the MS ring complex of Salmonella typhimurium does not require any other flagellar proteins**. *J Bacteriol* 1997, **179**:813-817.
28. Zhu K, Gonzalez-Pedrajo B, Macnab RM: **Interactions among membrane and soluble components of the flagellar export apparatus of Salmonella**. *Biochemistry* 2002, **41**:9516-9524.
29. Hirano T, Yamaguchi S, Oosawa K, Aizawa S: **Roles of FliK and FlhB in determination of flagellar hook length in Salmonella typhimurium**. *J Bacteriol* 1994, **176**:5439-5449.
30. Ohnishi K, Ohto Y, Aizawa S, Macnab RM, Iino T: **FlgD is a scaffolding protein needed for flagellar hook assembly in Salmonella typhimurium**. *J Bacteriol* 1994, **176**:2272-2281.
31. Ikeda T, Homma M, Iino T, Asakura S, Kamiya R: **Localization and stoichiometry of hook-associated proteins within Salmonella typhimurium flagella**. *J Bacteriol* 1987, **169**:1168-1173.
32. Homma M, Kutsukake K, Iino T, Yamaguchi S: **Hook-associated proteins essential for flagellar filament formation in Salmonella typhimurium**. *J Bacteriol* 1984, **157**:100-108.
33. Homma M, Iino T: **Locations of hook-associated proteins in flagellar structures of Salmonella typhimurium**. *J Bacteriol* 1985, **162**:183-189.
34. Fan F, Ohnishi K, Francis NR, Macnab RM: **The FliP and FliR proteins of Salmonella typhimurium, putative components of the type III flagellar export apparatus, are located in the flagellar basal body**. *Mol Microbiol* 1997, **26**:1035-1046.
35. Ohnishi K, Fan F, Schoenhals GJ, Kihara M, Macnab RM: **The FliO, FliP, FliQ, and FliR proteins of Salmonella typhimurium: putative components for flagellar assembly**. *J Bacteriol* 1997, **179**:6092-6099.
36. Minamino T, Iino T, Kutuskake K: **Molecular characterization of the Salmonella typhimurium flhB operon and its protein products**. *J Bacteriol* 1994, **176**:7630-7637.
37. Minamino T, Macnab RM: **Components of the Salmonella flagellar export apparatus and classification of export substrates**. *J Bacteriol* 1999, **181**:1388-1394.
38. Minamino T, MacNab RM: **Interactions among components of the Salmonella flagellar export apparatus and its substrates**. *Mol Microbiol* 2000, **35**:1052-1064.

39. Fan F, Macnab RM: **Enzymatic characterization of FliI. An ATPase involved in flagellar assembly in Salmonella typhimurium**. *J Biol Chem* 1996, **271**:31981-31988.
40. Vogler AP, Homma M, Irikura VM, Macnab RM: **Salmonella typhimurium mutants defective in flagellar filament regrowth and sequence similarity of FliI to F0F1, vacuolar, and archaebacterial ATPase subunits**. *J Bacteriol* 1991, **173**:3564-3572.
41. Williams AW, Yamaguchi S, Togashi F, Aizawa SI, Kawagishi I, Macnab RM: **Mutations in fliK and flhB affecting flagellar hook and filament assembly in Salmonella typhimurium**. *J Bacteriol* 1996, **178**:2960-2970.
42. Minamino T, Doi H, Kutsukake K: **Substrate specificity switching of the flagellum-specific export apparatus during flagellar morphogenesis in Salmonella typhimurium**. *Biosci Biotechnol Biochem* 1999, **63**:1301-1303.
43. Minamino T, Macnab RM: **Domain structure of Salmonella FlhB, a flagellar export component responsible for substrate specificity switching**. *J Bacteriol* 2000, **182**:4906-4914.
44. Auvray F, Ozin AJ, Claret L, Hughes C: **Intrinsic membrane targeting of the flagellar export ATPase FliI: interaction with acidic phospholipids and FliH**. *J Mol Biol* 2002, **318**:941-950.
45. Minamino T, MacNab RM: **FliH, a soluble component of the type III flagellar export apparatus of Salmonella, forms a complex with FliI and inhibits its ATPase activity**. *Mol Microbiol* 2000, **37**:1494-1503.
46. Minamino T, Chu R, Yamaguchi S, Macnab RM: **Role of FliJ in flagellar protein export in Salmonella**. *J Bacteriol* 2000, **182**:4207-4215.
47. Fraser GM, Bennett JC, Hughes C: **Substrate-specific binding of hook-associated proteins by FlgN and FliT, putative chaperones for flagellum assembly**. *Mol Microbiol* 1999, **32**:569-580.
48. Bennett JC, Thomas J, Fraser GM, Hughes C: **Substrate complexes and domain organization of the Salmonella flagellar export chaperones FlgN and FliT**. *Mol Microbiol* 2001, **39**:781-791.
49. Nambu T, Minamino T, Macnab RM, Kutsukake K: **Peptidoglycan-hydrolyzing activity of the FlgJ protein, essential for flagellar rod formation in Salmonella typhimurium**. *J Bacteriol* 1999, **181**:1555-1561.
50. Hirano T, Minamino T, Macnab RM: **The role in flagellar rod assembly of the N-terminal domain of Salmonella FlgJ, a flagellum-specific muramidase**. *J Mol Biol* 2001, **312**:359-369.
51. Minamino T, Gonzalez-Pedrajo B, Yamaguchi K, Aizawa SI, Macnab RM: **FliK, the protein responsible for flagellar hook length control in Salmonella, is exported during hook assembly**. *Mol Microbiol* 1999, **34**:295-304.
52. Muramoto K, Makishima S, Aizawa SI, Macnab RM: **Effect of cellular level of FliK on flagellar hook and filament assembly in Salmonella typhimurium**. *J Mol Biol* 1998, **277**:871-882.
53. Koroyasu S, Yamazato M, Hirano T, Aizawa SI: **Kinetic analysis of the growth rate of the flagellar hook in Salmonella typhimurium by the population balance method**. *Biophys J* 1998, **74**:436-443.
54. Muramoto K, Makishima S, Aizawa S, Macnab RM: **Effect of hook subunit concentration on assembly and control of length of the flagellar hook of Salmonella**. *J Bacteriol* 1999, **181**:5808-5813.
55. Makishima S, Komoriya K, Yamaguchi S, Aizawa SI: **Length of the flagellar hook and the capacity of the type III export apparatus**. *Science* 2001, **291**:2411-2413.

56. Blocker A, Komoriya K, Aizawa S: **Type III secretion systems and bacterial flagella: insights into their function from structural similarities**. *Proc Natl Acad Sci U S A* 2003, **100**:3027-3030.
57. Cornelis GR: **The Yersinia Ysc-Yop 'type III' weaponry**. *Nat Rev Mol Cell Biol* 2002, **3**:742-752.
58. Feldman MF, Cornelis GR: **The multitalented type III chaperones: all you can do with 15 kDa**. *FEMS Microbiol Lett* 2003, **219**:151-158.
59. Parsot C, Hamiaux C, Page AL: **The various and varying roles of specific chaperones in type III secretion systems**. *Curr Opin Microbiol* 2003, **6**:7-14.
60. Ramamurthi KS, Schneewind O: **Substrate recognition by the Yersinia type III protein secretion machinery**. *Mol Microbiol* 2003, **50**:1095-1102.
61. Blocker A, Gounon P, Larquet E, Niebuhr K, Cabiaux V, Parsot C, Sansonetti P: **The tripartite type III secreton of Shigella flexneri inserts IpaB and IpaC into host membranes**. *J Cell Biol* 1999, **147**:683-693.
62. De Geyter C, Wattiez R, Sansonetti P, Falmagne P, Ruysschaert JM, Parsot C, Cabiaux V: **Characterization of the interaction of IpaB and IpaD, proteins required for entry of Shigella flexneri into epithelial cells, with a lipid membrane**. *Eur J Biochem* 2000, **267**:5769-5776.
63. Hakansson S, Schesser K, Persson C, Galyov EE, Rosqvist R, Homble F, Wolf-Watz H: **The YopB protein of Yersinia pseudotuberculosis is essential for the translocation of Yop effector proteins across the target cell plasma membrane and displays a contact-dependent membrane disrupting activity**. *Embo J* 1996, **15**:5812-5823.
64. Tardy F, Homble F, Neyt C, Wattiez R, Cornelis GR, Ruysschaert JM, Cabiaux V: **Yersinia enterocolitica type III secretion-translocation system: channel formation by secreted Yops**. *Embo J* 1999, **18**:6793-6799.
65. Koster M, Bitter W, de Cock H, Allaoui A, Cornelis GR, Tommassen J: **The outer membrane component, YscC, of the Yop secretion machinery of Yersinia enterocolitica forms a ring-shaped multimeric complex**. *Mol Microbiol* 1997, **26**:789-797.
66. Woestyn S, Allaoui A, Wattiau P, Cornelis GR: **YscN, the putative energizer of the Yersinia Yop secretion machinery**. *J Bacteriol* 1994, **176**:1561-1569.
67. Payne PL, Straley SC: **YscP of Yersinia pestis is a secreted component of the Yop secretion system**. *J Bacteriol* 1999, **181**:2852-2862.
68. Stainier I, Bleves S, Josenhans C, Karmani L, Kerbourch C, Lambermont I, Totemeyer S, Boyd A, Cornelis GR: **YscP, a Yersinia protein required for Yop secretion that is surface exposed, and released in low Ca2+**. *Mol Microbiol* 2000, **37**:1005-1018.
69. Payne PL, Straley SC: **YscO of Yersinia pestis is a mobile core component of the Yop secretion system**. *J Bacteriol* 1998, **180**:3882-3890.
70. Day JB, Plano GV: **The Yersinia pestis YscY protein directly binds YscX, a secreted component of the type III secretion machinery**. *J Bacteriol* 2000, **182**:1834-1843.
71. Blocker A, Jouihri N, Larquet E, Gounon P, Ebel F, Parsot C, Sansonetti P, Allaoui A: **Structure and composition of the Shigella flexneri "needle complex", a part of its type III secreton**. *Mol Microbiol* 2001, **39**:652-663.
72. Kimbrough TG, Miller SI: **Contribution of Salmonella typhimurium type III secretion components to needle complex formation**. *Proc Natl Acad Sci U S A* 2000, **97**:11008-11013.
73. Kubori T, Matsushima Y, Nakamura D, Uralil J, Lara-Tejero M, Sukhan A, Galan JE, Aizawa SI: **Supramolecular structure of the Salmonella typhimurium type III protein secretion system**. *Science* 1998, **280**:602-605.

74. Magdalena J, Hachani A, Chamekh M, Jouihri N, Gounon P, Blocker A, Allaoui A: **Spa32 regulates a switch in substrate specificity of the type III secreton of Shigella flexneri from needle components to Ipa proteins**. *J Bacteriol* 2002, **184**:3433-3441.
75. Kawagishi I, Homma M, Williams AW, Macnab RM: **Characterization of the flagellar hook length control protein fliK of Salmonella typhimurium and Escherichia coli**. *J Bacteriol* 1996, **178**:2954-2959.
76. Allaoui A, Woestyn S, Sluiters C, Cornelis GR: **YscU, a Yersinia enterocolitica inner membrane protein involved in Yop secretion**. *J Bacteriol* 1994, **176**:4534-4542.
77. Kostyuchenko VA, Leiman PG, Chipman PR, Kanamaru S, van Raaij MJ, Arisaka F, Mesyanzhinov VV, Rossmann MG: **Three-dimensional structure of bacteriophage T4 baseplate**. *Nat Struct Biol* 2003, **10**:688-693.
78. Mota LJ, Journet L, Sorg I, Agrain C, Cornelis GR: **Bacterial injectisomes: needle length does matter**. *Science* 2005, **307**:1278.
79. Journet L, Agrain C, Broz P, Cornelis GR: **The needle length of bacterial injectisomes is determined by a molecular ruler**. *Science* 2003, **302**:1757-1760.
80. Agrain C, Sorg I, Paroz C, Cornelis GR: **Secretion of YscP from Yersinia enterocolitica is essential to control the length of the injectisome needle but not to change the type III secretion substrate specificity**. *Mol Microbiol* 2005, **57**:1415-1427.
81. Minamino T, Saijo-Hamano Y, Furukawa Y, Gonzalez-Pedrajo B, Macnab RM, Namba K: **Domain organization and function of Salmonella FliK, a flagellar hook-length control protein**. *J Mol Biol* 2004, **341**:491-502.
82. Agrain C, Callebaut I, Journet L, Sorg I, Paroz C, Mota LJ, Cornelis GR: **Characterization of a Type III secretion substrate specificity switch (T3S4) domain in YscP from Yersinia enterocolitica**. *Mol Microbiol* 2005, **56**:54-67.
83. Pallen MJ, Penn CW, Chaudhuri RR: **Bacterial flagellar diversity in the post-genomic era**. *Trends Microbiol* 2005, **13**:143-149.
84. Hirano T, Shibata S, Ohnishi K, Tani T, Aizawa S: **N-terminal signal region of FliK is dispensable for length control of the flagellar hook**. *Mol Microbiol* 2005, **56**:346-360.

ANNEXES

List of the plasmids

Plasmid name	Protein encoded	Vector	References	Remarks
pCA1	$YscP_{\Delta 1\text{-}15}$	pBAD	[82]	
pCA2	$YscP_{393\text{-}515}$	pBAD		not stable
pCA3	$YscP_{pestis}$	pBAD	[79]	
pCA4	$YscP_{\Delta 97\text{-}465}$	pBAD		
pCA5	$YscP_{\Delta 16\text{-}25}$	pBAD	[79]	
pCA6	$YscP_{\Delta 26\text{-}35}$	pBAD	[79]	
pCA7	$YscP_{\Delta 36\text{-}45}$	pBAD	[79]	
pCA9	$YscP_{\Delta 46\text{-}96}$	pBAD	[79]	
pCA10	$YscP_{1\text{-}100}$ -Cya	pMSL56	[80]	
pCA11	$YscP_{370\text{-}515}$	pBAD		not stable
pCA12	$YscP_{1\text{-}50}$ -Cya	pMSL56		
pCA13	$YscP_{\Delta 58\text{-}477}$	pBAD		
pCA14	$YscP_{\Delta 57\text{-}384}$	pBAD		
pCA15	YscP-DHFR	pBAD		
pCA17	HIS-$YscP_{400\text{-}515}$	pET15b		
pCA18	$YscP_{\Delta 385\text{-}424}$	pBAD	[79]	
pCAP19	$YscP_{\Delta 425\text{-}464}$	pBAD		
pCA20	$YscP_{\Delta 46\text{-}96+\Delta 222\text{-}306}$	pBAD	[79]	
pCA22	$YscP_{\Delta 57\text{-}221}$	pBAD	[80]	
pCA23	$YscP_{\Omega}$	pBAD	[79]	
pCA24	$YscP_{\Omega lacZ}$	pBAD		
pCA25	$YscP_{16\text{-}100}$ -Cya	pMSL56		
pCA26	YscP $_{1\text{-}100(d16\text{-}25)}$-Cya	pMSL56		
pCAP27	YscP $_{1\text{-}100\ (d26\text{-}35)}$-Cya	pMSL56		
pCAP28	YscP $_{1\text{-}50\ (d36\text{-}45)}$-Cya	pMSL56		
pCA29	YscP $_{1\text{-}50\ (d16\text{-}45)}$-Cya	pMSL56		
pCA30	$YscP_{6\text{-}100}$ -Cya	pMSL56		
pCA31	$YscP_{16\text{-}50}$ -Cya	pMSL56	[80]	
pCAP32	YscP $_{1\text{-}50\ (d16\text{-}25)}$-Cya	pMSL56	[80]	
pCA33	$YscP_{1\text{-}50\ (d26\text{-}35)}$ -Cya	pMSL56	[80]	
pCA34	YscP $_{1\text{-}50\ (d36\text{-}45)}$ -Cya	pMSL56	[80]	
pCA35	$YscP_{\Delta 57\text{-}384}$- HIS	pET22+		
pCA36	$YscP_{6\text{-}50}$ -Cya	pMSL56		not stable

pCA37	YscP$_{138-384}$ -Cya	pMSL56	[80]	
pCA39	YscP$_{97-384}$-Cya	pMSL56	[80]	
pCA41	YscP$_{\Delta 1-56}$	pBAD		not stable
pCAP45	YscX-DHFR	pBAD		
pCAP47	YscP$_{\Delta 97-137}$	pBAD	[82]	
pCAP48	YscP$_{\Delta 137-177}$	pBAD	[82]	
pCAP49	YscP$_{\Delta 177-197}$	pBAD	[82]	
pCAP50	YscP$_{\Delta 197-216}$	pBAD	[82]	
pCAP51	YscP$_{97-384\ (d137-177)}$ -Cya	pMSL56	[80]	
pCAP52	YscP$_{97-384\ (d177-197)}$ -Cya	pMSL56	[80]	
pCAP53	YscP$_{97-384\ (d197-217)}$ -Cya	pMSL56	[80]	
pCAP54	YscP$_{97-384\ (d222-306)}$ -Cya	pMSL56	[80]	
pCAP55	YscP$_{97-384\ (d222-381)}$ -Cya	pMSL56	[80]	
pCAP56	YscP$_{\Delta 465-485}$	pBAD	[82]	
pCA57	YscP$_{\Delta 485-500}$	pBAD	[82]	
pCA58	YscP$_{384-465}$ -Cya	pMSL56	[80]	
pCA59	YscP$_{468\ -515}$ -Cya	pMSL56	[80]	
pCAP61	YscF-DHFR	pBAD		
pCAP62	YscO-DHFR	pBAD		
pCA67	YscP $_{\Delta 1-35}$- Cya	pMSL56		
pCAP71	YscP$_{107-137}$-Cya	pMSL56		
pCA72	YscP$_{97-137\ (d107-117)}$-Cya	pMSL56		
pCA73	YscP$_{97-384\ (d117-127)}$-Cya	pMSL56		
pCA75	YscP $_{\Delta 26-35+\Delta 485-500}$	pBAD		
pCA76	YscP $_{\Delta 1-15+\Delta 485-500}$	pBAD	[80]	
pCAP77	YscP $_{Q488A}$	pBAD	[82]	
pCAP78	YscP $_{Q472A}$	pBAD	[82]	
pCA79	YscP $_{Q482A}$	pBAD	[82]	
pCAP80	YscP $_{P486A}$	pBAD	[82]	
pCAP81	YscP $_{E479A}$	pBAD	[82]	
pCAP82	YscP $_{R480A}$	pBAD	[82]	
pCA83	YscP $_{L442A}$	pBAD	[82]	
pCA85	YscP $_{R418A}$	pBAD	[82]	
pCA86	YscP $_{P440A}$	pBAD	[82]	
pCA87	YscP A_6	pBAD		
pCA88	YscP$_{1-405-}$*Xba*I-406-end	pBAD		
pCA89	YscP*Xba*I - *Bgl*II	pBAD		

pCA90	$YscP_{T3S4\ AscP}$	pBAD	[82]	
pCA91	$YscP_{T3S4\ FliK\textit{salmo}}$	pBAD	[82]	
pCA92	$YscP_{T3S4\ PscP}$	pBAD	[82]	
pCA93	$YscP_{T3S4\ FliK\textit{pestis}}$	pBAD	[82]	
pCA95	$YscP_{97\text{-}515}$	pBAD	[80]	
pCA96	$YscP_{190\text{-}515}$	pBAD		
pCA97	$YscP_{245\text{-}515}$	pBAD		
pCA98	$YscP_{331\text{-}515}$	pBAD		
pCA99	$YscP_{367\text{-}515}$	pBAD		
pCA115	$YscP_{\Delta 1\text{-}35}$	pBAD		not stable
pCA116	$YscP_{\Delta 1\text{-}35+\Delta 97\text{-}137}$	pBAD		not stable

Curriculum vitae

Personal information

Surname/ First name	**AGRAIN Céline**
Address	5 rue Roswag, 67600 Sélestat
Telephone	0388928172
E-mail	c.agrain@unibas.ch
Nationality	french
Date of birth	22.01.1978

Occupational field

Molecular Microbiologist

Education and work experience

Dates	from October 2002 to now
Title of qualification awarded	**PhD**
Principal subjects	Molecular Microbiology/ Microbial Pathogenesis
Name and address of employer	Department of Microbiology, Biozentrum, University of Basel, 50-70 Klingelbergstrasse, 4056 Basel
Supervisor	Prof. Dr. Guy Cornelis
Subject	*YscP, a key player in Type Three Secretion Systems of Yersinia enterocolitica*

Dates	from august 2001 to july 2002
Title of qualification awarded	**DEA** with distinctions
Principal subjects	Molecular and Cellular Biology
Name and address of employer	Laboratoire Dynamique, évolution et expression de génomes de microorganismes, CNRS FRE 2326, Institut de botanique, 28 rue Goethe, 67083 Strasbourg
Supervisor	Dr. Jean-Marie Meyer
Subject	*Characterization of ferri-pyoverdine receptors in Pseudomonas aeruginosa*

Dates	from october 2000 to june 2001
Title of qualification awarded	**Maitrise de biochimie mention biologie Moléculaire** with distinctions
Principal subjects	Biochemistry, Molecular biology, Microbiology and Genetics
University	University Louis Pasteur, Strasbourg

Dates	july-august 2000
Position held	**Trainee**
Name and address of employer	Laboratoire Dynamique, évolution et expression de génomes de microorganismes, CNRS FRE 2326, Institut de botanique, 28 rue Goethe, 67083 Strasbourg
Supervisor	Dr. Jean-Marie Meyer
Subject	*Siderotyping in Burkholderia*

Dates	from october 2000 to june 2001
Title of qualification awarded	**Licence de Biochimie** with distinctions

Publications

- Articles

Cornelis, G.R., **Agrain, C.** and Sorg, I. (2005). Length control in bacteria and bacteriophages. **Curr Op Microbiol** *submitted*

Agrain, C., Sorg, I., Paroz, C., and Cornelis, G.R. (2005). Secretion of YscP from *Yersinia enterocolitica* is essential to control the length of the injectisome needle but not to change the Type III secretion substrate specificity. **Mol Microbiol** 57 : 1415-1427

Agrain, C., Callebaut, I., Journet, L., Sorg, I., Paroz, C., Mota, L.J., and Cornelis, G.R. (2005). Characterization of a Type III secretion substrate specificity switch (T3S4) domain in YscP from Yersinia enterocolitica. **Mol Microbiol** 56 : 54-67.

Mota, L.J., Journet, L., Sorg, I., **Agrain, C.,** and Cornelis, G.R. (2005). Bacterial injectisomes: needle length does matter. **Science** 307: 1278.

Journet, L., **Agrain, C**., Broz, P., and Cornelis, G.R. (2003). The needle length of bacterial injectisomes is determined by a molecular ruler. **Science** 302: 1757-60.

- Posters

Agrain, C., Sorg, I., Journet, L., Paroz, C., Mota, L.J., and Cornelis, G.R. (2005). YscP, a key player in *Yersinia enterocolitica* Type Three Secretion System. Swiss Society of Microbiology (SSM) Congress, Geneva, Switzerland, 31/03-01/04. *Awarded 2nd poster prize.*

Mota, L.J., Journet, L., **Agrain, C.,** and Cornelis, G.R. (2005). The role of the injectisome needle on translocation of Yop proteins into macrophages by the Yersinia Ysc-Yop type III secretion system. Workshop EMBO/FEBS, Frontiers of Cellular Microbiology and Cell Biology, San Feliu de Guixols, Spain, 16/10-21/10.

Agrain, C., Callebaut, I., Journet, L., Sorg, I., Paroz, C., Mota, L.J., and Cornelis, G.R. (2004). Characterization of a Type III secretion substrate specificity switch (T3S4) domain, besides the molecular ruler region in YscP from *Yersinia enterocolitica*. Biozentrum Symposium, St-Chrischona, Switzerland, 14/10.

Agrain, C., Journet, L., and Cornelis, G.R. (2003). The functions and secretion signals of YscP of *Yersinia enterocolitica.* EMBO Lecture Course, Cellular and molecular biology of membranes, Cargèse, Corsica, France, 09/06-21/06.

Talks

Agrain, C., and Cornelis, G.R. (2004). YscP, la clef du système de secrétion de Type III chez *Yersinia enterocolitica*. Université Louis Pasteur, Strasbourg, France. 06/05

Agrain, C., Journet, L., and Cornelis, G.R. (2003). YscP, not only a ruler. EU MEMBACS meeting, Marbach, Konstanz, Germany, 06/11-08/11.